INTEGRATED MODELING OF STORM DRAIN AND NATURAL CHANNEL NETWORKS FOR REAL-TIME FLASH FLOOD FORECASTING AND STORMWATER PLANNING AND MANAGEMENT IN LARGE URBAN AREAS

By

HAMIDEH HABIBI

Presented to the Faculty of the Graduate School of

The University of Texas at Arlington in Partial Fulfillment of the Requirements

for the Degree of

DOCTOR OF PHILOSOPHY

THE UNIVERSITY OF TEXAS AT ARLINGTON

July 2017

Acknowledgements

I am extremely grateful to my advisor Dr. Dong-Jun Seo for his tremendous support during my PhD study. I would also like to thank my dissertation committee Drs. Nick Fang, Habib Ahmari, and Jean Gao for their comments. In addition, I am grateful to Drs. Sunghee Kim, Behzad Nazari, Hamideh Riazi, and Arezoo Rafieeinasab and all other members of our research group at the Urban Water Institute for their support.

Also, I would like to express my gratitude to many others who helped me during my PhD study including, Dr. Zhengtao Cui of the NWS Office of Water Prediction for help with HLRDHM modeling, Mses. Amy Cannon of the City of Arlington and Stephanie Griffin of the City of Grand Prairie for providing the storm drain and related data used in this work.

This material is based upon work supported by the National Science Foundation under Grant No. CyberSEES-1442735. This support is gratefully acknowledged.

Finally, I must express my gratitude to my wonderful parents, family, and friends for all their support and encouragement.

July 25, 2017

Abstract

INTEGRATED MODELING OF STORM DRAIN AND NATURAL CHANNEL NETWORKS FOR REAL-TIME FLASH FLOOD FORECASTING FOR STORMWATER PLANNING AND MANAGEMENT FOR LARGE URBAN AREAS

Hamideh Habibi, PhD

The University of Texas at Arlington, 2017

Supervising Professor: Dong-Jun Seo

Urban flash flooding is a serious problem in large highly populated areas such as the Dallas–Fort Worth metroplex (DFW). Being able to monitor and predict flash flooding at a high spatiotemporal resolution is critical to mitigating its threats and for cost effective emergency management. In this reserach, a high-resolution flash flood forecast system which operates in real time is developed for DFW using a gridded distributed hydrologic model and high-resolution quantitative precipitation estimates from the DFW Demostration Network of the Collaborative Adaptive Sensing of the Atmosphere (CASA) Program high-resolution X band radars and the National Weather Service (NWS) NEXRAD radar.

To mitigate hazards and to reduce negative impacts of flooding, urban municipalities operate storm drain networks of varying capacity and complexity. Whereas the conveyance capacities of storm drain systems are generally much smaller than those of the natural channel systems (Rafieeinasab et al. 2015), storm drain networks may significantly alter the severity of flooding and other impacts depending on the location of flooding and the magnitude of rainfall. For accurate flash flood forecasting and effective stormwater planning and management in urban areas, it is necessary to model not only the natural channel systems but also the large and complex networks of storm drains. Most distributed hydrologic models developed for real-time flood forecasting lack the ability to simulate storm drains explicitly. Most urban hydraulic models can simulate storm drains but are not suitable for real-time forecasting for large areas due to computational cost and modeling complexity. In this work, a modular storm drain model that can be easily coupled with existing gridded distributed hydrologic models for real-time flash flood forecasting and stormwater planning and management for large urban areas is described. The integrated model is applied to a 144.6 km^2 area consisting of five urban catchments in the Cities of Arlington and Grand Prairie in Texas, US, and the impact of the storm drain network via a combination of simulation experiments, sensitivity analysis and a limited comparison with observed flow is assessed. It is shown how the integrated model may be used to assess the effectiveness of storm drain network over a large area and how areas of potential concern for flooding

may be identified under the existing condition and under increased imperviousness. The results show that storm drain modeling increases peak outlet flow for significant events very slightly only for smaller catchments. The simulation experiments with and without storm drain modeling also show that the storm drains reduce surface flow very significantly for a short duration at almost all grid cells in the study area, and that at many locations the flow remains reduced for the entire duration. Sensitivity analysis indicates that significant uncertainties exist in modeling inlet flow and hence partitioning surface runoff into storm drain and natural channel flows. The sources of uncertainties include incomplete information on stormwater infrastructure and uncertainties associated with inlet size, efficiency, clogging and gutter flow modeling. Whereas uncertainty analysis for stormwater infrastructure would be an extremely expensive proposition for both modeling and computing with 1D storm drain-2D surface flow modeling for a large area, the integrated modeling approach developed in this work makes such analysis well within the realm of possibility. The proposed approach hence offers a practical pathway for integrated modeling of storm drains with gridded distributed hydrologic models for large urban areas.

Table of Contents

List of Illustrations

List of Tables

Chapter 1

General introduction

Flooding is one of the most significant natural hazards in urban areas and a major source of inconvenience of varying magnitude and frequency to the residents. In urban areas with high population density and large fractions of impervious surfaces, even a small-scale but intense rainfall event can cause deadly flash floods and extensive damages. To mitigate hazards and to reduce negative impacts from flooding, all urban municipalities operate storm drain networks of varying capacity, spatial extent and complexity. Whereas the conveyance capacities of storm drain systems are generally much smaller than those of the natural channel systems (Rafieenasab et al., 2015), storm drain networks may significantly alter the level of flooding hazards and other impacts depending on the location as well as the magnitude and spatiotemporal variability of rainfall. For accurate flash flood forecasting in urban areas, it is hence necessary to model not only the natural channel systems but also the large and complex networks of storm drains. The ability of modeling jointly the natural channels and storm drain systems for large urban areas is also important for planning and management of storm water infrastructure. Traditionally, storm water infrastructure has been designed on a site-by-site basis with the goal of keeping the post-development peak flow from flooding events the same as before. Such an approach, however, does not reduce

the runoff or the total volume of storm water, and hence may still produce flooding downstream. Also, because of the site-by-site design, stormwater infrastructure does not fully account for spatiotemporal integration of runoff and flow through natural and man-made systems or spatiotemporal variability of rainfall across scale. As such, the design and operation of the resulting system is likely to lack resiliency to work effectively on larger, watershed scales. Indeed, McCuen (1979) and Emerson et al. (2005) showed that an unplanned system of site-based storm water control measures or best management practices can actually increase flooding on a watershed scale owing to the effect of many facilities discharging into a receiving waterbody in an uncoordinated fashion - causing the very flooding problem the individual basins were built to solve.

The ability to model jointly the natural channel and storm drain systems for large urban areas also allows objective assessment of vulnerability of stormwater infrastructure from transient shocks of extreme precipitation under climate change and urbanization. Many researchers have assessed the impacts of climate change on urban drainage systems and analyzed the specific impacts on different small urban areas (e.g., Niemczynowicz 1989; Watt et al. 2003; Mailhot et al. 2006a; Guo 2006; Denault et al. 2006). While the results vary depending on the variation of urban catchment responses to heavy-to-extreme rainfalls, most conclude that the probability of surcharge and hence flooding increases in urban area. Therefore, there exists a critical need in stormwater management and planning in large urban

areas for being able to simulate how large storm drain networks may respond to extreme rainfall under changing land cover conditions and climate change.

Restoring and improving urban infrastructure is one of the grand challenges in engineering today (NAE 2015). This research addresses a critical gap in stormwater planning and management in large urban areas by developing a coupled computer model that can simulate how large storm drain networks respond to extreme rainfall under changing land cover conditions due to urbanization, and by advancing understanding of how the coupled system of man-made storm drain and natural channel networks respond to such shocks and changes. By making the coupled modeling possible for large urban areas, this research is expected to allow rigorous system approach to optimizing urban stormwater systems for both short- and long-term planning and management.

Recently, the National Oceanic and Atmospheric Administration's National Weather Service launched the National Water Model (NWM) which provides high-resolution water forecasts for the Nation. Currently, the NWM models natural channels only. This research also addresses the outstanding gap of cost-effective integrated modeling of natural and storm drain systems that can be implemented for urban areas of all sizes in the U.S. and elsewhere.

Integrated modeling of flow through natural channels and storm drains for small urban areas is not new. Approaches such as 1D-2D modeling (Leandro et al.

2009) have gained wide popularity and acceptance in recent years. For real-time applications over large areas, however, such approaches quickly become untenable because of modeling complexities and extremely large computational requirements. There are many urban hydraulic models of varying sophistication such as HEC-1 (USACE 1985), TR-20 and TR-55 (SCS 1983, 1986), MOUSE (DHI 1995), HydroWorks (HR) (Wallingford Ltd. 1997) and Storm Water Management Model (SWMM) (Huber and Dickinson 1988) just to name only several. Distributed hydrologic models can cover large areas and may be suitable for real time applications but cannot simulate storm drains explicitly. While the coupled modeling is widely practiced at small scales ($O(10^1 \sim 10^2)$ km^2), the existing modeling paradigm and capabilities do not easily scale up to large urban areas. This research takes a novel approach of equivalent-mapping the storm drain network to the distributed hydrologic model grid for the natural channel network, thereby rendering the coupled modeling simple and parsimonious for real-world applications, and highly modular and efficient for application for large areas.

In this study, first the flash flood forecast system for the Dallas-Fort Worth Metroplex (DFW), which operates in real-time with the use of weather radar and a distributed hydrologic model, is described. A new storm drain module that can be easily integrated with the gridded distributed hydrologic models is then described for real-time simulation of flow through both natural channels and storm drains for

large urban areas. The specific research questions addressed in this research include:

1. How to partition surface runoff into pipe and natural channel systems? What are the largest sources of uncertainty?
2. How to reduce the geometric complexity of a storm drain network into a simpler "equivalent" network?
3. How does the storm drain network alter the hydrologic response of urban catchments? How does the response vary according to the size of the catchment, land cover and the magnitude of the storm?
4. What is the relative importance of natural channels and storm drains in stormwater management and flood control at different spatiotemporal scales in large urban areas?

To address the 1st question, different strategies for partitioning surface runoff into storm drain and natural channel network are used and the performance of the integrated model is assessed. Also, to assess the uncertainties associated with partitioning surface runoff into flow into the storm drain network and that into the natural channels as well as to establish the bounds of the above partitioning, a systematic sensitivity analysis is carried out with respect to a limited number of model parameters. To address the 2nd question, an automated algorithm is developed to generate the flow direction for storm drain network and convert the original network to simple equivalent one. The resulting equivalent nework has the

same hydraulic and travel time characteristics of the original syetem. To address the 3rd and 4th questions, the performance of the model is assessed by routing runoff with and without storm drainage network under different land cover conditions and magnitude of desgin rainfall, and simulated flows at the catchment outlets are compared against the observed to assess the realism of the model for simulating natural channel flow.

The new and significant contributions of this research are: 1) real time high-resolution flash flood forecasting for DFW area, 2) development of an integrated model that can simulate flow through both natural channels and storm drains for real-time application of large urban areas, 3) development of an automatic algorithim for derivation of equivalent storm drain network from the original network and 4) advances in understanding of the uncertainty associated with partitioning runoff into storm drain and natural channel systems, hydrologic response of urban catchments to heavy-to-extreme rainfall using combined natural channel and storm drain systems, and the performance of stormwater infrastructure from transient shocks of extreme precipitation under changing conditions.This diseration is organized as follows. In Chapter 2, the high resolution flash flood forecast system developed for DFW is described. Chapter 3 describes the approach, study area, data used and the methodology for the integrated modeling of natural channel and storm drain networks. In Chapter 4, the algoritms developed for derivation of flow direction and equivalent storm drain network are explained. The

results are presented in Chapter 5, in two sections: 1) assess the performance of HLRDHM using two case studies of the flash flooding events of June 24, 2014 and April 13, 2015 in the City of Fort Worth, 2) assess the performance of integrated modeling of natural channels and storm drain networks which is presented in four partes: 1) compare simulation and observed flows at catchment outlets against, 2) integrated model simulation with and without storm drain modeling, 3) assess the impact of storm drains under different land cover conditions, and 4) examine the impact of the initial conditions (IC) of the storm drain flow model and assess the sensitivity of the conveyance volumes in the natural channel and storm drain networks to selected inlet flow model parameters. Chapter 6 provides the genral conclusions and future research recommendations.

Chapter 2

High-resolution flash flood forecasting for the Dallas-Fort Worth Motorplex (DFW)[1]

2.1. Introduction

More than three-quarters of the population of the United States lives in urban areas that comprise only about 3% of the total land area. According to the U.S. Census Bureau, the urban population increased by 12.1% from 2000 to 2010 compared to the overall increase of 9.7% for the same period. For the 486 large urbanized areas, the rate was even higher at 14.3%. Given the high population density, high-resolution observation and modeling capabilities are necessary for prediction of flash floods in urban areas. Increasing occurrences of extreme precipitation put such areas in an increasingly vulnerable position as even a small but intense rainfall event can cause deadly flash floods and extensive damages. If effective high-resolution prediction and warning capabilities exist for all urban areas, many lives would be saved and economic losses would be greatly reduced.

For high-resolution observation and modeling of large urban areas, the use of weather radar and distributed hydrologic modeling is a natural progression. In

[1] Used with permission from the CHI, the publisher of the Journal of Water Management Modeling, 2017

this work, the prototype high-resolution flash flood forecasting system under development for DFW is described and two case studies of the flash flooding event of June 24, 2014 and April 13, 2015 in Fort Worth are presented. Two radar-based Ouantative Precipitation Estimation (QPE) were used in this study: the higher-resolution (500m, 1 min) QPE from the X-band radar installed at the University of Texas at Arlington, which is part of the DFW Demonstration Network of Collaborative Adaptive Sensing of the Atmosphere (CASA) radars (see Figure 2), and the lower-resolution (4-km, 1-hr) multisensor QPE from the Multisensor Precipitation Estimator (MPE) operated by the Natinal Weather Service (NWS) West Gulf River Forecast Center (WGRFC). The model simulation results are qualitatively assessed based on the location and timing of local flooding reported by the residents of the City of Fort Worth throughout the event.

2.2. Study area and precipitation data used

The study area is the DFW in North Texas which is the fourth-largest metropolitan area in the US by population. The area of interest in this study is the Cities of Fort Worth, Arlington and Grand Prairie (see Figure 1).

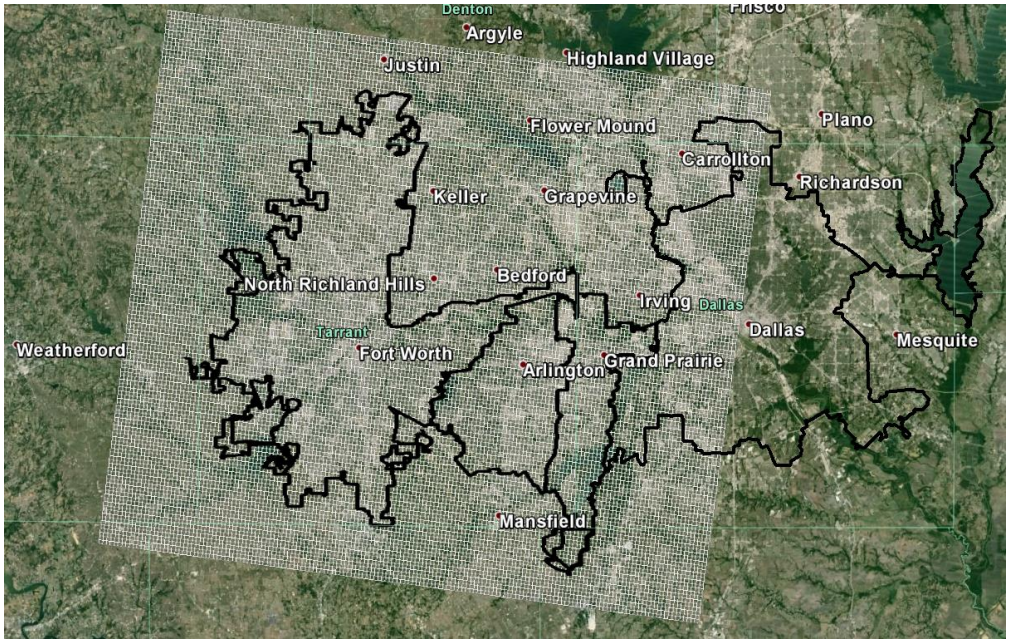

Figure 1 The HLRDHM domain encompassing Fort Worth, Arlington and Grand Prairie. Overlaid is the 500 m ×500 m CASA QPE grid.

For precipitation forcing, the QPEs from the Multisensor Precipitation Estimator (MPE, Seo et al. 2010, Kitzmiller et al. 2011) and from the DFW Demonstration Network of CASA radars are used. The MPE product, which is routinely used in operational hydrologic forecasting, is obtained from the West Gulf River Forecast Center (WGRFC) and has a spatiotemporal resolution of 1 hr and 4 km Hydrologic Rainfall Analysis Projection (HRAP). One of the limitations with Next-Generation Radar (NEXRAD) is that they do not observe the lower atmosphere away from the radar, which causes degradation of spatial resolution at far ranges. Also, the temporal resolution is constrained by a fixed set of volume coverage patterns. This lack of resolution arises because the radar operation is

independent of the weather conditions. To maximize its utility, the radar may adapt to the time-varying needs of the users (Junyent et al. 2010). To address these gaps in the current weather observation system, the NSF Engineering Research Center (ERC) for CASA developed a new weather warning system based on dense networks of small radars (McLaughlin et al. 2005) with adaptive scanning strategy (Junyent et al. 2010). The CASA Integrated Project was the first test bed of a networked CASA radar system composed of four X-band radars in Oklahoma. Each radar node was approximately 30 km apart from the next unit. The details of the radar network, hardware and software architectures are described in Junyent et al. (2010). The network was evaluated using rain gauge observations for a five-year period which showed a good agreement between radar QPE and rain gauge observations with a standard deviation of 25% and a bias of 3.7% (Chandrasekar et al. 2012).

Because CASA QPE is based on specific differential propagation phase, it is immune to absolute calibration errors (Bringi and Chandrasekar 2001). Attenuation is a known issue for precipitation estimation using X-band radars (Seo et al. 2010, Berne and Krajewski 2013). The CASA system uses the network reflectivity retrieval technique (Chandrasekar and Lim 2008) and the network-based attenuation correction technique (Lim et al. 2011) to mitigate the effects of attenuation. Lim et al. (2011) showed that the technique works robustly in real time in retrieving attenuation-corrected reflectivity.

A network of seven CASA X-band radars, referred to as the DFW Demonstration Network, has been deployed in the area thus far. Figure 2 shows the radar locations at the University of Texas at Arlington (UTA), Cleburne, Midlothian and Addison, Denton. Fort Worth, Mesquite and their coverage. Radar QPE from the network is based on:

$$R = 18.15KDP^{0.791} \quad (1)$$

where, R is rain rate (mm/hr), and KDP is specific differential phase (deg/km).

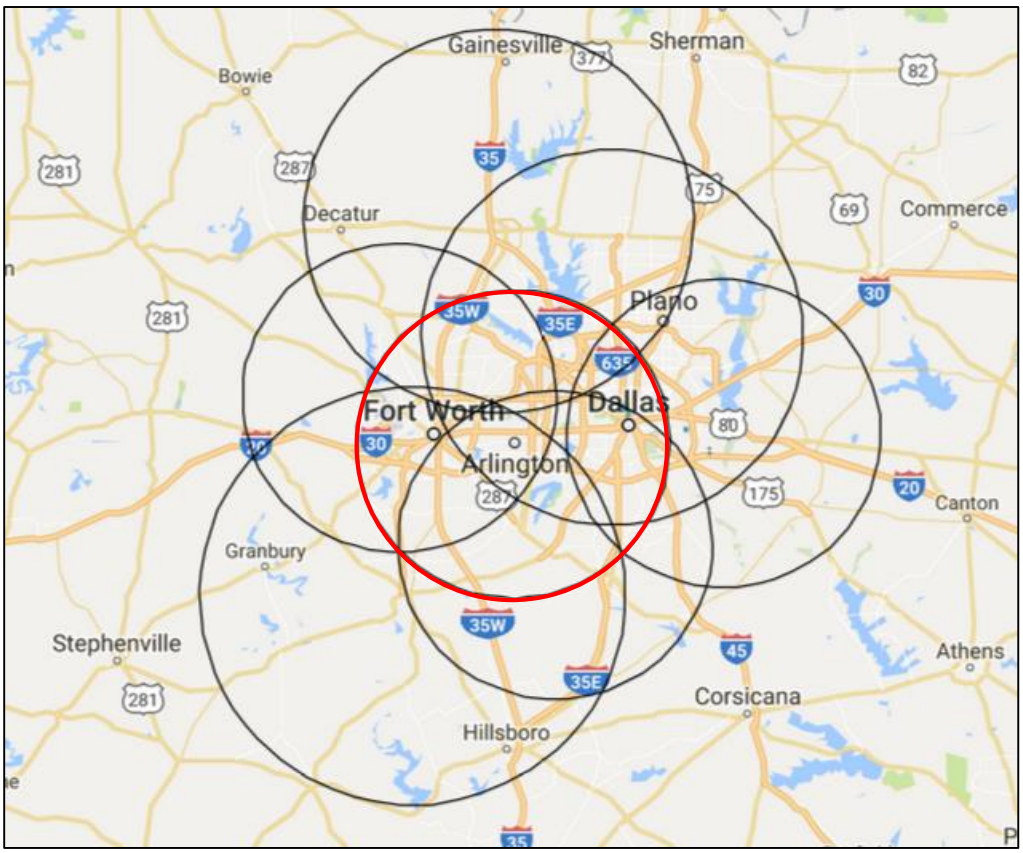

Figure 2 The DFW Demonstration Network (the red circle indicates the UTA radar coverage)

The spatiotemporal resolution of the QPE from the DFW Demonstration Network is 500 m and 1 min. The QPE products include instantaneous rain rate and 1- and 3-hr rainfall accumulations. Recently, comparative evaluation of different radar-based QPE products was carried out based on a limited period of record of about a year (Rafieeinasab et al. 2014, 2015). The results show that, in general, the CASA QPE is more accurate for larger precipitation amounts whereas the MPE estimates are more accurate for smaller amounts in the study area.

2.3. Hydrologic model

The distributed hydrologic model used in this work is the Hydrology Laboratory-Research Distributed Hydrologic Model (HL-RDHM) developed by the NWS Hydrology Laboratory (HL) (Koren et al., 2004). Koren et al. (2004) showed that HL-RDHM results are comparable to well-calibrated lumped model simulations, and that the former outperform the latter when spatial rainfall variability is significant. The operational version of HL-RDHM, or the Distributed Hydrologic Model (DHM), is used at various River Forecast Centers (RFC) for flash flood and river flood forecasting.

For rainfall-runoff modelling, the Sacramento soil moisture accounting (SAC-SMA) model is used. For routing of hillslope and channel flows, kinematic-wave routing is used. SAC-SMA was first introduced by Burnash et al. (1973) (see

Figure 3) and has been used widely from local to continental scales. SAC-SMA is a conceptual model of the land surface phase of the hydrologic cycle. It accounts for percolation, soil moisture storage, drainage and evaporation processes. The model inputs rainfall, evaporation and snow cover (optional) and outputs runoff to the channel system. The basic SAC-SMA has 16 parameters, of which the most important are given in Table 1.

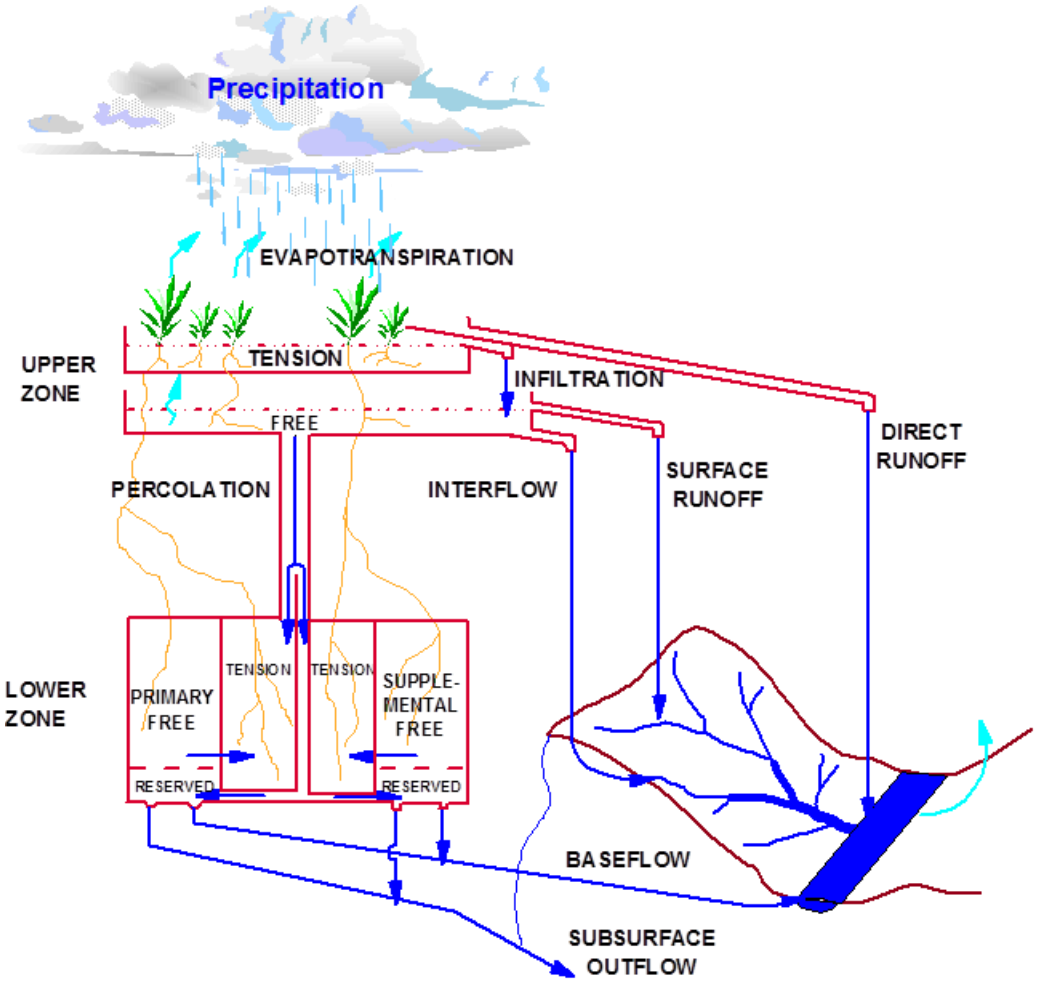

Figure 3 Schematic of the SAC-SMA model.

Koren et al. (2000, 2003) related the SAC-SMA parameters with soil properties such as porosity, field capacity and wilting point, and derived a priori settings for a subset of the SAC-SMA parameters using the State Soil Geographic Database (STATSGO) soil texture data in 11 soil layers.

Anderson et al. (2006) and Zhang et al. (2006) improved the quality of the a priori parameters by replacing the STATSGO data with the finer-scale Soil Survey Geographic Database (SSURGO). A priori grids of the SAC-SMA and kinematic-wave routing parameters are provided by NWS for the continental United States at a 4km x 4km resolution. For modelling at higher resolutions, it is necessary to re-derive the parameters using higher-resolution physiographic data.

Table 1 SAC-SMA parameters, the units and description

Parameters	Units	Description
UZTWM	mm	Upper Zone Tension Water Maximum storage
UZFWM	mm	Upper Zone Free Water Maximum storage
LZTWM	mm	Lower Zone Tension Water Maximum storage
LZFSM	mm	Lower Zone Free water Supplementary Maximum storage
LZFPM	mm	Lower Zone Free water Primary Maximum storage
UZK	day-1	Upper zone free water withdrawal rate
LZSK	day-1	Lower Zone Supplementary withdrawal rate
LZPK	day-1	Lower Zone Primary withdrawal rate
PCTIM	%/100	% permanent impervious area
ADIMP	%/100	% area contributing as impervious when saturated
RIVA	%/100	% area affected by riparian vegetarian, streams and lakes
ZPERC	none	Maximum percolation rate under dry condition
REXP	none	Percolation equation exponent
PFREE	%/100	%of percent going directly to lower zone free water

Because impervious areas play a very important role in rainfall-runoff processes in urban areas, it is necessary that they are delineated with high accuracy and resolution. In this study, the percent impervious area maps (PCTIM in Table 1) are derived based on a set of the GIS layers obtained from the Cities of Fort Worth, Arlington and Grand Prairie (see Table 2). Figure 4 shows the resulting PCTIM map with different resolutions over the DFW area.

Table 2 GIS layers from cities of Fort Worth, Arlington, and Grand Prairie used for estimation of PCTIM.

Map Layer	Fort Worth	Arlington	Grand Prairie	Dallas
Building footprint	√	√	√	√
Impervious cover of commercial	√	-	√	√
Pavements	√	√	-	√
Centerline of sidewalk	√	-	-	√
Centerline of streets	-	-	√	-

Hillslope and channel routing in HLRDHM is performed using kinematic-wave routing (Chow et al. 1988, Koren et al. 2004). HLRDHM routs runoff through the natural channels identifiable from the digital elevation model (DEM) by the Cell Outlet Tracing with an Area Threshold (COTAT) algorithm (Reed 2003).

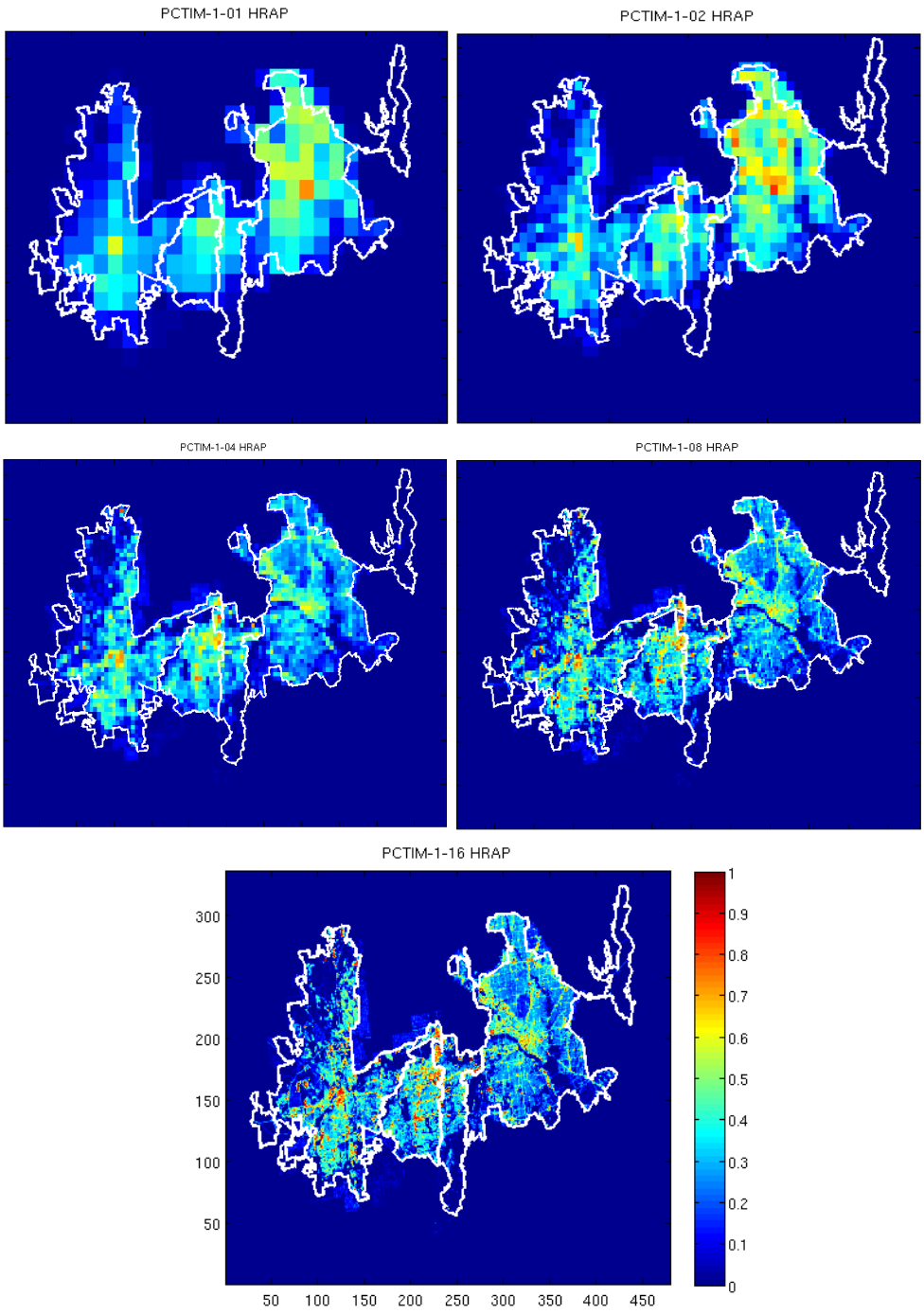

Figure 4 PCTIM maps at different resolution (1, 1/2, 1/4, 1/8 and 1/16 HRAP) within the Cities of Fort Worth, Arlington, Grand Prairie and Dallas.

Within each cell, fast runoff is first routed over conceptual hillslopes, and then the combination of channel inflow from hillslope routing, slow runoff (i.e. subsurface or ground), and inflow from upstream cells is routed via channel routing (Koren et al. 2004). A conceptual hillslope consists of multiple uniform hillslopes, the number of which depends on the stream channel density specified for the cell. The conceptual channel that transfers water from one cell to another usually represents the highest order stream in the cell selected. The cell-to-cell connectivity is used to transfer water from upstream to downstream cells and to the basin outlets. For hillslope routing, discharge per unit area of hillslope (q_h) is given by (Koren et al. 2004) as:

$$q_h = 2k_q \mathrm{D} \frac{\sqrt{S_h}}{n_h} h^{5/3} \quad (2)$$

Where k_q is unit transformation coefficient, D is stream channel density in km^{-1}, S_h is hillslope slope, n_h is hillslope roughness coefficient, and h is average depth of water on the hillslope.

For channel routing, the discharge for each cell,Q_c, is defined as:

$$Q_c = q_0 A^{q_m} \quad (3)$$

A = Wetted cross-sectional area,

q_0 = Specific discharge, i.e., discharge per unit channel cross section area, and

q_m = Exponent in the power-law relationship.

The specific discharge may be evaluated if A and Q_c are known. Mean annual flow may be derived from the mean average annual runoff data over the continental US available from the United States Geological Survey (USGS, Slack and Landwehr, 1992). The wetted channel cross section, A, may be obtained from:

$$A = Q/A \tag{4}$$

Where V is the mean velocity. The mean velocity may be evaluated using the empirical equation developed by Jobson (1996):

$$V = 0.094 + 0.0143\left(\frac{D_a^{1.25}\sqrt{g}}{Q}\right)^{0.919} S^{0.159}\frac{Q}{D_a} \tag{5}$$

Where D_a is upstream drainage area calculated using the flow direction and cell size grids, g is gravitational acceleration, and S is channel slope.

The two kinematic-wave channel routing parameters, q_0 and q_m, were derived using the above relationships and the National Elevation Dataset (NED) with 30 meter resolution from the NHDPlus Version 2 dataset (David et al. 2014). Figure 5 shows the derived specific discharge at different resolutions over the model domain.

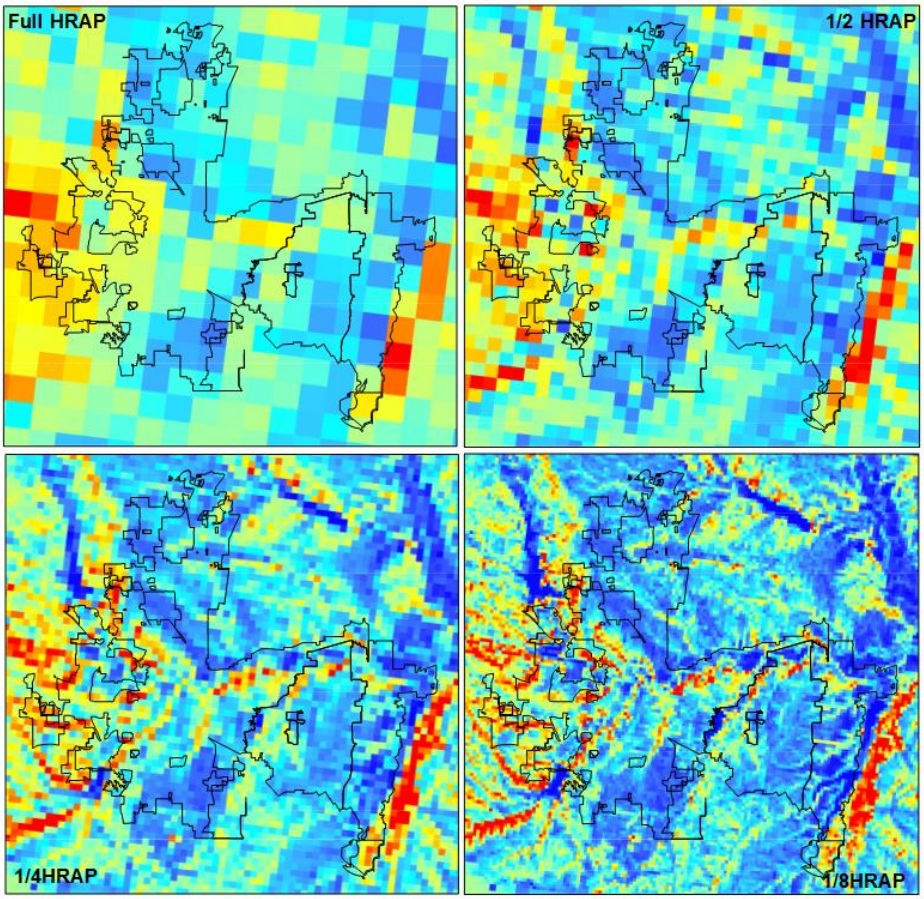

Figure 5 Maps of specific discharge at different spatial resolutions over the model domain: 4 km (upper-left), 2 km (upper-right), 1 km (lower-left) and 500 m (lower-right)

Threshold Frequency (TF) component of HL-RDHM (NWS 2009) expresses the streamflow map in terms of return periods which most engineers are familiar with. The idea of using threshold frequencies along with distributed hydrologic models (DHM-TF) for flash flood forecasting is discussed in detail by Reed et al. (2007).

HL-RDHM uses the Bulletin 17B method (log-pearson Type III frequency distribution) suggested by the Water Resources Council (1982) (http://water.usgs.gov/osw/bulletin17b/bulletin_17B.html) to compute the probability that a computed discharge will exceed the annual maximum discharge in any given year. The routines to compute map skew for the Bulletin 17B method were taken directly from the PeakFQ software distributed by the USGS. In implementing the Bulletin 17B method, the low outlier test is included, but not the high outlier test.

To calculate the annual maximum peak discharges for each cell in any year, HL–RDHM was run at a spatiotemporal resolution of 1 HRAP and 1 hour using the historical MPE data from 1996 to 2014 and a grid of annual maximum peaks at the end of each water year stored. Figure 6 shows annual maximum discharge for years 2000, 2005, 2010 and 2014.

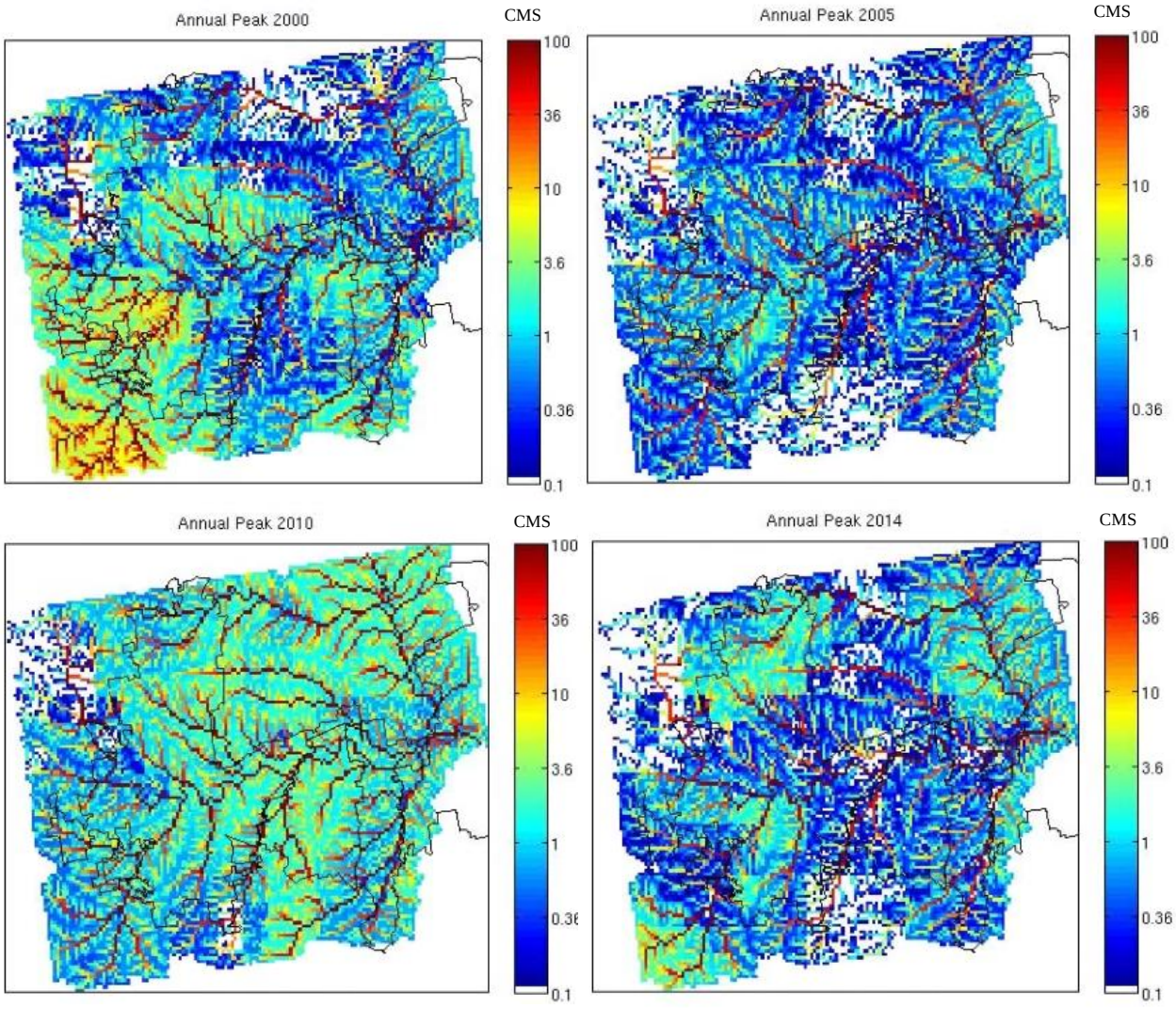

Figure 6 Annual maximum discharge for years 2000, 2005, 2010 and 2014.

Chapter 3

Integrated modeling of natural channel and storm drain and networks for real-time flash flood forecasting

3.1 Introduction

Flash flood events are one of the most significant natural hazards. They often cause loss of life and economic damages (Gaume et al. 2009). As stated in the US Flood Loss Report provided by the NWS, during the past 30-year period, flood losses averaged about $7.86 billion in damages with 82 fatalities per year. According to Dittman (1994), on average, there were 119 flood deaths per year in the United States.

Urban flooding has become a larger threat due to population growth, urbanization and climate change. According to the US Census Bureau, the United State population has been increasing since 1900. As a result of rapid population growth, migration from rural areas to cities increases which leads to intense urbanization that often increases flood risk (Chang and Franczyk, 2008). Changes in urban runoff volume and flood peaks have historically been blamed on increases in impervious area. The impervious surface increases the amount of surface runoff in relation to infiltration, and therefore increase the total volume of water in streams during or soon after the rain. Surface runoff travels quicker over impervious areas

and through sewers than it does in natural streams. This means that the flow will both arrive and die away faster, and therefore the peak flow will be greater (Butler et al., 2004). There are many studies which show urbanization is a major cause of amplified peak flow and increased flood risk (Changnon and Demissie, 1996; Brun and Band, 2000; Smith et al., 2002; Rosso and Rulli, 2002; Ott and Uhlenbrook, 2004; Zhu et al., 2007; Wheater and Evans, 2009).

According to recent studies, global warming, one of the main cause of hydrologic regime change, can induce the acceleration of the hydrologic cycle (Huntington, 2006 and Oki and Kanae, 2006), which can consequently impact frequency and intensity of rainfall events (Arnell, 2003; Hamlet and Lettenmaier, 2007; Milly et al., 2008). The United States Environmental Protection Agency (EPA) reported that in recent years, a larger percentage of precipitation has come in the form of intense single-day events (see Figure 1). The extreme single-day precipitation events remained fairly steady between 1910 and the 1980s, but has risen substantially since then. Over the entire period from 1910 to 2014, the portion of the country experiencing extreme single-day precipitation events increased at a rate of about half a percentage point per decade (EPA, 2015).

Therefore, increasing occurrences of extreme precipitation in urban areas with high population density and large fractions of impervious surfaces leave such areas in an increasingly vulnerable position where even a small scale but intense

rainfall event can cause deadly flash floods and extensive damages. Given the high population density, high-resolution observation and modeling capabilities are necessary for prediction of flash floods in urban areas.

To mitigate hazards and to reduce negative impacts of flooding, urban municipalities operate storm drain networks of varying capacity and complexity. Whereas the conveyance capacities of storm drain systems are generally much smaller than those of the natural channel systems (Rafieeinasab et al. 2015), storm drain networks may significantly alter the severity of flooding hazards and other impacts depending on the location of flooding and the magnitude of rainfall. To produce accurate predictions in urban areas, it is necessary to model not only the natural channel systems but also the large and complex networks of storm drains, which may contain thousands of pipes and open channels. Such capability is also important for planning and management of stormwater infrastructure which has traditionally been designed on a site-by-site basis with the goal of keeping the post-development peak flow from flooding events the same as before. Such an approach, however, does not reduce the runoff or the total volume of stormwater and may still produce flooding downstream as a result. Also, with site-by-site design, it is not possible to fully account for spatiotemporal variations of runoff and flow through natural and man-made hydraulic systems or spatiotemporal variability of precipitation beyond the site scale. Accordingly, the resulting stormwater system may not work effectively at larger watershed scales. Indeed, McCuen (1979) and

Emerson et al. (2005) showed that an unplanned system of site-based stormwater control measures or best management practices can actually increase flooding on a watershed scale owing to the effect of many facilities discharging into a receiving waterbody in an uncoordinated fashion - causing the very flooding problem the individual basins were built to solve (NRC 2008). The ability to model jointly the natural channel and storm drain systems for large urban areas also allows objective assessment of performance of stormwater infrastructure from transient shocks of extreme precipitation under changing conditions. Many researchers have assessed the impacts of climate change on urban drainage systems and analyzed the specific impacts on different small urban areas (e.g., Niemczynowicz 1989; Watt et al. 2003; Mailhot et al. 2006a; Guo 2006; Denault et al. 2006). Studies show that an increase in the intensity and frequency of extreme rainfall events may increase sewer overflows and urban flooding (Mailhot et al. 2006; Ashley et al. 2005). While the results vary depending on the urban catchment's response to extreme rainfalls, most conclude that the probability of surcharge and hence flooding increases in urban area. There hence exists a critical need in stormwater planning and management in large urban areas for a capability to assess how large storm drain networks may respond to extreme rainfalls under changing land cover conditions and climate change. Integrated modeling of flow through natural channels and storm drains for small urban areas is not new. Approaches such as 1D storm drain-2D surface flow modeling (Leandro et al. 2009) have gained wide popularity and

acceptance in recent years. For real-time applications over large areas, however, such approaches quickly become untenable because of complexities in modeling and extremely large computational requirements.

There are many urban hydraulic models of varying sophistication such as HEC-1 (U.S. Army Corps of Engineers 1985), TR-20 and TR-55 (Soil Conservation Service 1983, 1986), MOUSE (Danish Hydraulic Institute 1995), HydroWorks (HR Wallingford Ltd. 1997), and storm water management model (SWMM) (Huber and Dickinson 1988) but most of them are not practical for real-time applications of large metropolitan areas because of complexity and computational cost.

SWMM has been applied in numerous watersheds in United States cities and other part of the world (Selvalingam et al. 1987; Warwick and Tadepalli 1991; Bhaduri et al. 2001). It has been applied to all types of storm water management from urban drainage (Zaghloul 1998; Campbell and Sullivan 2002) to flood routing (Hsu et al. 2000). Nazari et al. (2014) used PCSWMM to model storm drains explicitly in two small inundation-prone catchments in the City of Fort Worth which took several months to make the model.

On the other hand, distributed hydrologic models which develop for real time applications of large urban areas cannot simulate storm drains explicitly. As reported by Rafieenasab et al. (2015), for hydrologic modeling of large areas,

explicit modeling of storm drains is a large challenge. Many efforts have been made to couple hydrologic and hydraulic models for flood modeling purposes. Nguyen et al. (2015) used Hydrology Research Distributed Hydrologic Model (HL-RDHM, 2009) as a rainfall-runoff generator and replaced the routing scheme of HL-RDHM with the 2D hydraulic model (BreZo) to develop a high resolution coupled hydrologic-hydraulic model for flash flood modeling at a river scale. Bonnifait et al. (2009) coupled TOPMODEL with a 1D hydraulic model named CARIMA for reconstructing the catastrophic flood event in the Gard region, France. Kim et al. (2012) developed an integrated model of the Triangulated Irregular Network-Real Time Integrated Basin Simulator (tRIBS) with an Overland Flow Model (OFM) for a watershed of 64 km^2 located in Oklahama, USA. In large scale basin, Biancamaria et al. (2009) developed a coupled hydrologic–hydraulic framework of the interactions between Soil-Biosphere–Atmosphere (ISBA) and LISFLOOD-FP (Neal et al., 2012) for the Ob River in Siberia. In a recent study, the widely used Variable Infiltration Capacity (VIC, Liang et al., 1994) was coupled with LISFLOOD-FP for forecasting daily flood inundation in large scale for the Lower Zambezi River (Schumann et al., 2013). Habibi et al. (2015) developed a prototype high-resolution flash flood prediction system for urban area using a high resolution modeling and precipitation data but their hydrologic model does not simulate storm drains, the results may not be realistic due to large collective capacity of storm drain network within their study area. So, the inability to explicitly simulate storm

drainage networks is seen as a major limitation in the application of distributed hydrology models.

As distributed hydrologic modeling with high resolution X-band radar rainfall products is already operational in real-time (Habibi et al., 2016), it would be highly beneficial to develop a storm drain module that can be implemented with the distributed hydrologic model, in order to produce accurate flash flood predictions. Therefore, in this study, an integrated model is developed that can simulate flow through both natural channels and storm drains for large urban areas in real time to addresses a critical gap in stormwater management and planning and to advance the knowledge and understanding of how the coupled system responds to extreme rainfall under changing land cover conditions due to urbanization. The following questions are aimed to address:

- How to partition surface runoff into pipe and natural channel systems? What are the largest sources of uncertainty?
- How to reduce the geometric complexity of a storm drain network into a simpler "equivalent" network?
- How does the storm drain network alter the hydrologic response of urban catchments? How does the response vary according to the size of the catchment, land cover and the magnitude of the storm?

- What is the relative importance of natural channels and storm drains in stormwater management and flood control at different spatiotemporal scales in large urban areas?

This chapter is organized as follows. Section 2 describes the approach, study area and data used. Section 3 describes the method developed and used. Section 4 presents the results. Section 5 presents the conclusions and future research recommendations.

3.2 Approach, study area and data used

In this section, the general approach to integrated modeling of storm drain and natural channel networks, the study area and the data used are described.

3.2.1 Approach

The general approach taken in this work for integrated modeling of natural channel and storm drain flows is to develop a modular storm drain module that can be readily interfaced with existing gridded distribute models with minimum changes to the latter. In this work, the U.S. National Weather Service's (NWS) Hydrology Laboratory Research Distributed Hydrologic Model (HLRDHM) (HLRDHM 2009; Koren et al., 2004) as the parent model is used. HLRDHM has been used in many research and operational applications (Habibi et al., 2016;

Moreda et al., 2006; Reed et al., 2007) and is recognized as one of the best performing distributed hydrologic models (Reed et al. 2004; Smith et al. 2012, 2004; Moreda et al. 2006). HLRDHM is based on regular rectangular grids in the Hydrologic Rainfall Analysis Project (HRAP) projection (Greene and Hudlow 1982). The HRAP grid has a 4 km×4 km resolution onto which the WSR-88D precipitation products (Klazura and Imy 1993) are mapped. The model can also support higher resolution grids such as 500m×500m (1/8 HRAP), and 250m×250m (1/16 HRAP), etc. The HLRDHM uses the Sacramento Soil Moisture Accounting Model (SAC-SMA) (Burnash et al., 1973) to simulate soil moisture, actual evapotranspiration and surface flow at each grid cell, and kinematic wave (Chow et al. 1988, Koren et al. 2004) for hillslope and a channel routing. Fast responses such as overland flow and direct runoff are routed at each cell through conceptual hillslope which drains into conceptual channel within the same grid cell. The slow responses such as interflow and baseflow are assumed to drain directly into the conceptual channel without being routed through hillslope.

In developing the storm drain module, modularity, simplicity and computational efficiency are of great importance to allow easy integration with any distributed models that employ gridded hillslope and channel routing. By operating the storm drain module on the same grid as the parent model, one only has to partition runoff into the natural channel and the storm drain at each grid box, route the natural channel and storm drain flows separately, and discharge the storm drain

flow into the natural channel at outfalls. In this way, adding the storm drain module to the gridded distributed model amounts only to adding a sink in hillslope routing if the grid box contains inlets and a source in channel routing if the grid box contains an outfall(s). The following approach is taken to storm drain modeling with HLRDHM. While the details described in this work are specific to the HLRDHM, the storm drain module may be integrated with any distributed model that has gridded hillslope and channel routing.

1) Determine the model resolution,
2) Derive the equivalent storm drain network from the actual storm drain network to the resolution of the HLRDHM, i.e., the parent gridded distributed hydrologic model,
3) For each time step, run SAC to determine surface and subsurface runoff for all grid cells,
4) For each time step, partition the surface runoff between the equivalent storm drain network and the natural channel network for all grid cells,
5) For each time step, route the storm drain flow through the equivalent storm drain network and discharge into the natural channels at outfall-containing grid cells,
6) For each time step, route the natural channel flow through the natural channel network, and
7) Repeat Steps 3 through 6 for all time steps.

3.2.2 Study area

The study area includes five urban catchments in the Cities of Arlington and Grand Prairie (U.S.). The five catchments have a combined area of about 144.6 km^2. Their size and time-to-peak at the outlet vary significantly from 3.4 to 54.6 km^2 and from 0.5 to 2.5 hrs, respectively (Rafieeinasab et al. 2015). Figure 7 shows the area map with the location of the radars and catchments boundaries, and Figure 8 shows the storm drain network in the study area along with topography. Table 3 provides a summary of basin's characteristics. Percentage impervious cover in thease basins varies from 31% in the least development to 58% in the most urbanized basin.

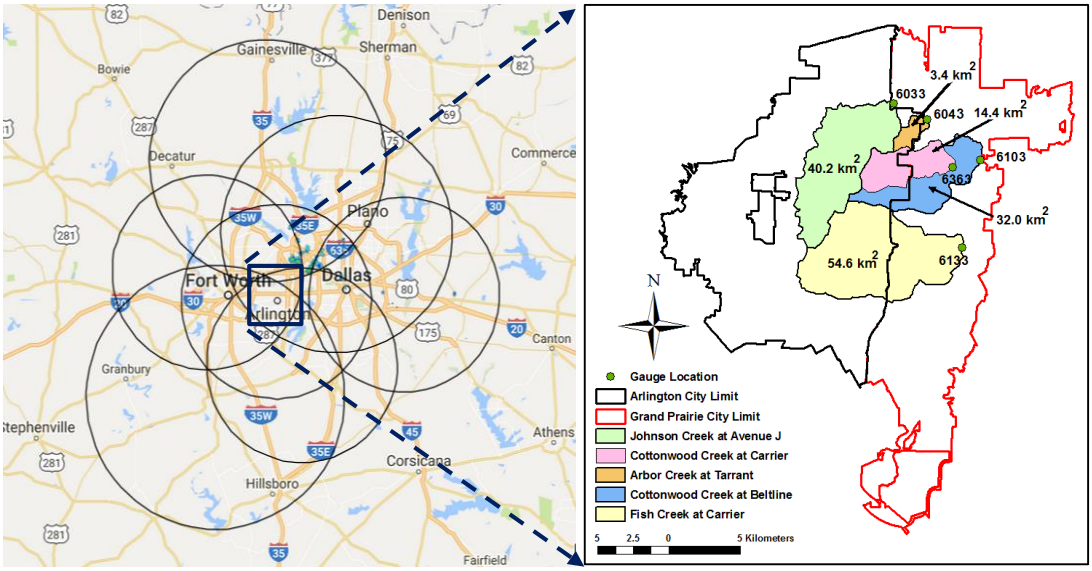

Figure 7 Location of the radars and catchments boundaries in the Cities of Arlington and Grand Prairie

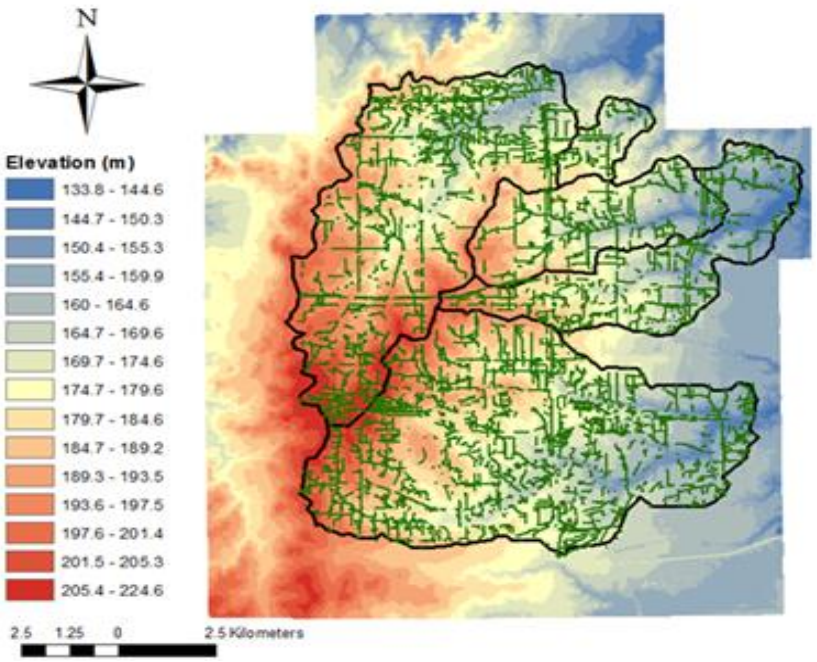

Figure 8 Storm drain network in the study area along with topography

The above model domain is large by stormwater modeling standards but represents only a small fraction of the large cities in DFW. The Cities of Dallas, Fort Worth, Arlington and Grand Prairie, which comprise the mid-section of DFW, have areas of 999.3, 904.4, 258.2 and 210.0 km^2, respectively. These four cities have a combined area of about 2,371.9 km^2 (Figure 9). The storm drain module sought in this work is able to operate over such large areas.

Table 3 Summary of catchments characteristics

Catchment Name	ID	Drainage Area (km^2)	Imperviousness (%)
Fish Creek at Carrier	6133	54.6	31
Johnson Creek	6033	40.2	48
Cottonwood Creek at Beltline	6103	32	37
Cottonwood Creek at Carrier	6363	14.4	40
Arbor Creek at Tarrent	6043	3.4	58

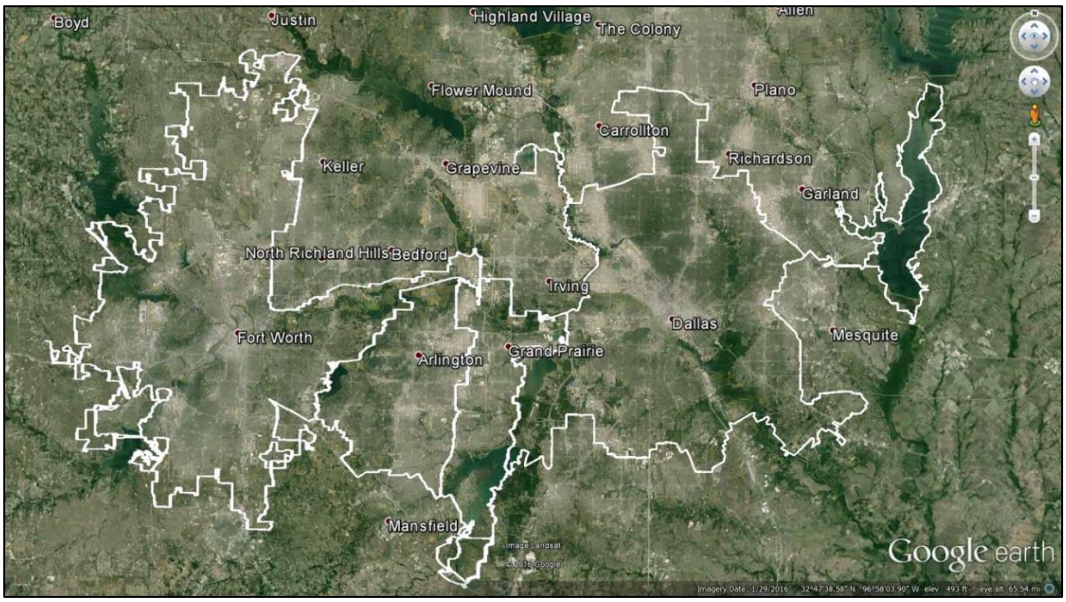

Figure 9 Fort Worth, Arlington, Grand Prairie and Dallas

3.2.3 Data used

The storm drain data used in this work are provided by the Cities of Arlington and Grand Prairie. The data includes information about pipes lines, inlets, outfalls and junctions. Figure 10 shows the storm drain data within the five catchments. There are 1200 outfalls and 11600 inlets in the study area. Slope and diameter for some pipes are missing in the storm drain database provided by the Cities of Arlington and Grand Prairie. Missing information were estimated according to the following rules. If the pipe diameter is unknown, the pipe size was selected based on the standard pipe size chart and the sizes of the up- and downstream pipes. If the slope of the pipe was unknown, the ground slope was used.

HL-RDHM is utilized for rainfall-runoff modeling and natural channels routing. The spatial resolution of the model was set to 1/16 HRAP (250 m * 250 m) which is the highest spatial resolution available in HL-RDHM. A priori grids of the SAC-SMA (11 parameters listed in Table 1) and kinematic-wave routing parameters (specific discharge and exponent in the power-law relationship describe in section 2.3) are derived at 1/16 HRAP resolution and used in this work. Figure 11 shows percent impervious area maps (PCTIM in Table 1) over the five catchments at 250 m resolution, which is derived based on the information listed in Table 2.

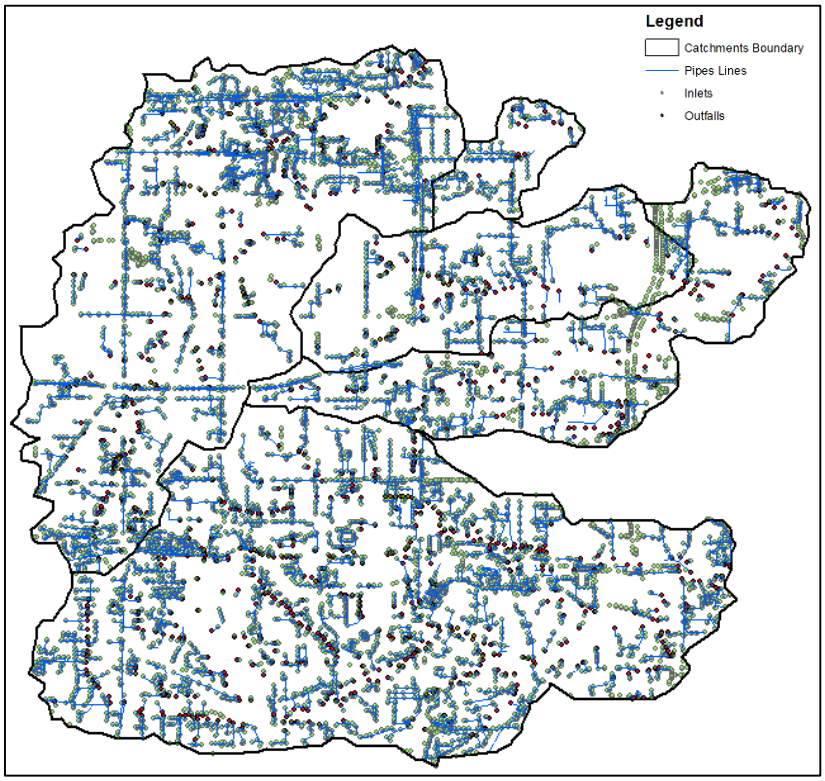

Figure 10 Storm drain data within the five catchments.

Also the street fraction within the selected resolution are derived using the street GIS layers (Figure 12) that ranges from 0 to 0.4.

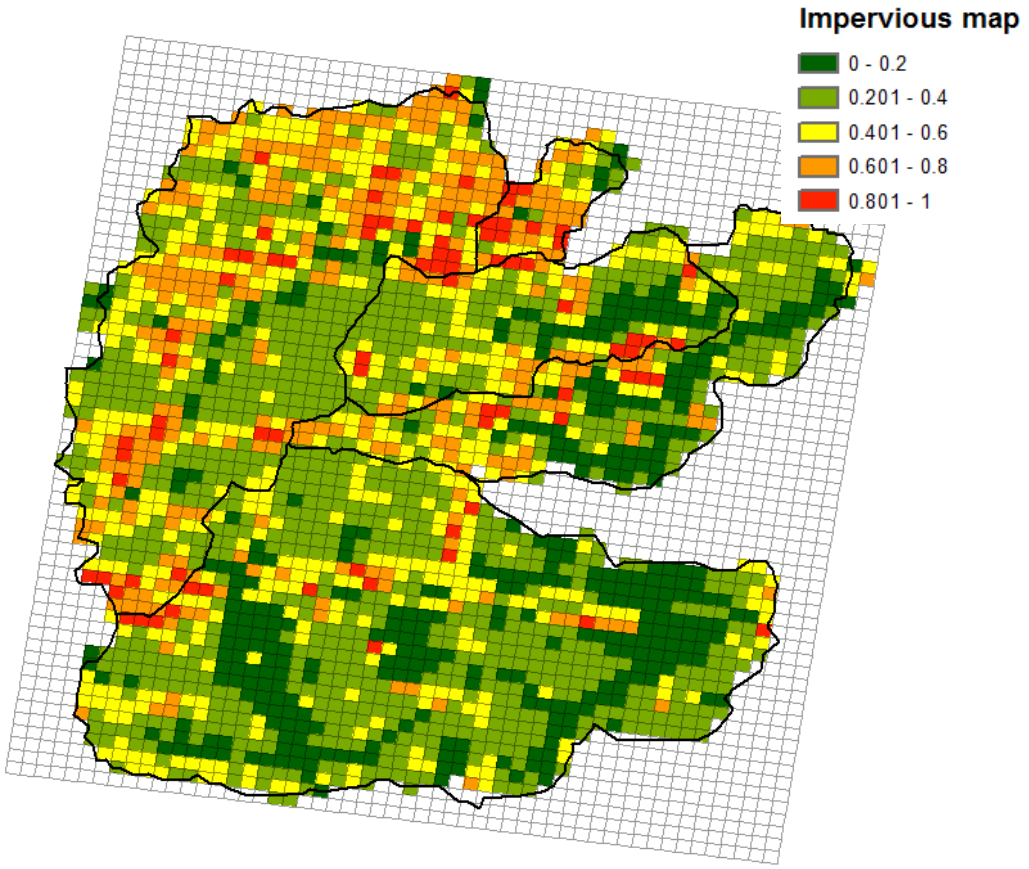

Figure 11 Impervious cover within the five catchments at 1/16 HRAP resolution

High spatiotemporal resolution QPE is one of the essential requirements for the prediction of urban flash floods, which are usually associated with heavy rainfall over a short period of time. The DFW Demonstration Network of the Collaborative Adaptive Sensing of the Atmosphere (CASA) program which

consists of a combination of high resolution X band radars and a standard National Weather Service (NWS) Next-Generation Radar (NEXRAD) system operating at S band frequency provides high spatiotemporal-resolution quantitative precipitation estimates (QPE, Chen and Chandrasekar, 2015).

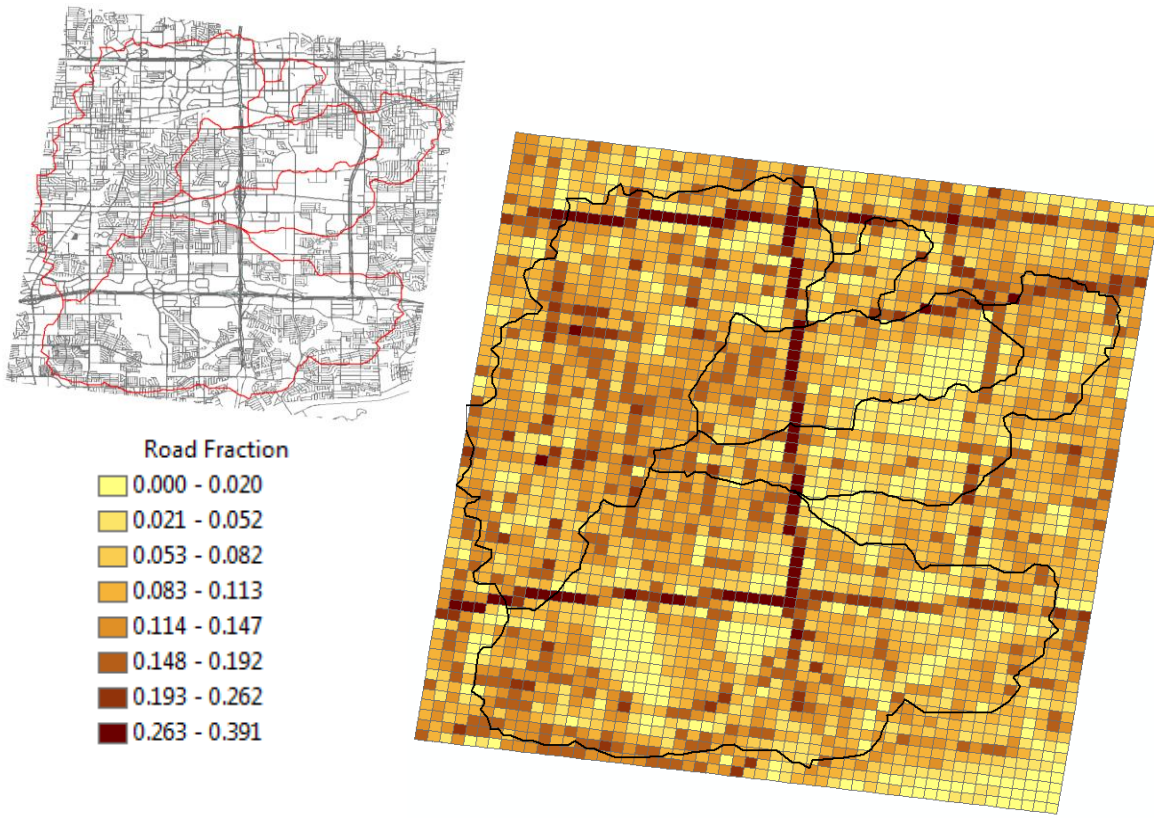

Figure 12 Road fraction over the study area at 1/16 HRAP resolution

The spatiotemporal resolution of this product is 500 m and 1 minute. Recently, comparative evaluation of different radar-based QPE products was carried out based on a limited period of record of about a year (Rafieeinasab et al.

2014, 2015). The results show that, in general, the CASA QPE is more accurate for larger precipitation amounts whereas the Multisensor Precipitation Estimator (MPE, Seo et al. 2010) estimates are more accurate for smaller amounts in the study area.

To evaluate the performance of the integrated model, streamflow simulations with the observations are compared. For the study basins, observed water level from pressure transducer sensors are available every 15 min from the High Water Warning System (HWWS) owned and operated by the Cities of Arlington and Grand Prairie. These observations were used previously to validate streamflow simulations (Rafieeinasab et al., 2015a) using rating curves derived via 1-D steady state non-uniform hydraulic modeling (Kean and Smith 2005, 2010; Norouzi et al., 2015). Also, UTA in collaboration with University of Michigan will deploy 13 additional water level and water quality sensors at multiple locations (8, 2, and 3 sensors at the Cities of Fort Worth, Arlington and Grand Prairie, respectively) within the study area (Figure 13). Additional data will be gathered via crowdsourcing in near real-time and post-event observations of flooding. For that, an application named iseeFlood developed for cell phones which simulation results will be verified using the reports received during extreme events.

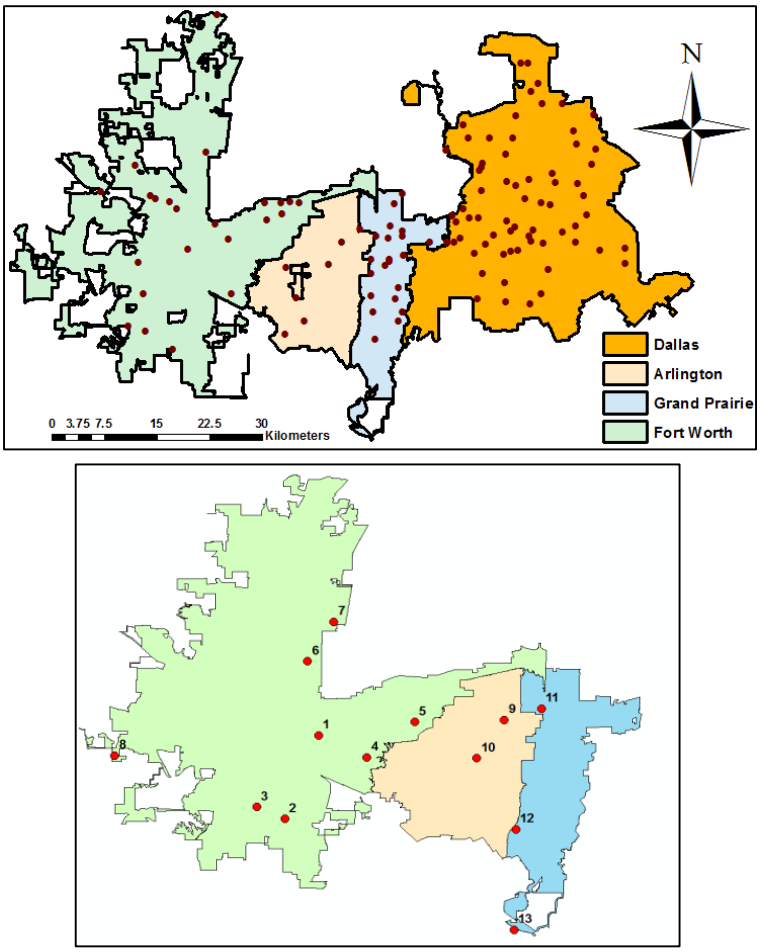

Figure 13 High Water Warning Systems (HWWS) locations owned by the cities (upper panel) and 13 additional water level and quality sensors (lower panel)

3.3 Integrated modeling of natural channel and storm drain networks

The rainfall-runoff model, SAC, in HLRDHM produces surface and subsurface runoff. Surface runoff is routed over conceptual hillslopes. Part of routed overland flow drains into pipe network if there is sufficient capacity in the storm drain network and the rest enters the channel network. Subsurface runoff is

assumed to enter the natural channel system directly from the soil. Flow in the storm drain network moves toward downstream and enters natural channel system at outfall locations and the combined flow is routed through the natural channels toward the catchment outlet. Figure 14 represents the flowchart of one-way interaction between storm drain and channel routing module in HL-RDHM. In this figure, existing and new processes are shown with black and green arrows, respectively.

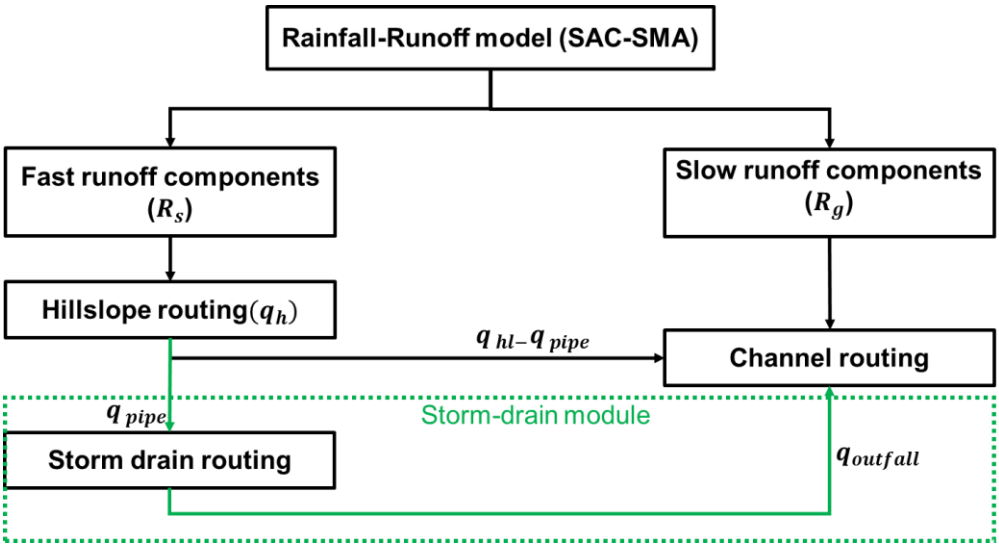

Figure 14 Storm drain and natural channel routing module in HL-RDHM.

In the HLRDHM, the water depth over the conceptual hillslopes in each grid cell is modeled via kinematic wave routing as follows:

$$\frac{\partial h}{\partial t} + L_h \frac{\partial q_{L_h}}{\partial x} = R_s \tag{6}$$

$$q_{L_h} = \frac{1}{L_h}\frac{1}{n}h^{5/3}S^{1/2} = 2D\frac{1}{n}h^{5/3}S^{1/2} \quad (7)$$

where h denotes the water depth on the hillslopes (m), R_s denotes the surface runoff rate (m/s), q_{L_h} denotes the total discharge per unit area from all hillslopes in the grid box (m/s), L_h denotes the hillslope length (m) given by the area of a grid cell (m^2) divided by the total width of the hillslopes over which surface flow occurs (m), S is the slope of the hillslopes (dimensionless), n is the hillslope manning's roughness coefficient ($s/m^{1/3}$), D is the drainage density (m^{-1}), and t denotes time (s). The identity of $1/L_h=2D$ in Eq.(7) stems from the assumed symmetry in the conceptual hillslopes which drain into the natural channel that runs through the middle of the grid box. For further details, the reader is referred to Koren et al. (2014).

With the inclusion of storm drain flow, the channel routing model of HLRDHM can be expressed as:

$$\frac{\partial A}{\partial t} + \frac{\partial Q}{\partial x} = \frac{(R_g + q_{L_h})f_c}{L_c} - \frac{Q_{inlet}}{L_c} + \frac{Q_{outfall}}{L_c} \quad (8)$$

$$Q = Q_s A^m \quad (9)$$

Where A is the wetted cross section of the natural channel (m^2), Q is discharge (m^3/s), R_g is slow runoff component (subsuface runoff rate from SAC), q_{L_h} is routed overland flow rate per unit area at the hillslope (m/s), f_c is a grid cell

area (m^2), L_c is a channel length within a cell, q_{inlet} denotes the total flow into the storm drains per unit area within the grid box (m/s), $q_{outfall}$ denotes the total flow through all outfalls per unit arae within the grid box (m^3/s), m is an exponent parameter, and Q_s is specific discharge (m/s). In Eq.(8), q_{inlet} in each grid cell cannot exceed the total flow (q_{L_h}) generated from the hillslope at that grid cell or the total flow generated from the pavement area of the grid cell, Q_{pvmt} (see Subsection 3.3.1), i.e., $Q_{inlet} \le \min\{q_{L_h} f_c, Q_{pvmt}\}$.

A priori grids of Q_s and m are available from the NWS for the U.S. based on the 30-m resolution National Elevation Dataset (NED) from the NHDPlus Version 2 (NHDPlusV2, David et al. 2011). The cell-to-cell connectivity is derived with the Cell Outlet Tracing with an Area Threshold algorithm (Reed, 2003) which is used to transfer water from upstream to downstream cells and to the basin outlets. In this work, the routing model parameters and the channel connectivity are rederived at 1/16 HRAP resolution using the NWS-developed programs. Figure 15 shows the resulting natural channel network and flow direction for the study area. Note that, with Eq.(8), storm drain modeling amounts to modeling time-varying Q_{inlet} and $Q_{outfall}$ at all grid boxes which is described below.

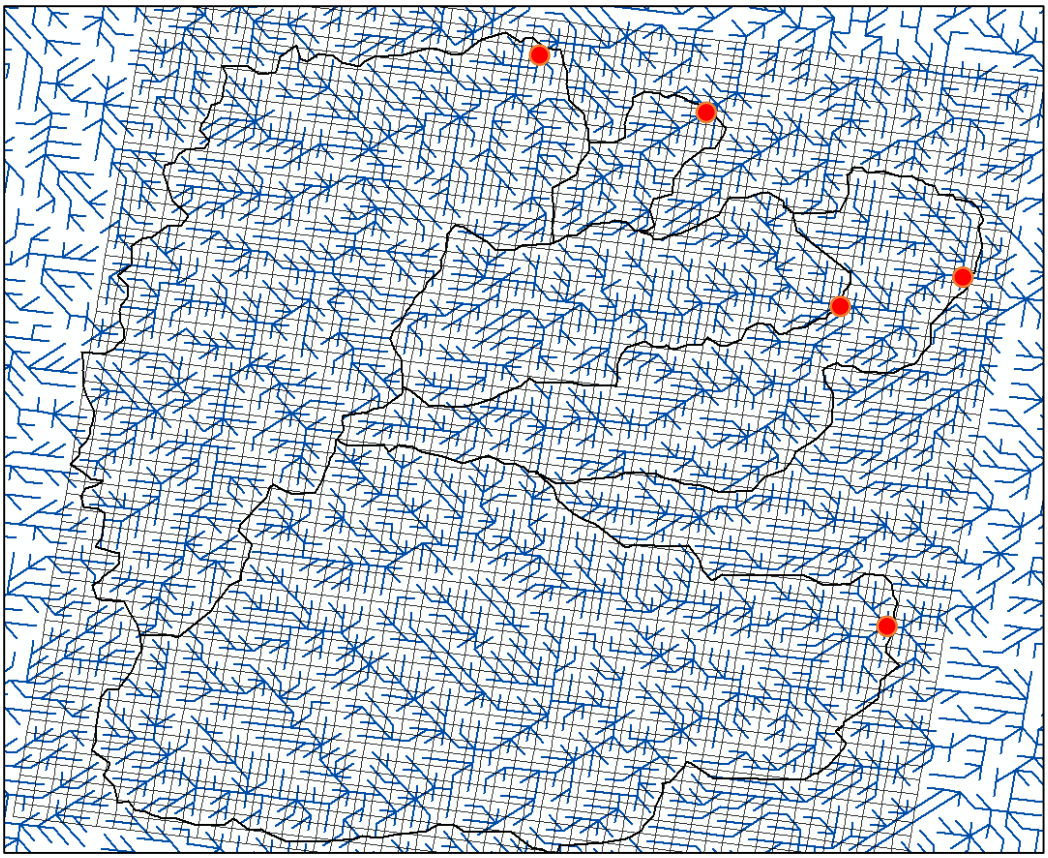

Figure 15 Natural channel network and flow direction for the study area (the red dots are the outlet of the catchments)

3.3.1 Flow into storm drains

Flow into the equivalent storm drain network is determined by modeling inlet flows under the following assumptions: 1) runoff generated on the inlet-bearing roadways drains first into the equivalent storm drain network unless the storm drain network is full, 2) if the storm drain network is full, the runoff drains into the natural channel in that grid box, and 3) all inlets in the same grid box share the same capacity. There are four types of inlets typically used for urban drainage:

curb, grate, linear drains and combination (of curb opening and grate) inlets (Akan and Houghtalen 2003, TxDOT 2016). In the study area, curb opening inlets dominate and it is hence assumed that all inlets are of this type (Figure 16).

Inflow through a curb opening inlet depends on the water depth at the inlet opening and the height of the opening. If the depth of flow in the gutter is less than or equal to 1.4 times the height of the inlet opening, the inlet is assumed to operate as a weir (TxDOT 2016). If there are N inlets in the grid cell, the total flow into the equivalent storm drain network at that grid box is given by:

$$Q_{inlet} = NC_w L_w y^{3/2} \qquad if \qquad y \leq 1.4d \tag{10}$$

Where Q_{inlet} denotes the flow into the equivalent storm drain network (m^3/s), C_w denotes the weir coefficient of 1.6 ($m^{0.5}/s$), L_w denotes the length of the curb inlet opening (m), y denotes the water depth at the inlet opening (m), and d denotes the height of the inlet opening (m). If y > d, the inlet is assumed to operate as an orifice. The total flow through N such orifices is given by:

$$Q_{inlet} = NC_o dL_o \sqrt{2gy} \qquad if \qquad y > d \tag{11}$$

Where C_o denotes the orifice coefficient of 0.67, L_o denotes the length of the orifice (m), and g denotes the gravitational acceleration ($m.s^{-2}$). At depths between 1.0 and 1.4 times the opening height, flow is in a transition stage and is determined based on the smaller of the weir and orifice flows.

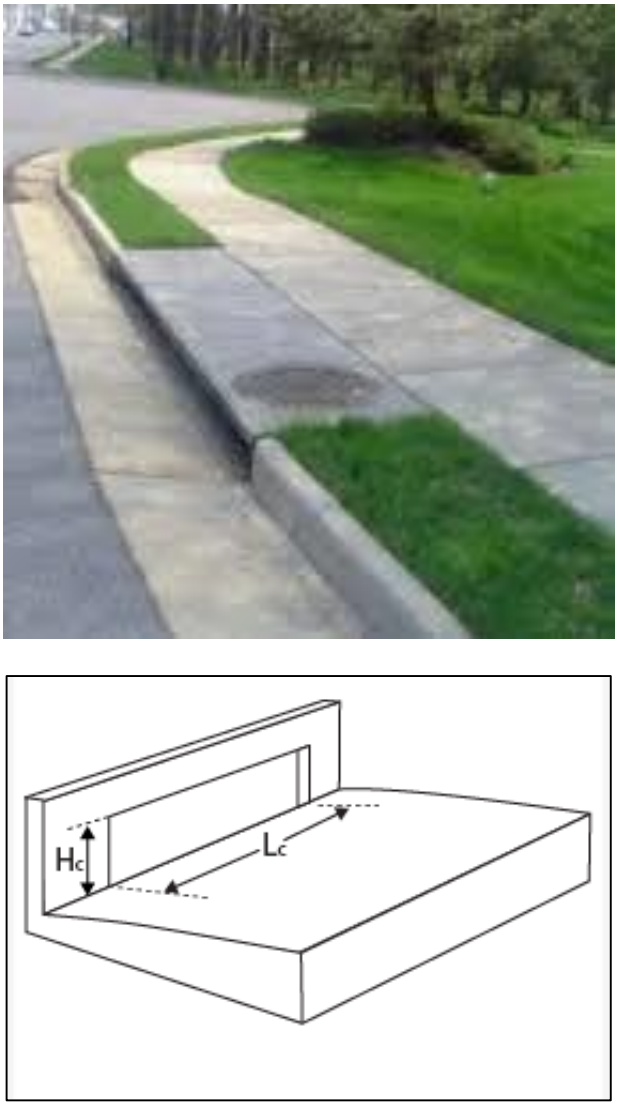

Figure 16 Curb inlet

To determine y, water depth on the pavement in each grid box is modeled using kinematic wave routing analogous to that for hillslope routing in Eqs.(6) and (7):

$$\frac{\partial h_{pvmt}}{\partial t} + L_{pvmt}\frac{\partial q_{pvmt}}{\partial x} = i \tag{11}$$

$$q_{pvmt} = \frac{1}{L_{pvmt}}\frac{1}{n_{pvmt}} h_{pvmt}^{5/3} S^{1/2} \tag{12}$$

Where h_{pvmt} denotes the water depth on the pavement (m), i denotes the rain rate for the grid cell (m/s), q_{pvmt} denotes the flow on the pavement per unit area (m/s), L_{pvmt} denotes the pavement length (m) assumed to be $\sqrt{f_c}$ (m), and n_{pvmt} denotes the Manning's roughness coefficient for the pavement. The water depth on the pavement, h_{pvmt}, is used for y in Eqs.(10) and (11). If Q_{inlet} is smaller than the total hillslope flow into the channel, $q_{L_h} f_c$, the remaining flow $q_{L_h} f_c - Q_{inlet}$ is assumed to drain into the natural channel as shown in Eq.(8). In a highly unlikely case of $Q_{inlet} > q_{L_h} f_c$, Q_{inlet} is set to $q_{L_h} f_c$ as indicated in Eq.(8). In reality, the curb-opening inlets intercept gutter flow whereas Eqs.(11) and (12) model sheet flow. Also, a number of parameters in the routing and inlet flow models is subject to significant uncertainty. To assess the uncertainties associated with partitioning surface runoff into flow into the storm drain network and that into the natural channels as well as to establish the bounds of the above partitioning, a systematic sensitivity analysis is carried out with respect to a limited number of model parameters (see Subsection 4.4).

3.3.2 Storm drain flow modeling

Flow through the equivalent storm drain network is modeled based on simplification of the continuity and momentum equations under the kinematic wave assumption:

$$dV / dt = Q_{in} - Q_{out} \tag{13}$$

$$S_f = S_0 \tag{14}$$

Where V denotes the volume of water in the pipe (m^3), Q_{in} denotes the inflow rate (m^3/s) and Q_{out} denotes the outflow rate (m^3/s). If the upstream of the pipe represents an inlet(s), $Q_{in}=Q_{inlet}$. If the downstream of the pipe represents an outfall(s), $Q_{out}=Q_{outfall}$. The above simplification is valid if the variations in the hydrograph are gradual enough to result in a quasi-steady flow for each pipe (Motiee et al., 1996) and if the pipe is not surcharged. The momentum equation can be expressed via the Manning's equation as:

$$A_p = \left(\frac{n_p \, P_p^{\,2/3}}{\sqrt{S_0}}\right)^{\frac{3}{5}} Q_{out}^{\frac{3}{5}} \tag{15}$$

Where A_p denotes the wetted cross-sectional area of the pipe (m^2), n_p denotes the Manning coefficient for the pipe, P_p denotes the wetted perimeter of the pipe (m), and S_0 denotes the slope of the pipe. In Eq.(15), A_p and P_p are computed from the downstream water depth.

The reader is reffered to Appendix F for the source code of storm drain flow modeling. Figure 17 shows the flowchart of the integrated model operation. Note that, while multiple elements have been newly added as described above, the only change necessary to the HLRDHM code is adding the source and sink terms in Eq.(8).

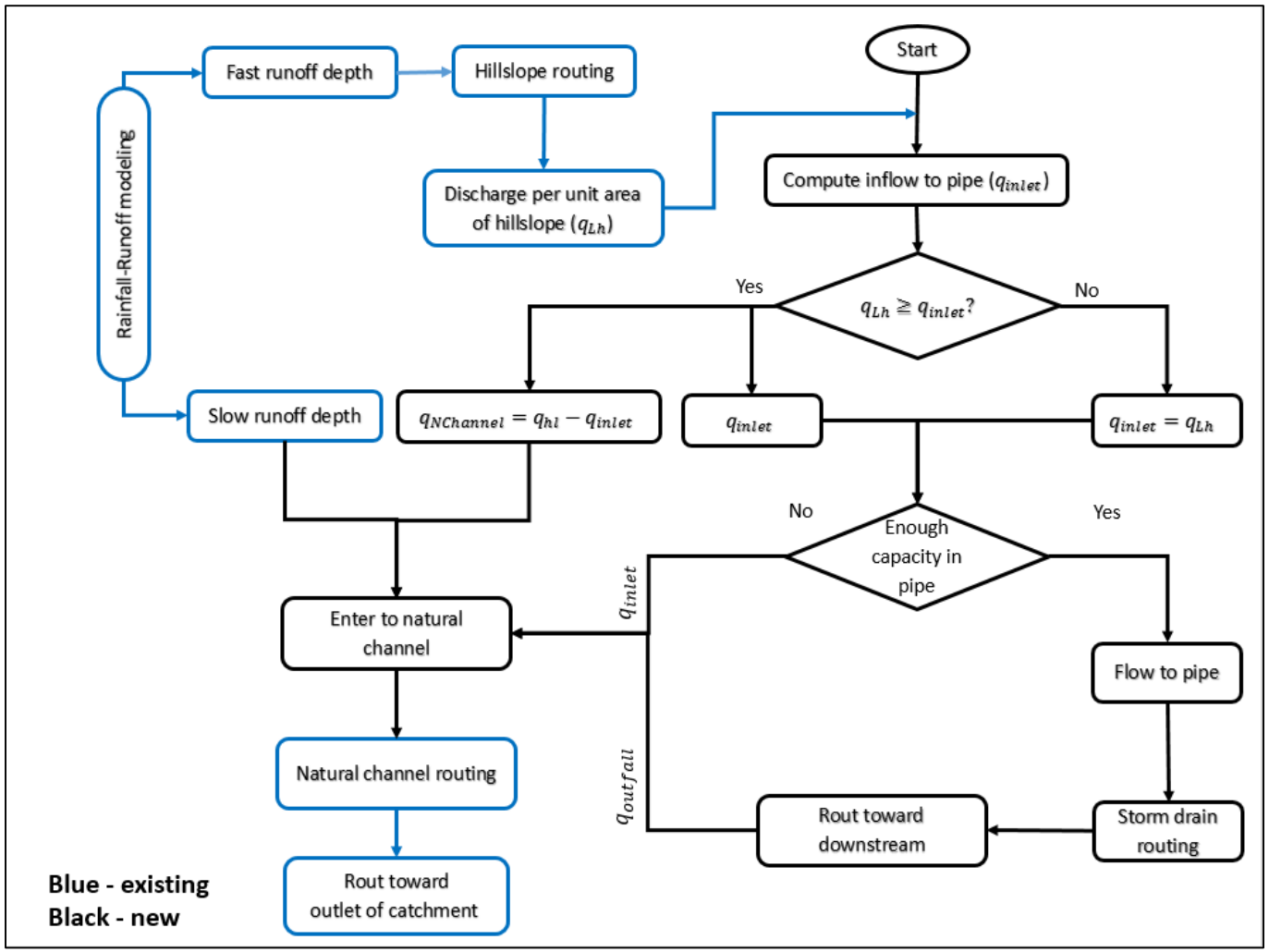

Figure 17 Flowchart of the integrated model operation

Chapter 4

Equivalent storm drain network

Large urban areas contain large and complex storm drainage networks and it is not practical to model all of them. For example, there are over 100,000 pipes and open channels within the Dallas-Fort Worth (DFW) metropolitan area (Figure 18). The purpose of equivalent storm drain network is to represent the real network with a hydraulically equivalent virtual network that has as closely as possible a single virtual pipe in each grid box.

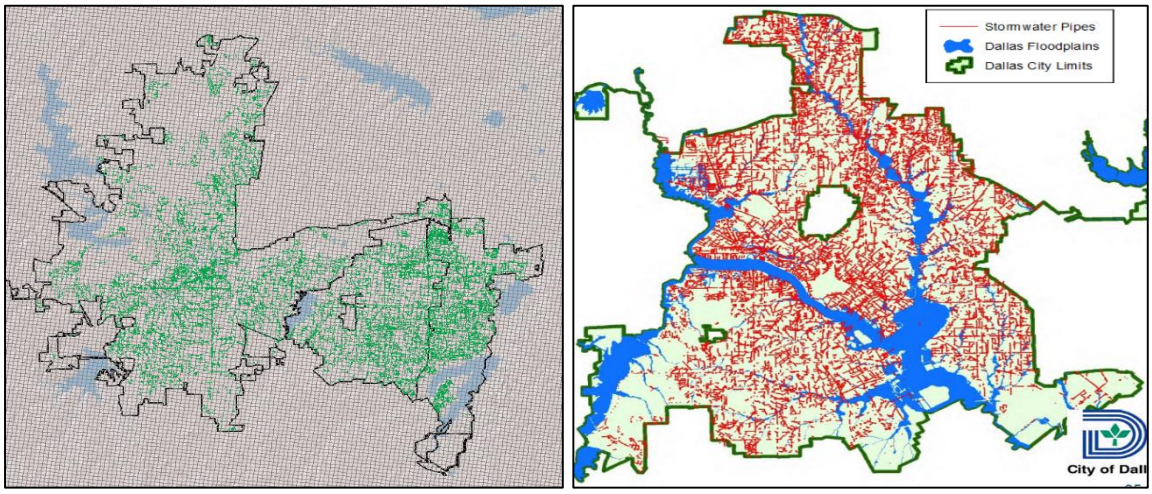

Figure 18 Storm drain networks in DFW area

In this way, one may link the storm drain module to the gridded distributed model only by adding sink and source terms in the existing channel routing model as shown in Eq.(8). Deriving the equivalent storm drain network amounts to

coarsening the real storm drain network such that the former approximates the mass and momentum balance of the latter with acceptable accuracy. Pipe networks generally consist of series and parallel pipes. All such configurations may be combined and converted into a simple equivalent pipe (Jeppson 1974). Modeling equivalent pipe systems of series and parallel pipes under steady state and full flow conditions is not new (Edvard et al, 1995; Larock et al, 2000). Most approaches are based on adjusting the diameter, length or roughness of the pipes while keeping the others the same. The resulting equivalent network produces the same pressure heads and head losses as the original network for all flow rates. The main limitation with the above simplification, however, is that, although the resulting network is hydraulically equivalent to the original network, it does not preserve travel time due to the steady-state assumption. To approximate both the hydraulics and the travel time for series and parallel pipes, Raczynski et al. (2008) developed the hydraulic and travel time equivalent technique. In this technique, equivalent pipe diameter is determined based on travel time equivalence relationships. Equivalent pipe roughness is then computed using hydraulic equivalence equations to maintain hydraulic consistency. For further details, the reader is referred to Raczynski et al. (2008).

4.1 Hydraulic and travel time equivalent

To determine the equivalent pipe, first the equivalent diameter of the aggregated pipes, D_e, is determined using the average total travel time of series and parallel pipes (Raczynski et al, 2008). A single pipe's travel time (t_{pipe}) is:

$$t_{pipe} = \frac{L}{V} = \frac{L}{Q/A} = \frac{LA}{Q} \quad (16)$$

Where V, Q, A and L are the velocity, discharge, area and length of a pipe. The average total travel time across a set of series pipes is the sum of the travel times in each pipe:

$$t_{total} = \sum_{i=1}^{n} t_{pipe,i} \quad or \quad \frac{1}{Q_{total}} \sum_{i=1}^{n} L_i A_i \quad (17)$$

For parallel pipes, the total travel time is determined by discharge-weighted average travel time:

$$t_{total} = \sum_{i=1}^{n} \frac{Q_i}{Q_{total}} t_{pipe,i} \quad or \quad \frac{1}{Q_{total}} \sum_{i=1}^{n} L_i A_i \quad (18)$$

The equivalent pipe must produce the same travel time as the original system, therefore:

$$t_{total} = \frac{L_e A_e}{Q_{total}} \quad (19)$$

As a result of substituting t_{total} for both parallel and series pipes, Eq.(20) is derived which proves that, for both pipe configurations, equivalent pipe characteristics are independent of flow rate:

$$L_e = \frac{\sum_{i=1}^{n} L_i A_i}{A_e} \tag{20}$$

Where A_e, or D_e is defined by user (the largest pipe diameter among the pipes).

The computed equivalent length, L_e, ensures that the travel time in the equivalent pipe will equal to the series or parallel pipes. It does not, however, ensure that the system will be hydraulically equivalent. To maintain hydraulic consistency between original and equivalent system, pipe roughness will then be determined from equivalent pipe relationships derived using conservation of energy across a set of pipes in parallel or series. The following equations are derived from Manning head loss equation to calculate the equivalent length for series and parallel pipes. In the development of equivalent network, barching pipes are assumed as parallel pipes.

Parallel pipe equivalence (Raczynski et al, 2008):

$$\frac{1}{{L_e}^{0.5}} = \sum_{i=1}^{n} \left(\frac{R_i}{R_e}\right)^{\frac{2}{3}} \frac{A_i}{A_e} \frac{N_e}{N_i} \frac{1}{{L_i}^{0.5}} \tag{21}$$

Series pipe equivalence (Raczynski et al, 2008)

$$L_e = \sum_{i=1}^{n} \left(\frac{R_e}{R_i}\right)^{\frac{4}{3}} \left(\frac{A_i}{A_e}\right)^2 \left(\frac{N_i}{N_e}\right)^2 L_i \quad (22)$$

Where N_i and R_i are roughness and hydraulic radius of the pipes in parallel or series and N_e and R_e are the same parameters for the equivalent system. There is one unknown parameter in the above equations, N_e, as A_e, R_e and L_e, are fixed using Eq.(20) so the equivalent system that matches both hydraulic and water balance characteristics is developed.

To derive equivalent storm drain network it is necessary to determine the flow directions (connectivity sequence) of the real network first. The following sections describe automatic algorithms developed for derivation of flow direction and equivalent storm drain network.

4.2 Flow direction of storm drain network algorithm

This algorithm uses GIS layers of inlets, junctions, outlets and pipes identifiers and their coordinates as inputs, and produce flow direction (connectivity sequence) of storm drains as output. The algorithm starts from the most downstream point of a branch and moves toward upstream in the following sequence of operations:

1. Generate the coordinates of all inlets, junctions, storm fittings, and outlets using ArcGIS,

2. Generate the coordinates of the start and end points for each pipe using ArcGIS,
3. Export all coordinates in each layer into a text file for all layers,
4. Select an outfall from the outfall text file,
5. Identify all pipes that drain to the selected outfall,
6. Determine the flow direction for each pipe identified in Step 5 based on elevation, and
7. Locate the immediate upstream point and repeat Steps 5 and 6.
8. Repeat the above steps for branches within the real network.

The storm drains identified in this way are then connected to the natural channels through the HRAP coordinates and cell numbers that exist in both connectivity files. The followings are the step by step of the procedure for derivation of flow direction of the original storm drain network shown in Figure 19. The reader reffered to Appendix E for the source code of this algorithm.

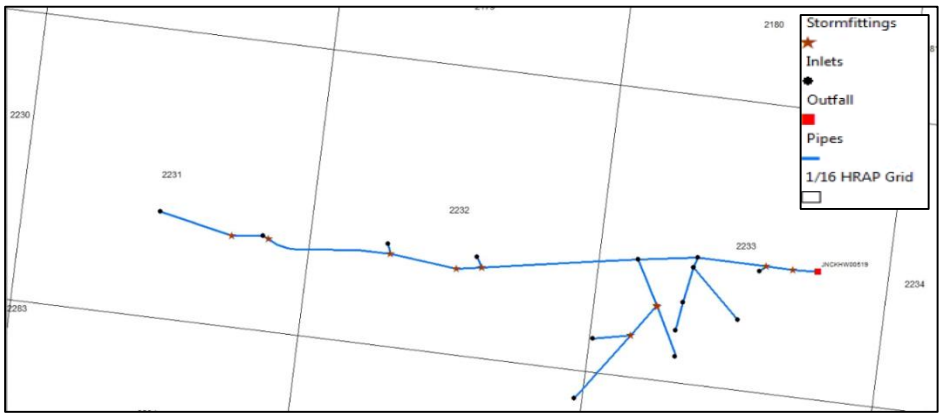

Figure 19 A smaple branch located in Johnson Creek Catchment

1. Generate the coordinates of all inlets, junctions, storm fittings, and outlets using ArcGIS (Figure 20).

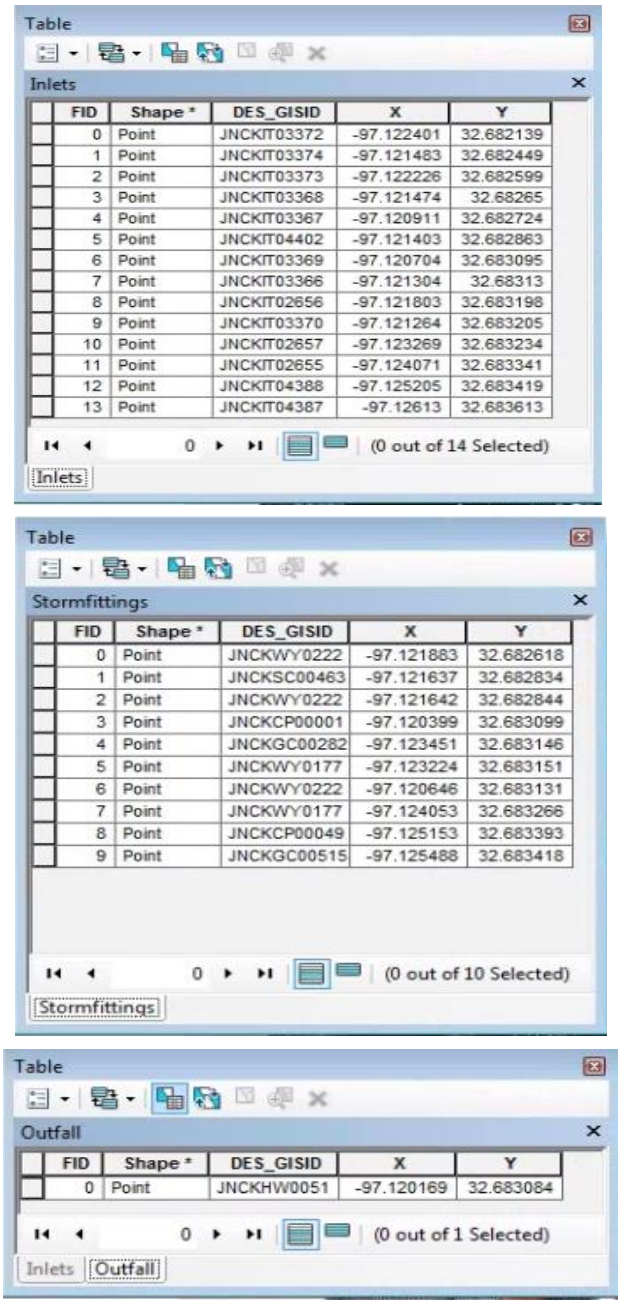

Figure 20 Latitude and longtitude coordinates of inlets, storm fittings and outfall

2. Generate the coordinates of the start and end points for each pipe using ArcGIS (Figure 21). As it can be seen in the table below, there are missing information in the upstream and downstream columns.

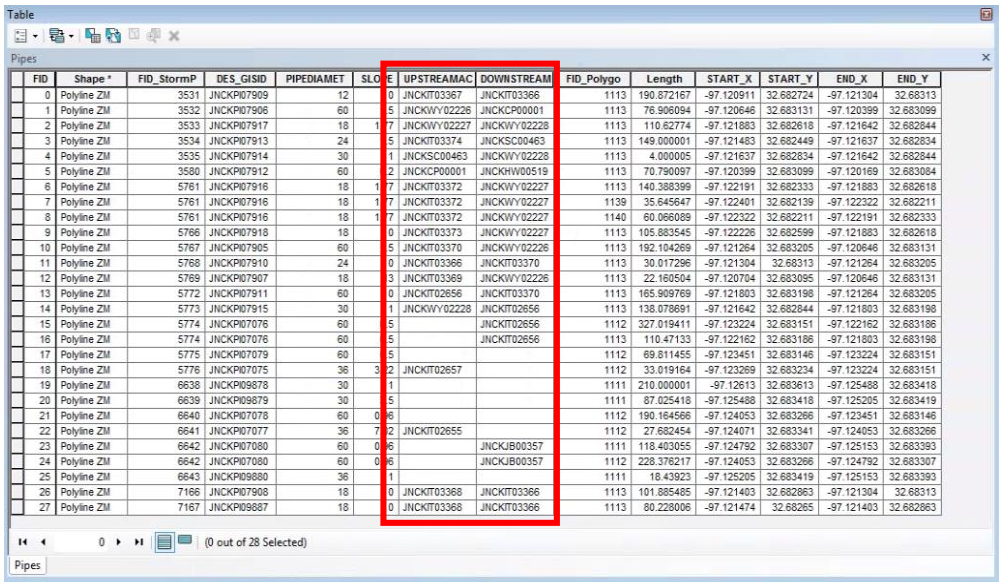

FID	Shape *	FID_StormP	DES_GISID	PIPEDIAMET	SLO	E	UPSTREAMAC	DOWNSTREAM	FID_Polygo	Length	START_X	START_Y	END_X	END_Y
0	Polyline ZM	3531	JNCKPI07909	12		0	JNCKIT03367	JNCKIT03366	1113	190.872167	-97.120911	32.682724	-97.121304	32.68313
1	Polyline ZM	3532	JNCKPI07906	60		5	JNCKWY02226	JNCKCP00001	1113	76.906094	-97.120646	32.683131	-97.120399	32.683099
2	Polyline ZM	3533	JNCKPI07917	18	1	7	JNCKWY02227	JNCKWY02228	1113	110.62774	-97.121883	32.682618	-97.121642	32.682844
3	Polyline ZM	3534	JNCKPI07913	24		5	JNCKIT03374	JNCKSC00463	1113	149.000001	-97.121483	32.682449	-97.121637	32.682834
4	Polyline ZM	3535	JNCKPI07914	30		1	JNCKSC00463	JNCKWY02228	1113	4.000005	-97.121637	32.682834	-97.121642	32.682844
5	Polyline ZM	3580	JNCKPI07912	60		2	JNCKCP00001	JNCKHW00519	1113	70.790097	-97.120399	32.683099	-97.120169	32.683084
6	Polyline ZM	5761	JNCKPI07916	18	1	7	JNCKIT03372	JNCKWY02227	1113	140.388399	-97.122191	32.682333	-97.121883	32.682618
7	Polyline ZM	5761	JNCKPI07916	18	1	7	JNCKIT03372	JNCKWY02227	1139	35.645647	-97.122401	32.682139	-97.122322	32.682211
8	Polyline ZM	5761	JNCKPI07916	18	1	7	JNCKIT03372	JNCKWY02227	1140	60.066089	-97.122322	32.682211	-97.122191	32.682333
9	Polyline ZM	5766	JNCKPI07918	18		0	JNCKIT03373	JNCKWY02227	1113	105.883545	-97.122226	32.682599	-97.121883	32.682618
10	Polyline ZM	5767	JNCKPI07905	60		5	JNCKIT03370	JNCKWY02226	1113	192.104269	-97.121264	32.683205	-97.120646	32.683131
11	Polyline ZM	5768	JNCKPI07910	24		0	JNCKIT03366	JNCKIT03370	1113	30.017296	-97.121304	32.68313	-97.121264	32.683205
12	Polyline ZM	5769	JNCKPI07907	18		3	JNCKIT03369	JNCKWY02226	1113	22.160504	-97.120704	32.683095	-97.120646	32.683131
13	Polyline ZM	5772	JNCKPI07911	60		0	JNCKIT02656	JNCKIT03370	1113	165.909769	-97.121803	32.683198	-97.121264	32.683205
14	Polyline ZM	5773	JNCKPI07915	30		1	JNCKWY02228	JNCKIT02656	1113	138.078691	-97.121642	32.682844	-97.121803	32.683198
15	Polyline ZM	5774	JNCKPI07076	60		5		JNCKIT02656	1112	327.019411	-97.123224	32.683151	-97.122162	32.683186
16	Polyline ZM	5774	JNCKPI07076	60		5		JNCKIT02656	1113	110.47133	-97.122162	32.683186	-97.121803	32.683198
17	Polyline ZM	5775	JNCKPI07079	60		5			1112	69.811455	-97.123451	32.683146	-97.123224	32.683151
18	Polyline ZM	5776	JNCKPI07075	36	3	2	JNCKIT02657		1112	33.019164	-97.123269	32.683234	-97.123224	32.683151
19	Polyline ZM	6638	JNCKPI09878	30		1			1111	210.000001	-97.12613	32.683613	-97.125488	32.683418
20	Polyline ZM	6639	JNCKPI09879	30		5			1111	87.025418	-97.125488	32.683418	-97.125205	32.683419
21	Polyline ZM	6640	JNCKPI07078	60	0	6			1112	190.164566	-97.124053	32.683266	-97.123451	32.683146
22	Polyline ZM	6641	JNCKPI07077	36	7	2	JNCKIT02655		1112	27.682454	-97.124071	32.683341	-97.124053	32.683266
23	Polyline ZM	6642	JNCKPI07080	60	0	6		JNCKJB00357	1111	118.403055	-97.124792	32.683307	-97.125153	32.683393
24	Polyline ZM	6642	JNCKPI07080	60	0	6		JNCKJB00357	1112	228.376217	-97.124053	32.683266	-97.124792	32.683307
25	Polyline ZM	6643	JNCKPI09880	36		1			1111	18.43923	-97.125205	32.683419	-97.125153	32.683393
26	Polyline ZM	7166	JNCKPI07908	18		0	JNCKIT03368	JNCKIT03366	1113	101.885485	-97.121403	32.682863	-97.121304	32.68313
27	Polyline ZM	7167	JNCKPI09887	18		0	JNCKIT03368	JNCKIT03366	1113	80.228006	-97.121474	32.68265	-97.121403	32.682863

Figure 21 Latitude and longtitude coordinates of starting and ending points of pipes

3. Export all coordinates in each layer into a text file for all layers.

4. Select an outfall from the outfall text file. The outfall name of this branch is “JNCKHW00519” and its latitude and longitude are “32.683084” and “-97.120169”, respectively.

5. Identify all pipes that drain to the selected outfall (Figure 22). The algorithm looks for any pipes that connect to the outfall point using the coordinates identified in Step 4. The highlighted pipe in figure bellow is the one that algorithm finds.

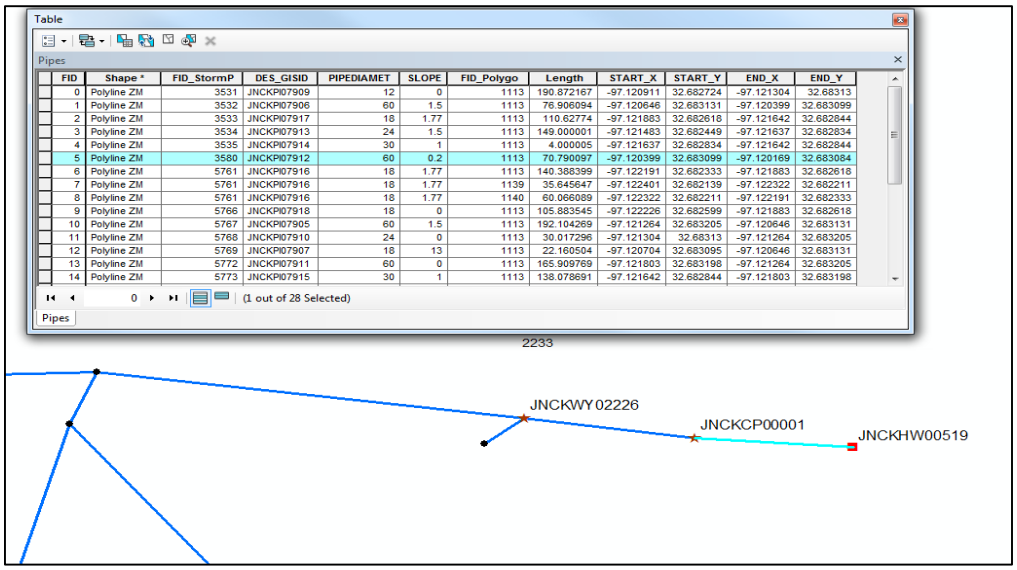

Figure 22 A pipe that drains to the selected outfall (JNCKHW00519)

6. Determine the flow direction for each pipe identified in Step 5 based on elevation. The direction of flow in Step 5 would be from “JNCKCP00001” to “JNCKHW00519”.

7. Locate the immediate downstream point which is “JNCKCP00001” and repeat Steps 5 and 6 (Figure 23). The direction of flow would be from “JNCKWY02226” to “JNCKCP00001”.

The next downstream point is “JNCKWY02226” and repeat Steps 5 and 6 (Figure 24). The direction of flow would be from “JNCKIT03369” to “JNCKWY02226” and “JNCKIT03370” to “JNCKWY02226”

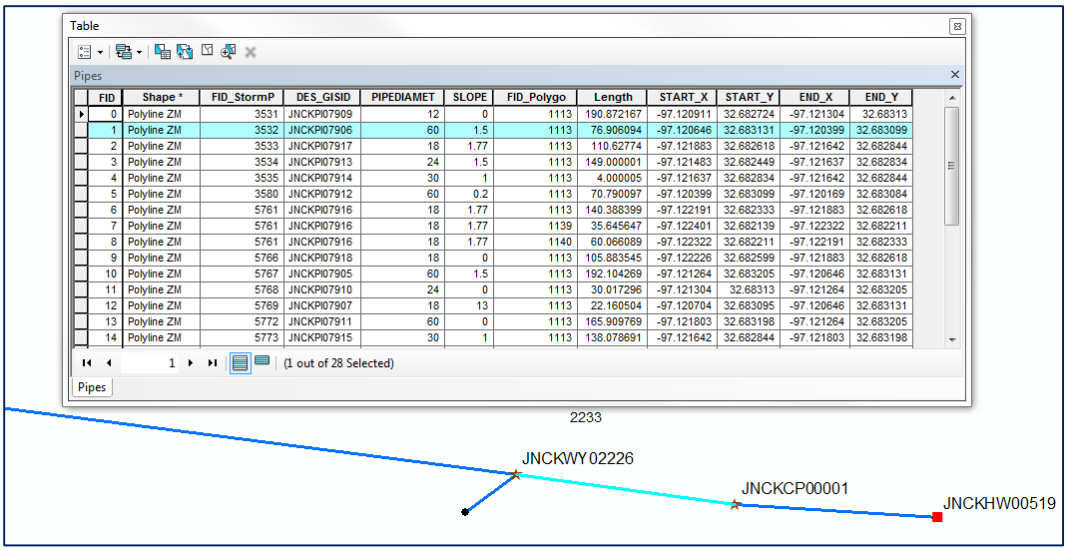

Figure 23 A pipe that drains to JNCKCP00001

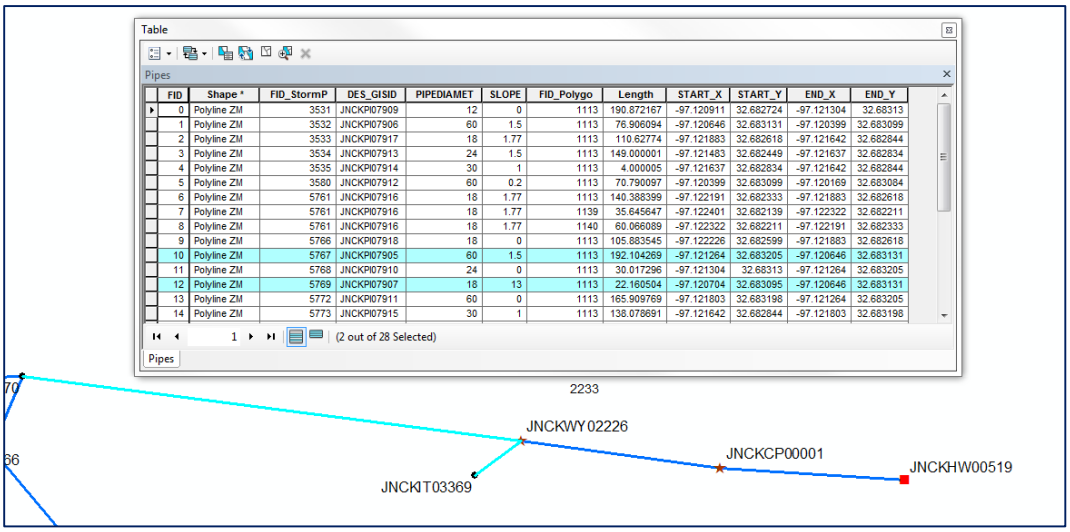

Figure 24 Pipes that drain to JNCKWY02226

The next downstream point are “JNCKIT03369” and “JNCKIT03370”. As it can be seen from Figure 25, no pipes are connected to the inlet “JNCKIT03369” so the algorithim stops at this location and repeat Steps 5 and 6 for the point

"JNCKIT03370". The flow direction would be from "JNCKIT02656" to "JNCKIT03370" and "JNCKIT03366" to "JNCKIT03370".

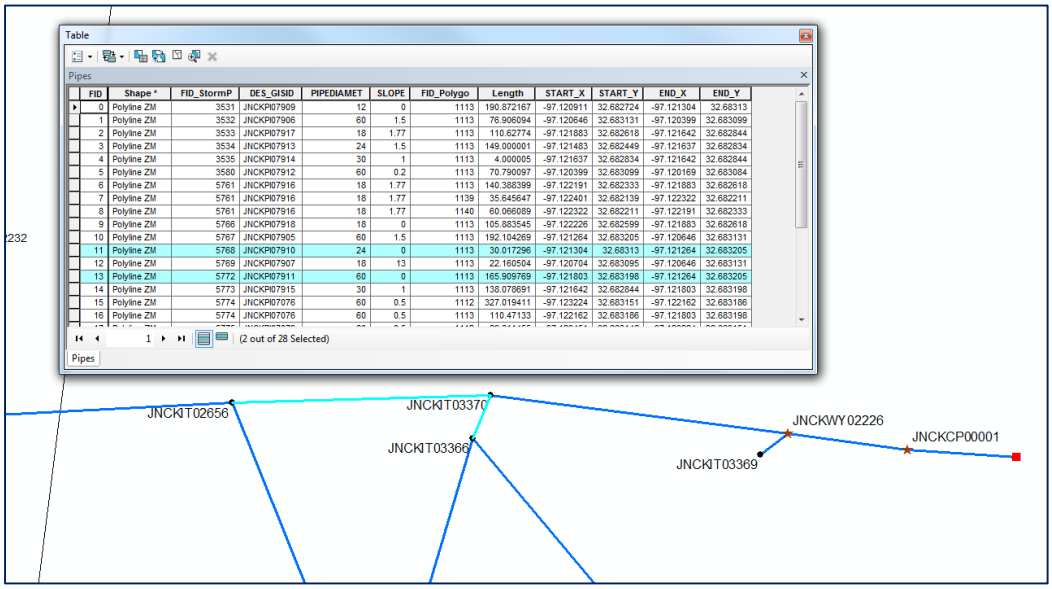

Figure 25 Pipes that drain to JNCKIT03370

The procedure will continue until there is no more pipes connected to a point. The highlighted dots in Figure 26 show the locations that the algorithm stops when it reaches.

8. Save the final result into a file and repeat the procedure for another outfall.

Figure 27 and 28 show the final results of flow direction for the branch. As it can be seen form Figure 27, the arrows show the direction of flow in the branch

and the upstream and downstream columns in Figure 28 show the connectivity sequence of the branch using their identifications.

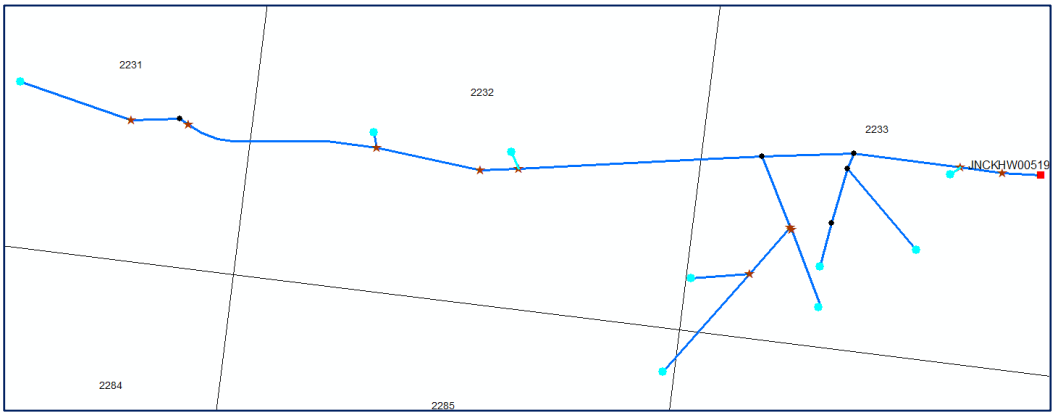

Figure 26 Locations where the algorithm stops

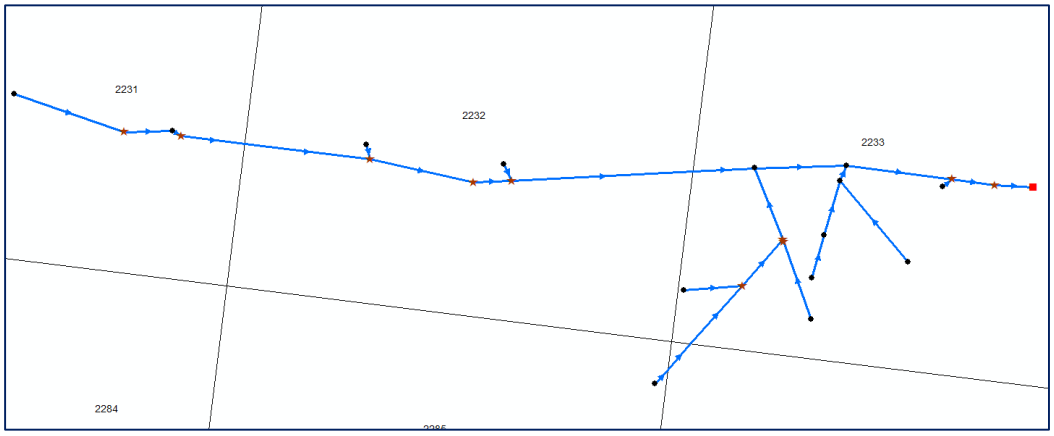

Figure 27 Flow direction of the branch

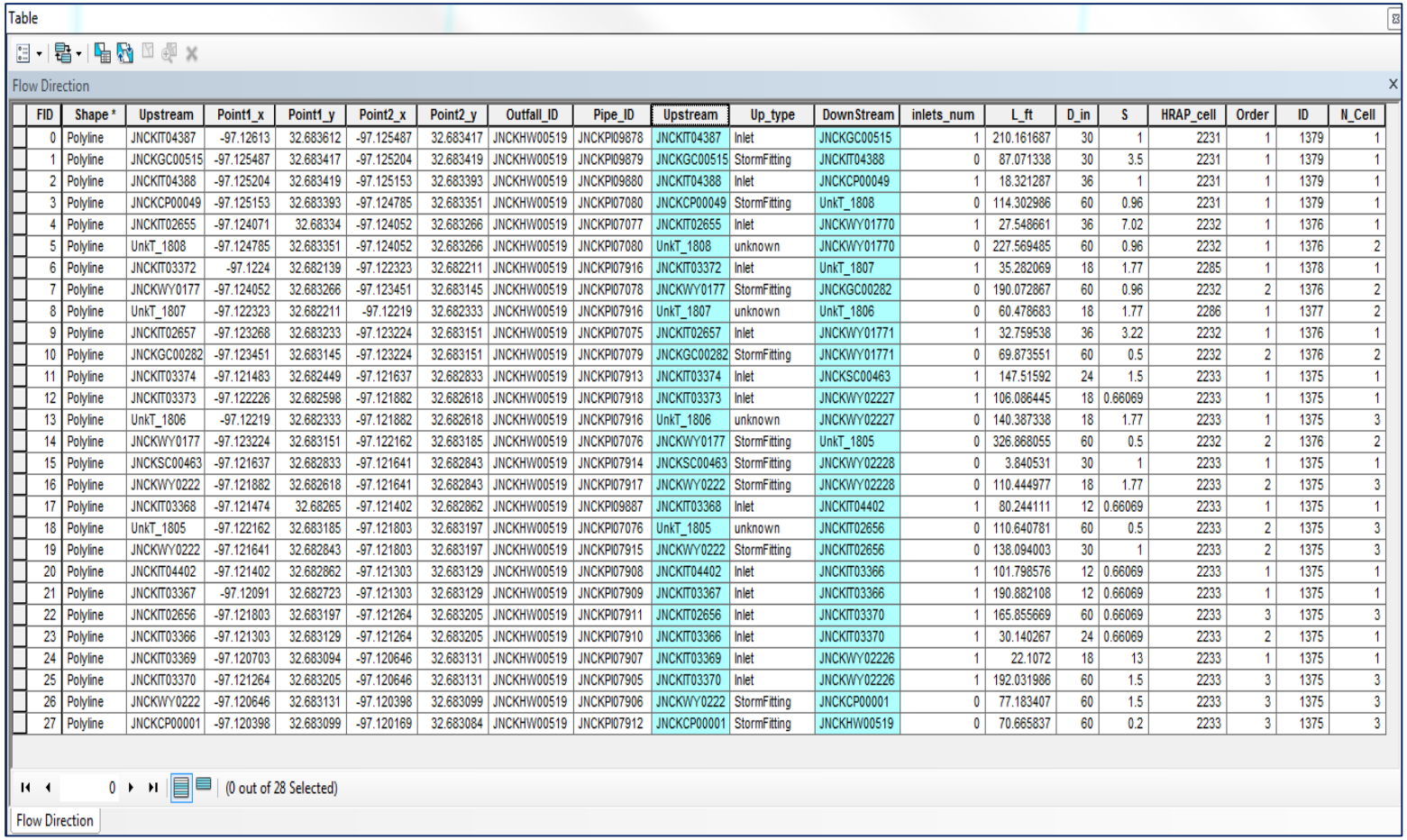
Table

Flow Direction

FID	Shape *	Upstream	Point1_x	Point1_y	Point2_x	Point2_y	Outfall_ID	Pipe_ID	Upstream	Up_type	DownStream	inlets_num	L_ft	D_in	S	HRAP_cell	Order	ID	N_Cell
0	Polyline	JNCKIT04387	-97.12613	32.683612	-97.125487	32.683417	JNCKHW00519	JNCKPI09878	JNCKIT04387	Inlet	JNCKGC00515	1	210.161687	30	1	2231	1	1379	1
1	Polyline	JNCKGC00515	-97.125487	32.683417	-97.125204	32.683419	JNCKHW00519	JNCKPI09879	JNCKGC00515	StormFitting	JNCKIT04388	0	87.071338	30	3.5	2231	1	1379	1
2	Polyline	JNCKIT04388	-97.125204	32.683419	-97.125153	32.683393	JNCKHW00519	JNCKPI09880	JNCKIT04388	Inlet	JNCKCP00049	1	18.321287	36	1	2231	1	1379	1
3	Polyline	JNCKCP00049	-97.125153	32.683393	-97.124785	32.683351	JNCKHW00519	JNCKPI07080	JNCKCP00049	StormFitting	UnkT_1808	0	114.302986	60	0.96	2231	1	1379	1
4	Polyline	JNCKIT02655	-97.124071	32.68334	-97.124052	32.683266	JNCKHW00519	JNCKPI07077	JNCKIT02655	Inlet	JNCKWY01770	1	27.548661	36	7.02	2232	1	1376	1
5	Polyline	UnkT_1808	-97.124785	32.683351	-97.124052	32.683266	JNCKHW00519	JNCKPI07080	UnkT_1808	unknown	JNCKWY01770	0	227.569485	60	0.96	2232	1	1376	2
6	Polyline	JNCKIT03372	-97.1224	32.682139	-97.122323	32.682211	JNCKHW00519	JNCKPI07916	JNCKIT03372	Inlet	UnkT_1807	1	35.282069	18	1.77	2285	1	1378	1
7	Polyline	JNCKWY0177	-97.124052	32.683266	-97.123451	32.683145	JNCKHW00519	JNCKPI07078	JNCKWY0177	StormFitting	JNCKGC00282	0	190.072867	60	0.96	2232	2	1376	2
8	Polyline	UnkT_1807	-97.122323	32.682211	-97.12219	32.682333	JNCKHW00519	JNCKPI07916	UnkT_1807	unknown	UnkT_1806	0	60.478683	18	1.77	2286	1	1377	2
9	Polyline	JNCKIT02657	-97.123268	32.683233	-97.123224	32.683151	JNCKHW00519	JNCKPI07075	JNCKIT02657	Inlet	JNCKWY01771	1	32.759538	36	3.22	2232	1	1376	1
10	Polyline	JNCKGC00282	-97.123451	32.683145	-97.123224	32.683151	JNCKHW00519	JNCKPI07079	JNCKGC00282	StormFitting	JNCKWY01771	0	69.873551	60	0.5	2232	2	1376	2
11	Polyline	JNCKIT03374	-97.121483	32.682449	-97.121637	32.682833	JNCKHW00519	JNCKPI07913	JNCKIT03374	Inlet	JNCKSC00463	1	147.51592	24	1.5	2233	1	1375	1
12	Polyline	JNCKIT03373	-97.122226	32.682598	-97.121882	32.682618	JNCKHW00519	JNCKPI07918	JNCKIT03373	Inlet	JNCKWY02227	1	106.086445	18	0.66069	2233	1	1375	1
13	Polyline	UnkT_1806	-97.12219	32.682333	-97.121882	32.682618	JNCKHW00519	JNCKPI07916	UnkT_1806	unknown	JNCKWY02227	0	140.387338	18	1.77	2233	1	1375	3
14	Polyline	JNCKWY0177	-97.123224	32.683151	-97.122162	32.683185	JNCKHW00519	JNCKPI07076	JNCKWY0177	StormFitting	UnkT_1805	0	326.868055	60	0.5	2232	2	1376	2
15	Polyline	JNCKSC00463	-97.121637	32.682833	-97.121641	32.682843	JNCKHW00519	JNCKPI07914	JNCKSC00463	StormFitting	JNCKWY02228	0	3.840531	30	1	2233	1	1375	1
16	Polyline	JNCKWY0222	-97.121882	32.682618	-97.121641	32.682843	JNCKHW00519	JNCKPI07917	JNCKWY0222	StormFitting	JNCKWY02228	0	110.444977	18	1.77	2233	2	1375	3
17	Polyline	JNCKIT03368	-97.121474	32.68265	-97.121402	32.682862	JNCKHW00519	JNCKPI09887	JNCKIT03368	Inlet	JNCKIT04402	1	80.244111	12	0.66069	2233	1	1375	1
18	Polyline	UnkT_1805	-97.122162	32.683185	-97.121803	32.683197	JNCKHW00519	JNCKPI07076	UnkT_1805	unknown	JNCKIT02656	0	110.640781	60	0.5	2233	2	1375	3
19	Polyline	JNCKWY0222	-97.121641	32.682843	-97.121803	32.683197	JNCKHW00519	JNCKPI07915	JNCKWY0222	StormFitting	JNCKIT02656	0	138.094003	30	1	2233	2	1375	3
20	Polyline	JNCKIT04402	-97.121402	32.682862	-97.121303	32.683129	JNCKHW00519	JNCKPI07908	JNCKIT04402	Inlet	JNCKIT03366	1	101.798576	12	0.66069	2233	1	1375	1
21	Polyline	JNCKIT03367	-97.12091	32.682723	-97.121303	32.683129	JNCKHW00519	JNCKPI07909	JNCKIT03367	Inlet	JNCKIT03366	1	190.882108	12	0.66069	2233	1	1375	1
22	Polyline	JNCKIT02656	-97.121803	32.683197	-97.121264	32.683205	JNCKHW00519	JNCKPI07911	JNCKIT02656	Inlet	JNCKIT03370	1	165.855669	60	0.66069	2233	3	1375	3
23	Polyline	JNCKIT03366	-97.121303	32.683129	-97.121264	32.683205	JNCKHW00519	JNCKPI07910	JNCKIT03366	Inlet	JNCKIT03370	1	30.140267	24	0.66069	2233	2	1375	1
24	Polyline	JNCKIT03369	-97.120703	32.683094	-97.120646	32.683131	JNCKHW00519	JNCKPI07907	JNCKIT03369	Inlet	JNCKWY02226	1	22.1072	18	13	2233	1	1375	1
25	Polyline	JNCKIT03370	-97.121264	32.683205	-97.120646	32.683131	JNCKHW00519	JNCKPI07905	JNCKIT03370	Inlet	JNCKWY02226	1	192.031986	60	1.5	2233	3	1375	3
26	Polyline	JNCKWY0222	-97.120646	32.683131	-97.120398	32.683099	JNCKHW00519	JNCKPI07906	JNCKWY0222	StormFitting	JNCKCP00001	0	77.183407	60	1.5	2233	3	1375	3
27	Polyline	JNCKCP00001	-97.120398	32.683099	-97.120169	32.683084	JNCKHW00519	JNCKPI07912	JNCKCP00001	StormFitting	JNCKHW00519	0	70.665837	60	0.2	2233	3	1375	3

0 (0 out of 28 Selected)

Flow Direction

Figure 28 Connectivity sequence of the branch

4.3 Equivalent storm drain network algorithm

The outputs of flow direction in storm drain network (described in section 4.2) are used to develop equivalent network using an automatic algorithm developed in R programming language which is described below:

1) Select an outfall in the real network and read flow directions for the branch of the real network that drains to the outfall,
2) Select the most upstream grid box in the branch,
3) Search for any connecting pipes.
4) Apply Eqs.(20) and (21) or Eqs.(20) and (22) to parallel or series pipes, respectively, to calculate the equivalent pipe characteristics,
5) Repeat Steps 3 and 4 until the real pipes within the grid box are reduced to a single equivalent pipe,
6) Repeat Steps 2 through 5 for all grid boxes that contain the branch until the outlet is reached,
7) Repeat the above steps for branches within the real network.

The followings are the step by step of the procedure for derivation of equivalent storm drain network shown in Figure 19.

1. Select an outfall and read flow directions for the branch of the real network that drains to the outfall (table in Figure 28).
2. Select the most upstream grid box in the branch (Figure 29).

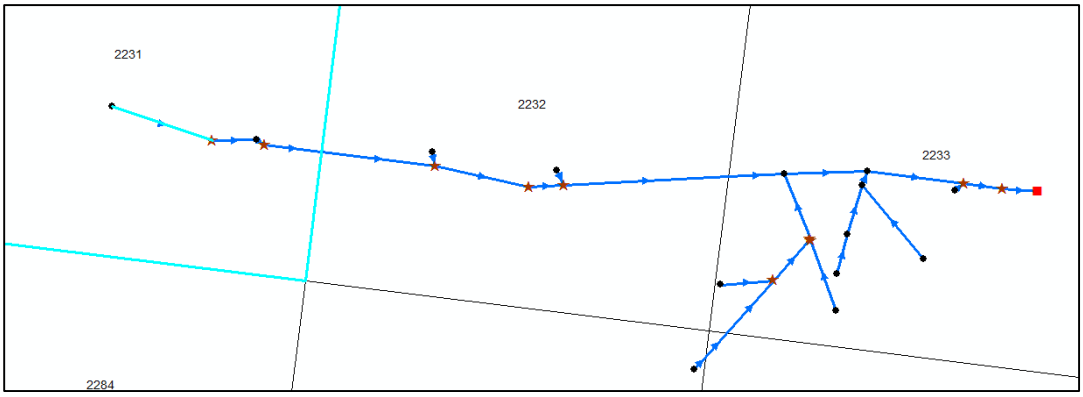

Figure 29 Upstream pipe in grid box 2231

3. Search for any connected pipes. The highlighted pipes are connected in series.

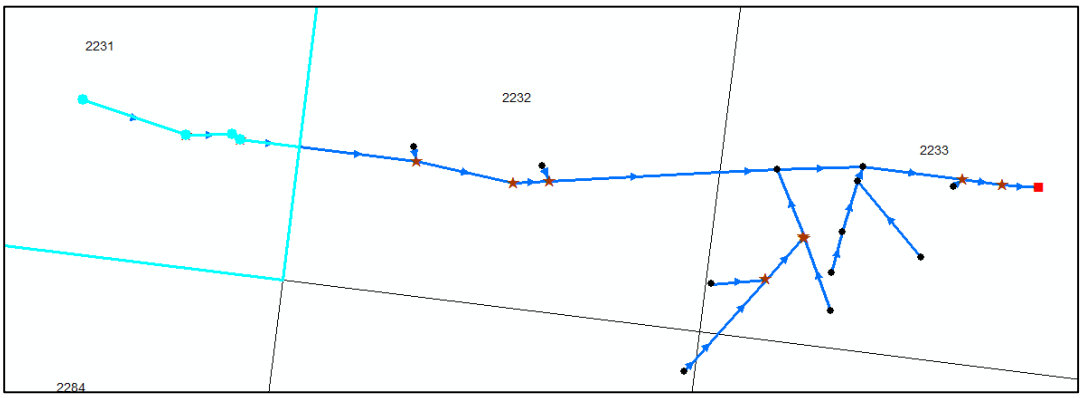

Figure 30 Connected pipes in grid box 2231

4. Apply Eqs.(20) and (21) or Eqs.(20) and (22) to parallel or series pipes, respectively, to calculate the equivalent pipe characteristics.

5. Repeat Steps 3 and 4 until the real pipes within the grid box are reduced to a single equivalent pipe (Figure 30).

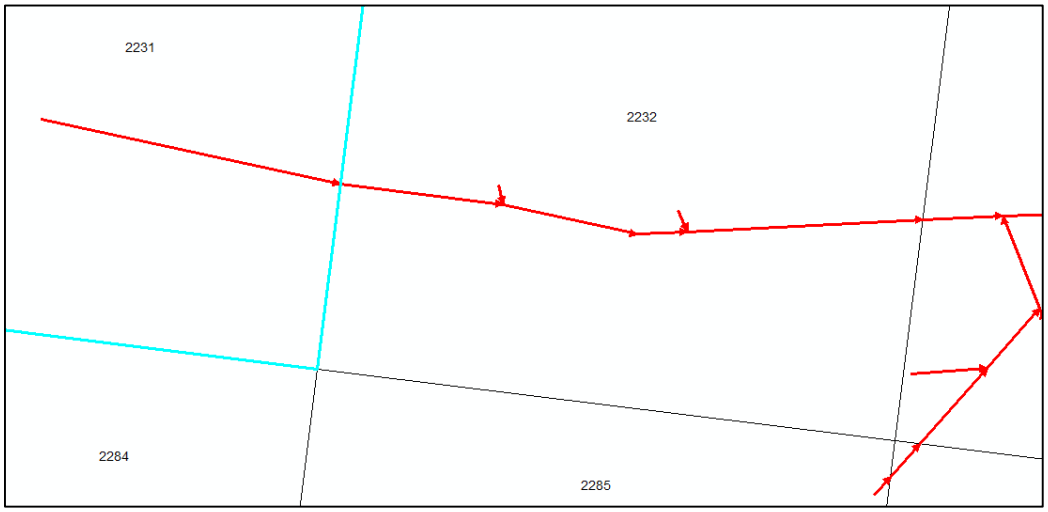

Figure 31 Equivalent pipe in grid box 2231.

6. Repeat Steps 2 through 5 for all grid boxes that contain the branch until the outlet is reached.

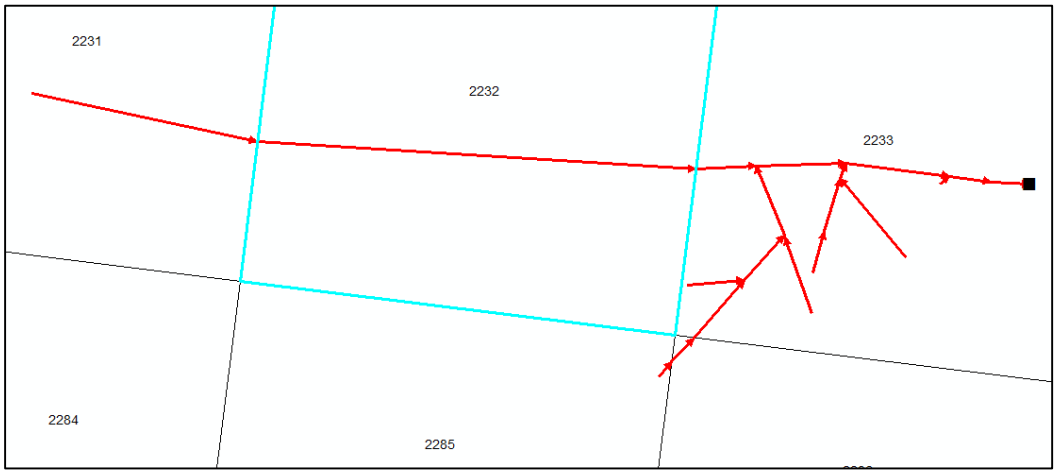

Figure 32 Equivalent pipe in grid box 2232

The algorithm stops when it reaches to the outfall of the network (Figure 33). The final results contain five equivalent pipes instead of 28 pipes in the original network. In Figure 33, although it seems that “UnkT_1808” pipe is not connected to any pipes but as it can be seen in the table (red box), the pipe is connected to a downstream pipe (“UnkT_1806”).

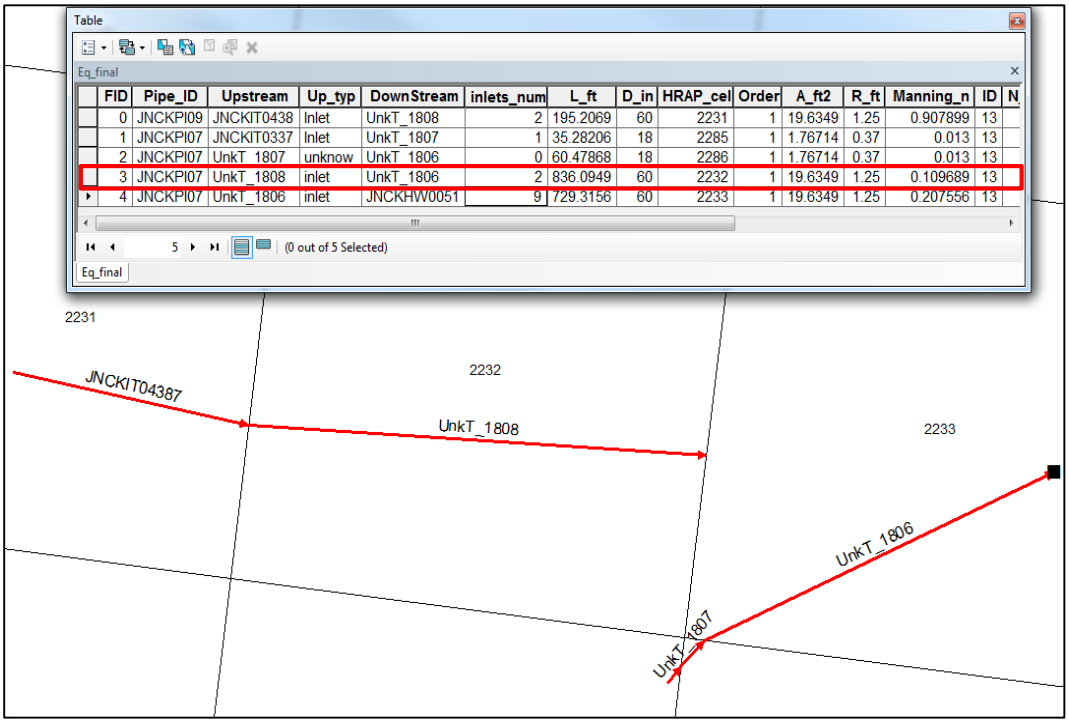

Figure 33 Equivalent storm drain shown in Figure 30

Figure 34 shows the working flowchart of algoritms of flow direction and equivalent storm drain networks.

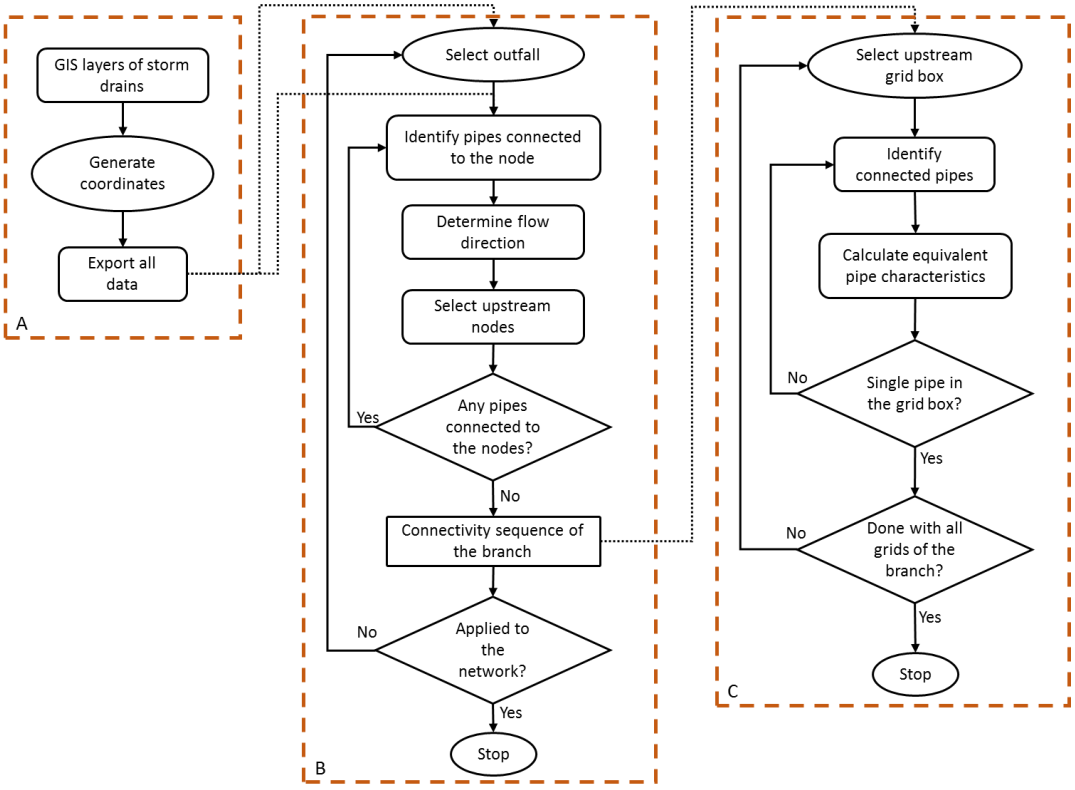

Figure 34 Flowchart of A) ArcGIS process, B) algorithm of flow direction for original storm drain network, and C) algorithm of equivalent storm drain network

4.4 Application of equivalent storm drain network

The automated algorithms described in sections 4.1 and 4.2 are used to develop the Equivalent Storm Drain Network (ESDN) for the five urban catchments. Figure 35 show the original and resulting equivalent storm drain networks for study are on a 250 m grid. In the figure, this original network contains about 22,000 pipes which reduced to 2000 in the equivalent system. Some storm drain open channels are self-contained and are not connected to any other structures. Such channels are considered as natural channels and are excluded in construction of the equivalent storm drain network.

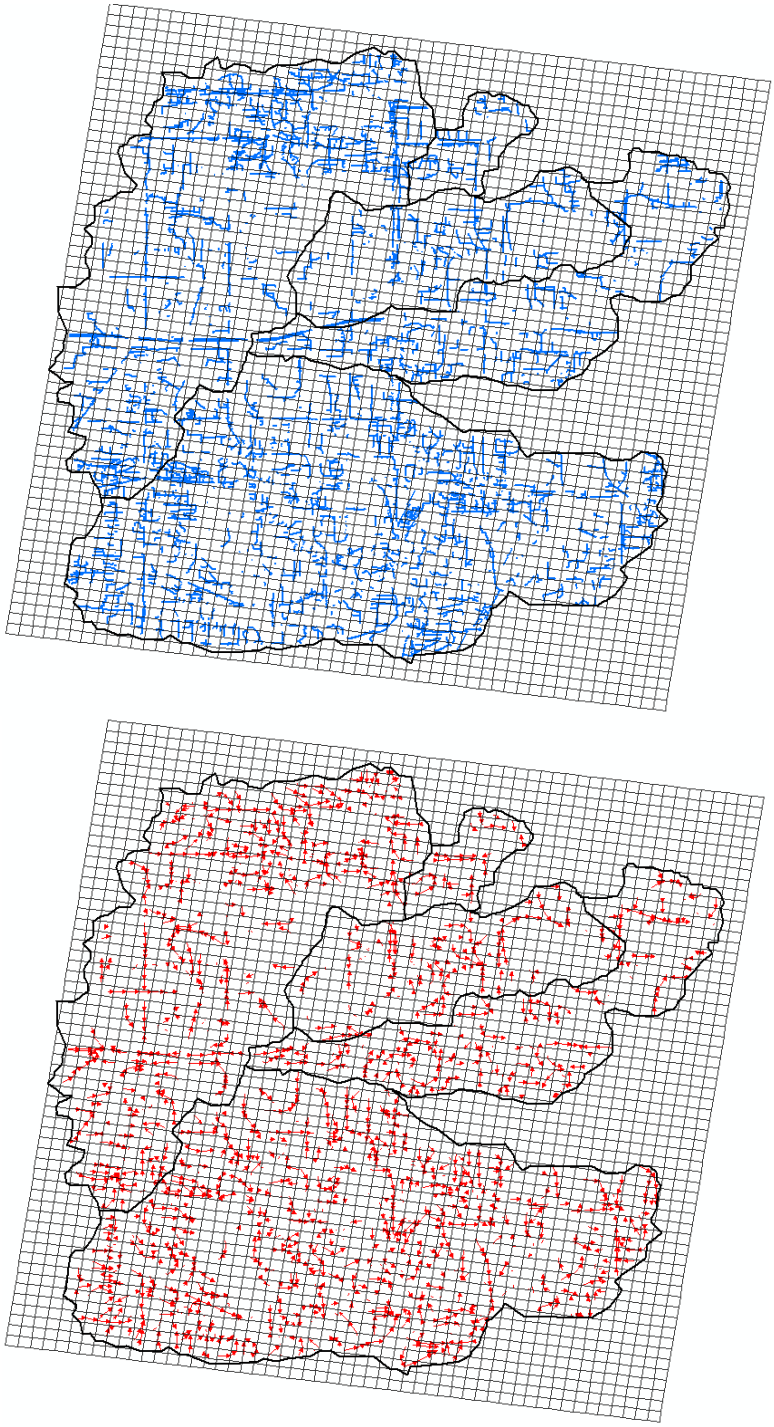

Figure 35 Original (upper panel) and equivalent (lower panel) storm drain network for the five urban catchments.

To check the goodness of the approximations with the equivalent systems, the flow routing results of the full and equivalent systems using rainfall event of January 16, 2016 in Arlington are compared. Three systems in the Johnson Creek Catchment are selected for the comparison purpose. The equivalent network and the selected pipe systems are shown in Figure 36.

On January 16, 2017, a rainfall event occurred in Arlington from which 4 inches of rain fell in about 6 hours. In Figure 37 the routing results using the full and equivalent networks for selected branches in the Johnson Creek Catchment is compared. For routing, kinematic wave is used for both networks using the same inflows (see Subsection 3.3.4). The figure shows that flow hydrographs at selected outfalls of the equivalent network are very close to those of the original network. The comparisons are similar for other catchments so they are not shown here. The above results indicate that the equivalent network represents the real storm drain network very well.

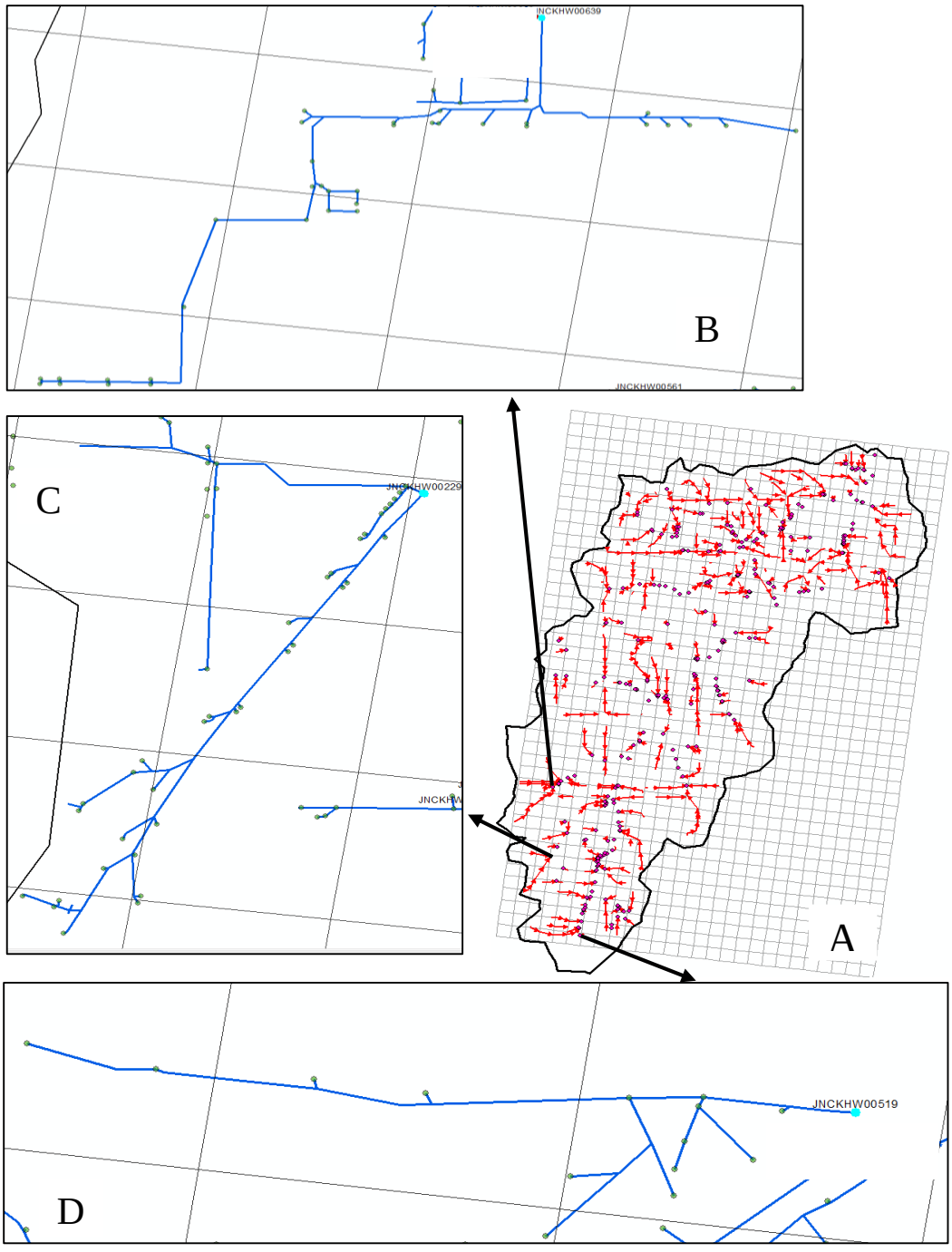

Figure 36 A) Equivalent storm drain network for Johnson Creek Catchment, B) real branch 1, C) real branch 2 and D) real branch 3

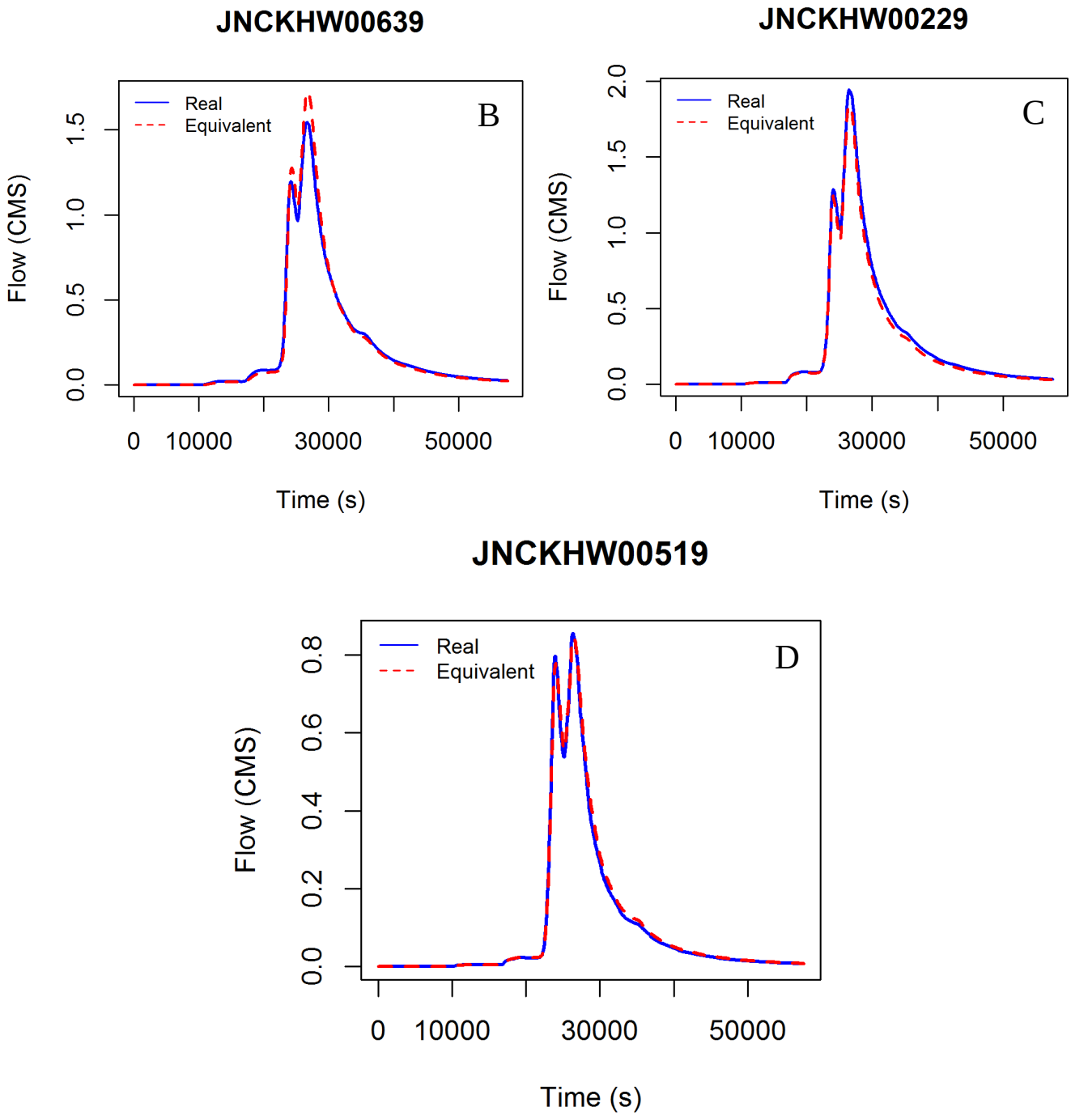

Figure 37 Flow hydrographs at outfall locations of original and equivalent branches shown in Figure 36

Chapter 5

Results and discussions

In this chapter, first, the performance of HL-RDHM is assessed using two case studies of the flash flooding events of June 24, 2014 and April 13, 2015 in the City of Fort Worth, then the real-time flash flood prediction system for DFW Metroplex is developed, and finally the results of integrated modeling of natural channel and storm drain network are presented.

5.1 High-resolution flash flood forecasting for DFW

5.1.1 Flash flooding event of June 24, 2014

To assess the performance of the system, flash flooding event of June 24, 2014, in Fort Worth that 2 to 3 inches of rain fell in just 90 minutes is used. The largest in June since 2007, the rain event was the result of small impulses moving through the upper level in which disturbances rotated around the low. The heaviest rain occurred where the boundaries intersected (Dallas news 2014). Over a span of three hours in the afternoon of June 24, Fort Worth fire officials responded to 420 calls. More than 40 of them were high-water rescues, more than 20 were for downed power lines, and eight fire calls were made during the flooding (Fox4 news 2014).

To warm up the model states, HL-RDHM was run at a spatiotemporal resolution of 1 HRAP and 1 hr using the MPE data from 1996 to 2014. The model

was then run at spatiotemporal resolution of 1/8 HRAP (~500 m) and 1 min for June 24, 2014, using CASA QPE and MPE over the domain. For qualitative assessment of the model results, the flooding reports received by the City of Fort Worth from the residents throughout the event are used. Figure 38 shows the total precipitation for June 24, 2014, as observed by MPE (upper panel) and CASA QPE (lower panel).

As readily seen in Figure 38, the higher resolution CASA QPE presents details much better than the lower resolution MPE. There are, however, areas in the CASA QPE where rainfall amounts appear depressed due to attenuation. Note that, for this study, the CASA QPE was based only on the radar at the University of Texas at Arlington (XUTA) located at the center of the radar umbrella in the lower panel of Figure 38. It is noted that the CASA QPE products will soon be based on multiple radars, thereby greatly mitigating the ill effects of attenuation.

Figures 39 and 40 show the hourly precipitation, hourly runoff and streamflow ending or valid at 4 pm on June 24, 2014, for the MPE and CASA QPE-based results, respectively. Note in Figure 40 that CASA QPE is used within the XUTA umbrella but MPE is used elsewhere. In the figures, the circles denote the locations of flooding as reported by the residents. The red circles indicate that flooding was first reported within the hour ending at 16:00.

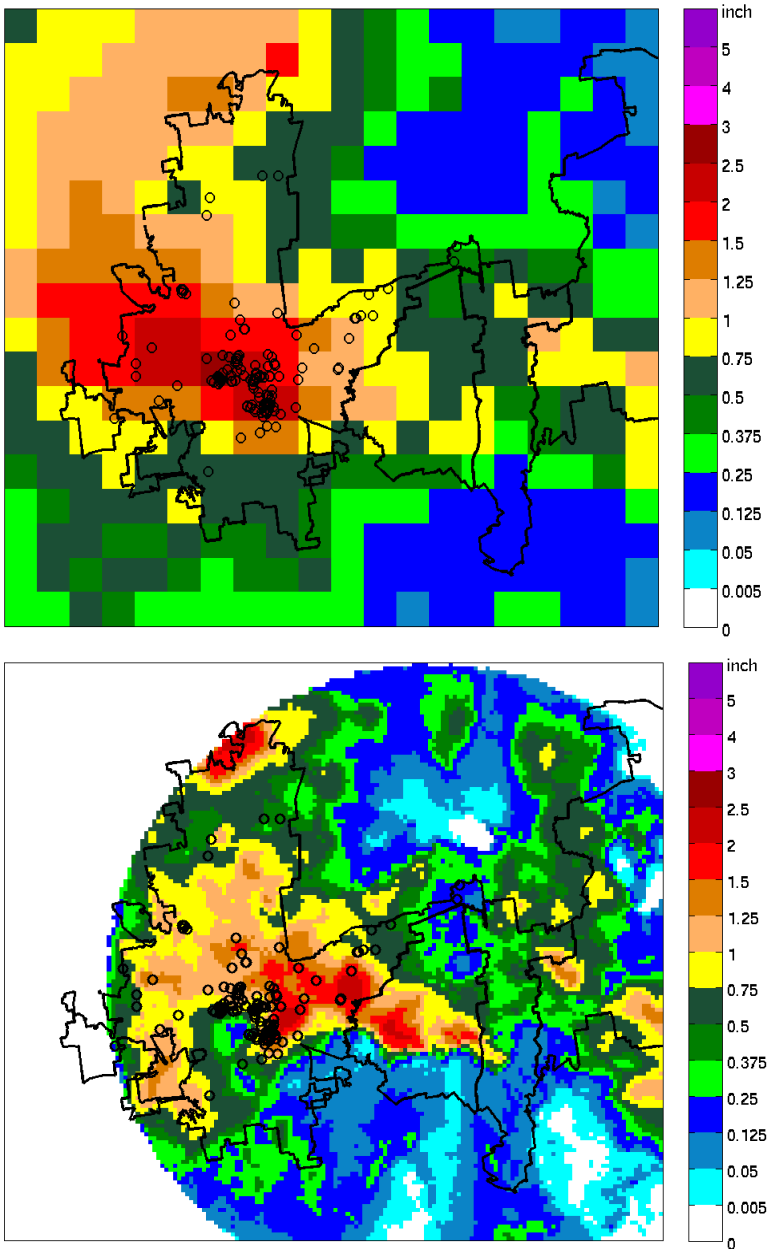

Figure 38 Total precipitation for June 24, 2014: upper panel) MPE (1 HRAP, 1 hr) and lower panel) CASA QPE (1/8 HRAP, 1 min)

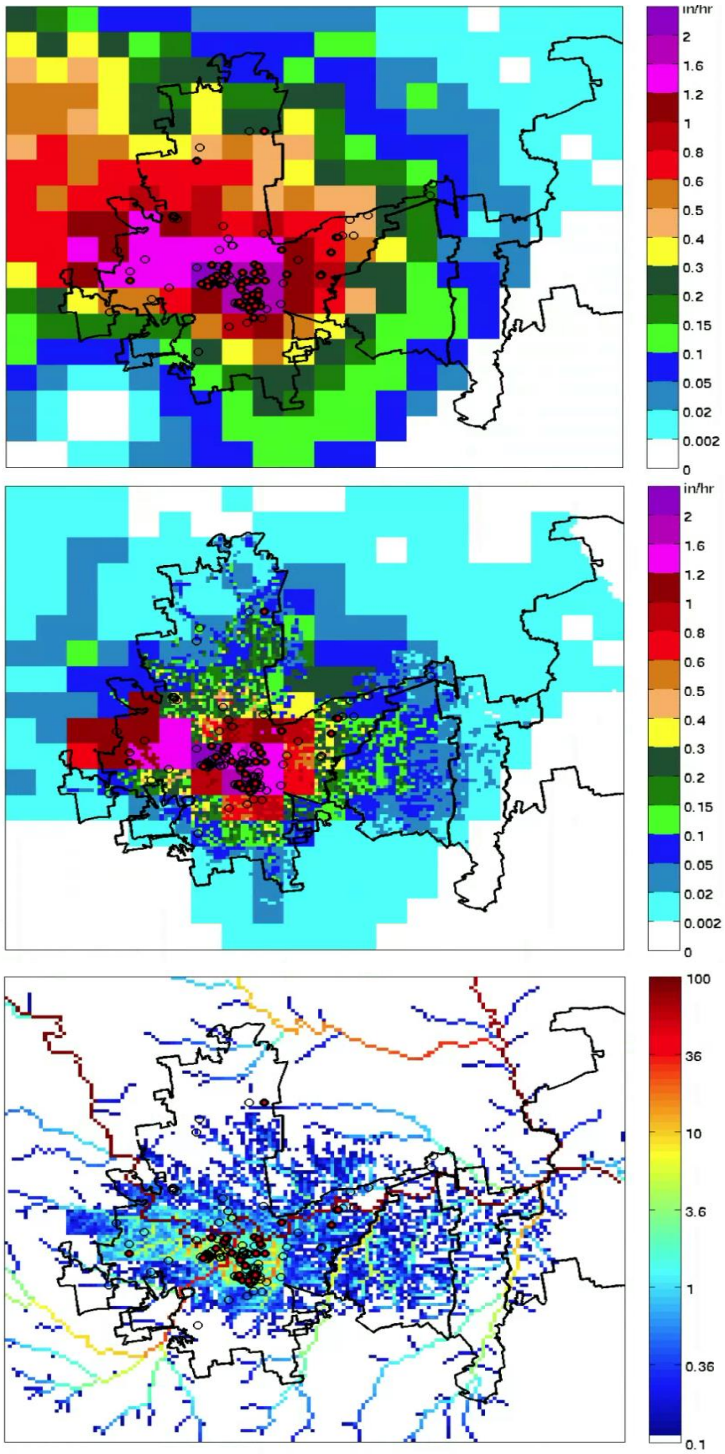

Figure 39 hourly MPE precipitation (upper panel), hourly MPE-forced runoff (middle panel) and MPE-forced streamflow (in CMS, lower panel) valid at 4 pm on June 24, 2014

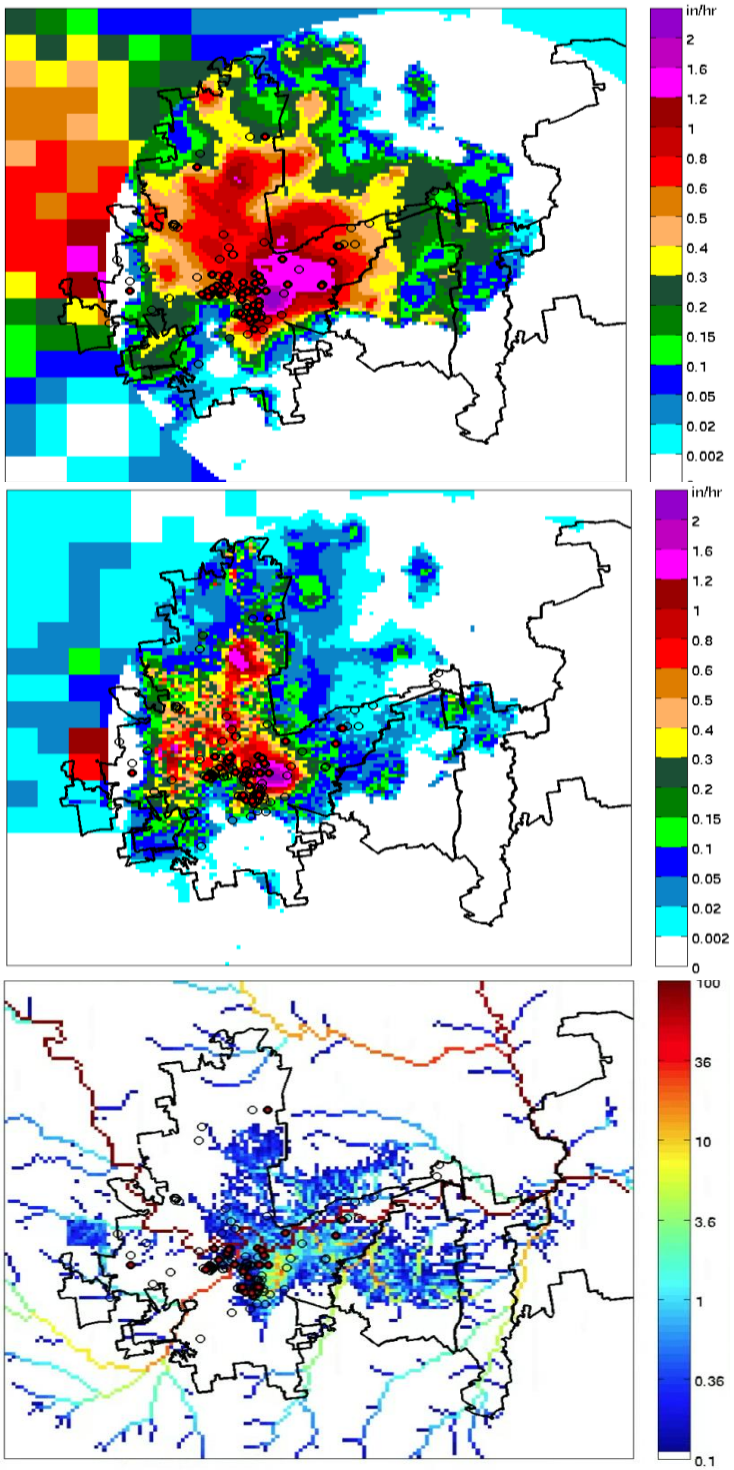

Figure 40 hourly CASA precipitation (upper panel), hourly CASA QPE-based runoff (middle panel), and CASA QPE-based streamflow (lower panel) valid at 4 pm on June 24, 2014

Figure 39 shows that most of the reports are located in the areas of heavy precipitation, and that the runoff and streamflow maps successfully narrow down the areas where most reports originated. The CASA QPE-forced results in Figure 40, on the other hand, show the ill effects of attenuation due to the fact that the QPE is derived only from a single X-band radar. As noted above, the effects of attenuation are expected to be addressed with network based QPE.

Comparison of the simulation results in Figures 39 and 40 indicates that higher-resolution QPE and modeling improves location and temporal specificity of flooding threats, and that high-quality QPE is necessary to benefit from high-resolution modeling.

5.1.2 Flash flooding event of April 13, 2015

A quick-moving thunderstorm dumped heavy rain across Tarrant County on Monday, April 13 2015, causing brief flooding in an area of Fort Worth. In that day, Fort Worth firefighters were called to help stranded motorists at several central city locations, and at least one person had to be rescued from her car, which was caught in the high water on a Street. The flooding reports received by the City of Fort Worth from the residents throughout the event are used for qualitative assessment of the model results. Figure 41 shows the total rainfall (upper left), runoff (upper right), maximum streamflow (lower left) and maximum return period

(lower right) for 2015-04-13, as observed by CASA QPE. In the figures, the circles denote the locations of flooding as reported by the residents. As it can be seen from the figures, most of the reports are located in the areas of heavy precipitation, and that the runoff and streamflow maps successfully narrow down the areas where most reports originated.

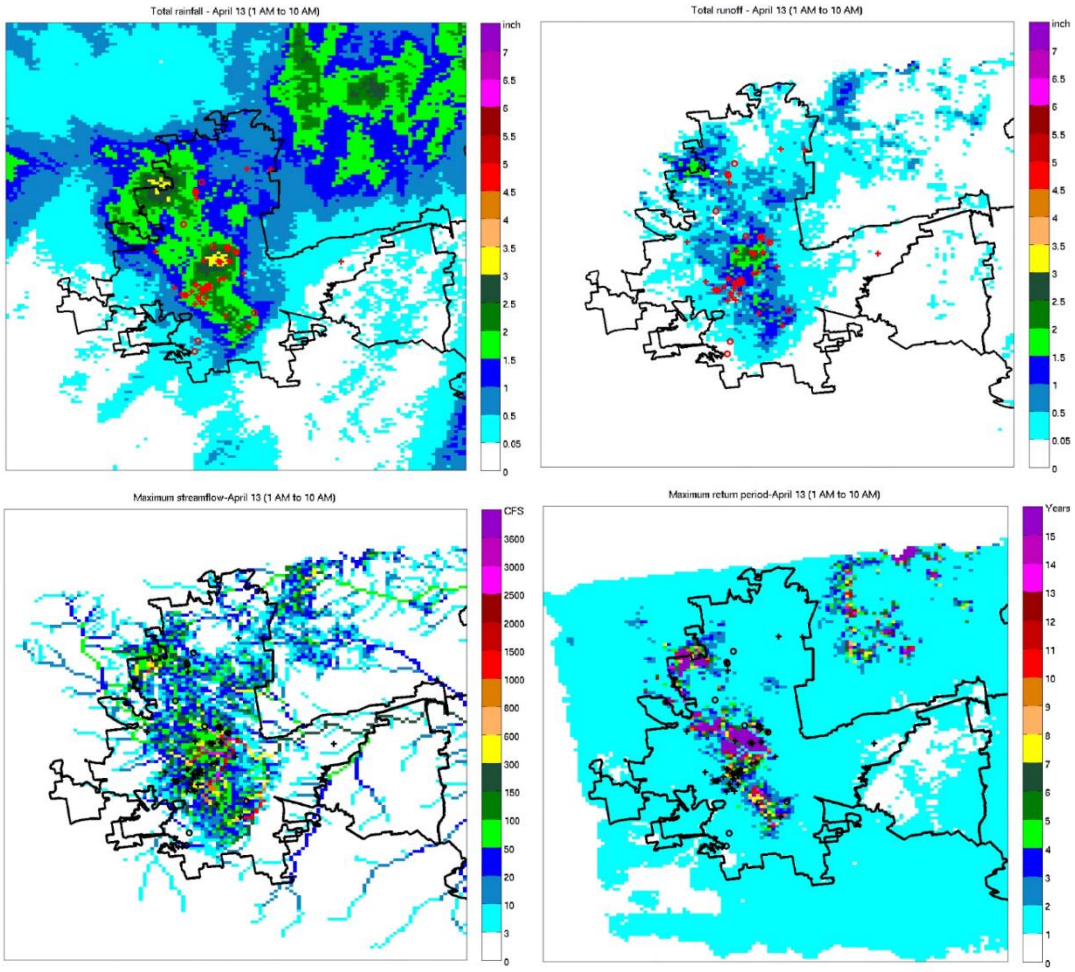

Figure 41 Total precipitation (upper left), total runoff (upper right), and maximum streamflow (lower left) and maximum retur period (lower right) on April 13, 2015

5.1.3 Flash flood forecasting system

Using the high resolution hydrologic model (HL-RDHM, 1min and 500m) and precipitation data (CASA QPE, 1min and 500m), a prototype of real time flash flood forecasting system for the DFW area has been developed. The simulation results including, runoff rate, one hour runoff, three hour runoff, stream flow, and return period are being generated and transferred to the CASAWX interface (https://droc1.srh.noaa.gov/dfw/) in real time (see Figure 42).

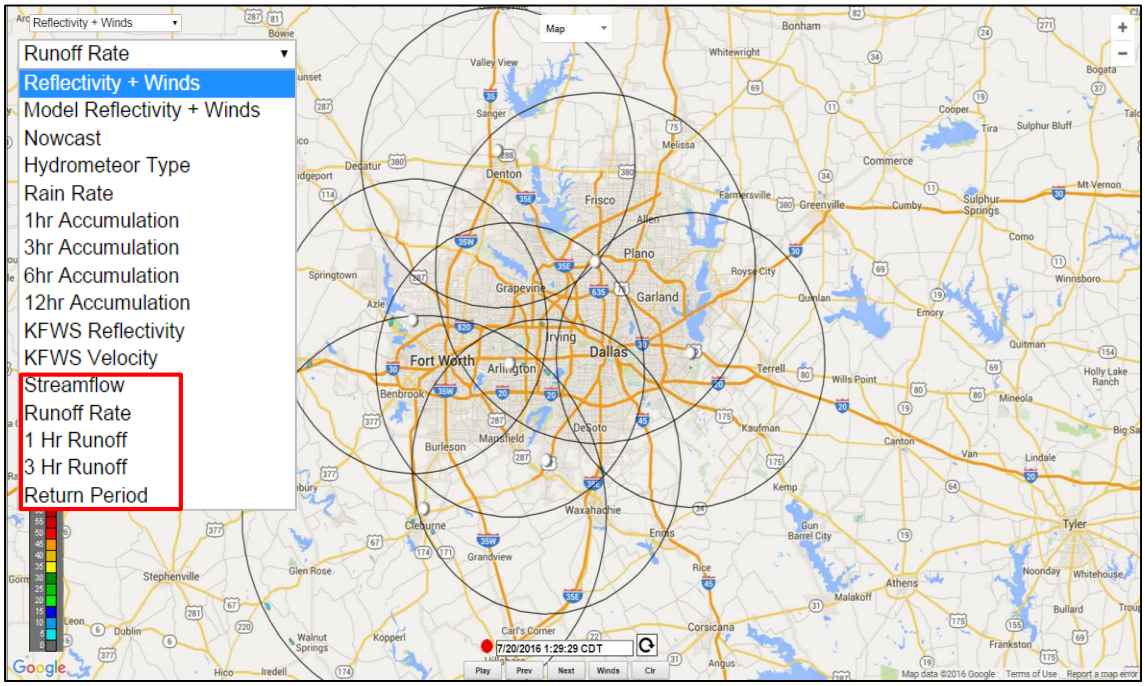

Figure 42 CASAWX network prroducts (http://droc1.srh.noaa.gov/dfw/)

5.2 Integrated modeling of natural cahnnel and storm drain network

In this section, the results are presented in four parts. In the first part, simulated flow at the catchment outlets against the observed is compared to assess the realism of the model for simulating natural channel flow. In the second part, the results from integrated model simulation with and without storm drain modeling at all locations within each catchment are described. This allows assessment of the contribution area-dependent impact of storm drains to surface flow. In the third part, the impact of storm drains on peak flow under the existing land cover conditions and under a 15% increase in imperviousness in the study area are presented. Lastly, the impact of the Iinitial Conditions (IC) of the storm drain flow model is examined and the sensitivity of the conveyance volumes in the natural channel and storm drain networks to selected inlet flow model parameters are assessed.

5.2.1 Comparison with observed flow at catchment outlet

The HLRDHM was evaluated previously for the study area by Rafieeinasab et al. (2015) by comparing model-simulated streamflow without storm drain modeling against observed flow. The streamflow was estimated from water level observations using model-derived rating curves (Norouzi et al. 2015). More recently, Norouzi (2016) carried out additional evaluation which included

comparison of HLRDHM-simulated soil moisture against observed soil moisture. He found that distinctly different infiltration processes are at work even within a small area in the Johnson Creek Catchment, and that SAC is generally not able to reproduce accurately observed soil moisture in the study area. Rafieeinasab et al. (2015) indicated that full-capacity open channel storm drainages can convey several times more flow than full-flow storm drain pipes in the study area, and that, for an extreme event such as Tropical Storm Hermine in 2010, the natural channels convey about 3 and 15 times as much flow as the full-capacity open channel storm drains and pipes, respectively. Tropical Storm Hermine produced 160 mm of rainfall over a 24-hr period in the study area which corresponds to a return period of about 25 years. The equivalent storm drain network modeled in this work include not only the storm drainage pipes but also the open channel storm drains to which storm drainage pipes are connected. All other storm drain open channels are considered as part of the natural channel network. Hence, one may expect the conveyance capacity of the equivalent storm drain network to be relatively modest compared to that of the natural channel network. Also, the available water level observations available for this study are located only at the catchment outlets. They hence combine flows through the natural channels and storm drains. For the above reasons, comparison of streamflow at the outlets of sizable catchments is not likely to reveal the impact of storm drains. On the other hand, one may still compare the natural channel flow simulations without storm drain modeling with the observed

flow to assess the quality of the baseline model simulation. Figures 43 and 44 show the hyetographs (top) and the simulated vs. observed hydrographs (bottom) for two events occurred in late Nov and Dec of 2015, respectively, in the 14.4 km^2 Cottonwood Creek at Carrier (Outlet 6363). The total rainfall amounts are 120 mm over a 24-hr period for the late Nov event and 90 mm over a 48-hr period for the late Dec event which correspond to return periods of approximately 5 and 2 years, respectively. The rainfall data used is the CASA QPE at 1/8 HRAP and 1-min resolution. The HLRDHM resolution is at 1/16 HRAP resolution. Figure 43 indicates that the model simulation is able to capture the events quite well but it is not able to pick up very fast-varying streamflow responses and exhibits flow magnitude-dependent errors for the late Dec event.

Certain types of errors in these simulations are not at all surprising in that they are based on the a priori model parameters for both soil moisture accounting and routing with no attempt at calibration. Overall, it is seen that the model is capable of producing realistic streamflow responses to rainfall events. Comparison of streamflow simulations with (red dashed line) and without (blue dashed line) storm drain modeling in Figure 43 indicates that the differences between the two are indistinguishable for the large Nov event, but that, for the smaller Dec event, the peak flows at the outlet have slightly increased with storm drain modeling. As explained above and shown in Figure 43, outlet flow integrates both natural channel and storm drain flows and hence is not very useful in assessing the impact of storm

drains. For impact assessment at much small spatial scales, a set of twin simulation experiments are carried out as described below. The reader referes to Appendix A and B for other comparioson with observation flow at outlets of GP6363 and GP6043, respectively.

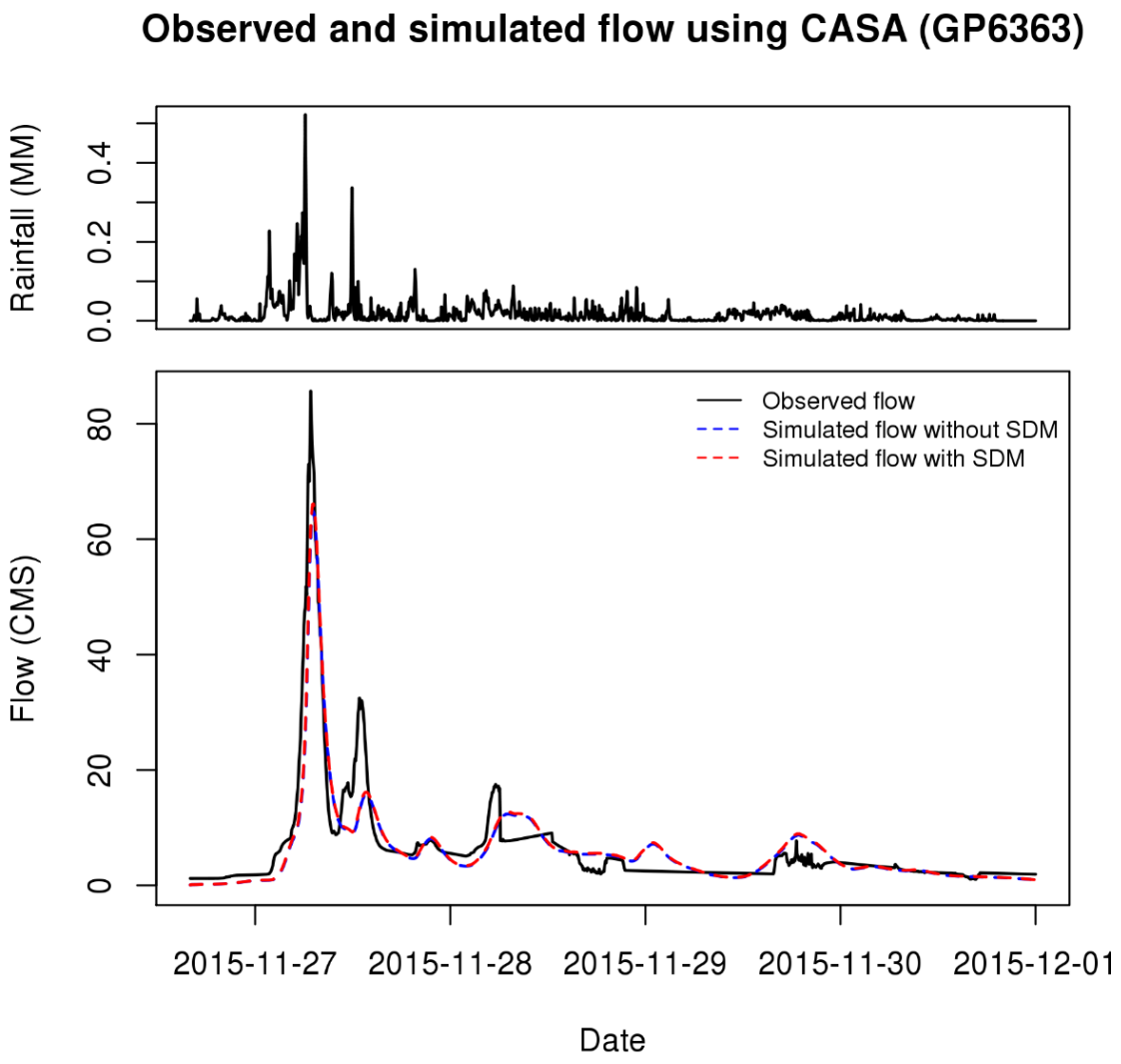

Figure 43 Streamflow observation and simulation with and without storm drain modeling using CASA QPE for GP6363 for late November 2015

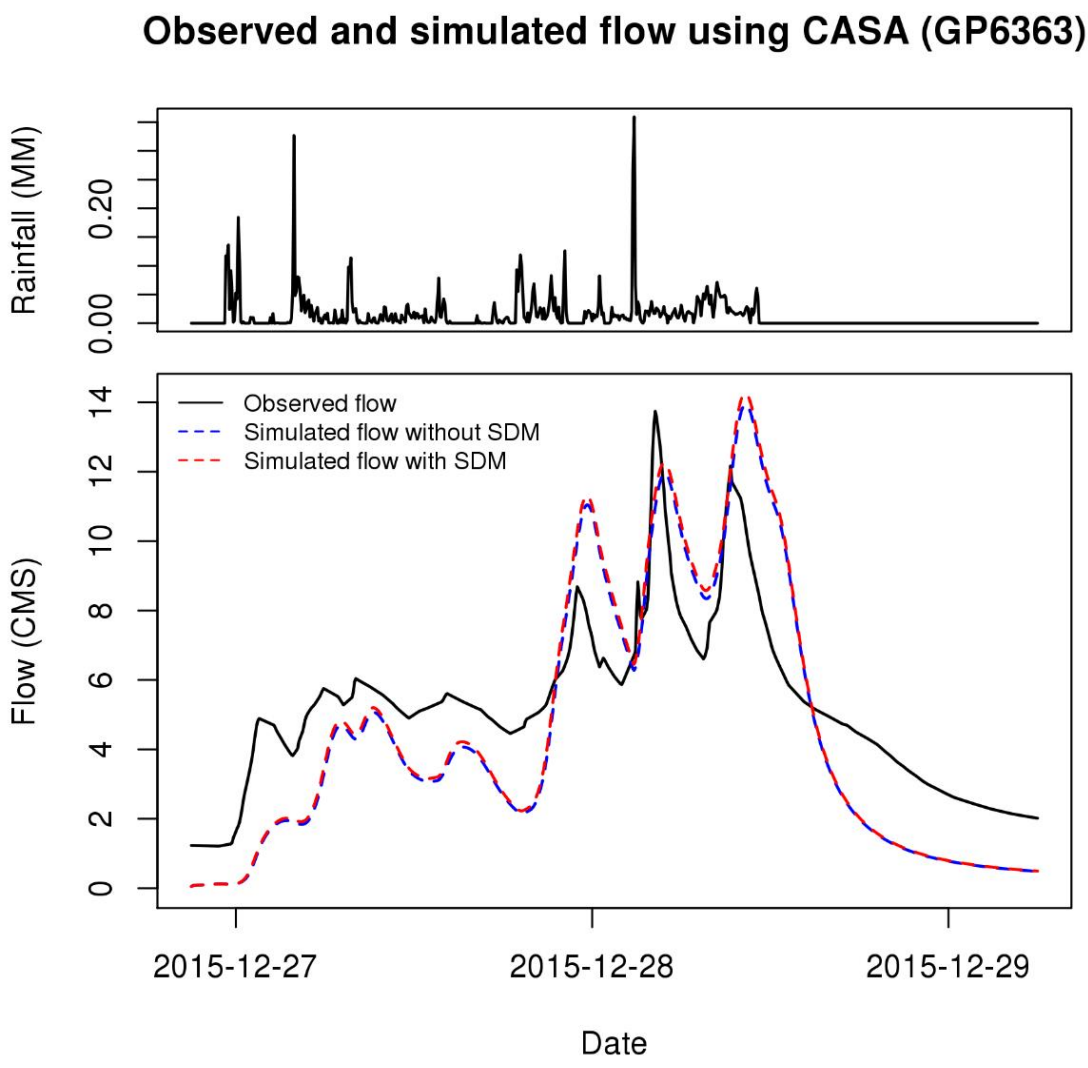

Figure 44 Streamflow observation and simulation with and without storm drain modeling using CASA QPE for GP6363 for late December 2015

5.2.2 Impact of storm drains at different scales of contributing area

In the DFW area, integrated design of stormwater infrastructure calls for 25-yr 24-hr design rainfall for conveyance which includes minimizing localized site flooding of streets, sidewalks, and properties by a combination of on-site stormwater controls and conveyance systems, and for 100-yr 24-hr design rainfall for flood mitigation which includes providing adequate downstream conveyance systems, installing stormwater controls on-site to maintain or improve existing downstream conditions and/or maintaining existing on-site runoff conditions in lieu of a downstream assessment (NCTCOG 2015). In this work, spatially uniform 100-yr 5-min and 24-hr rainfall of constant rate are applied to assess the impact of storm drain network on surface flow in response to impulse- and step-function forcings of rainfall, respectively. Figure 45 shows the simulated hydrographs of channel flow with (red solid line) and without (blue solid line) storm drain modeling at all grid boxes in the Johnson Creek Catchment (Outlet 6033) due to a spatial uniform rainfall pulse of 280.7 mm lasting 5 min. Because the hydrographs shown in the figure represent the response of the contributing areas to what is essentially an impulse, they may be considered as scaled unit hydrographs. Note that, the smaller the contributing area is, the faster the hydrologic response is.

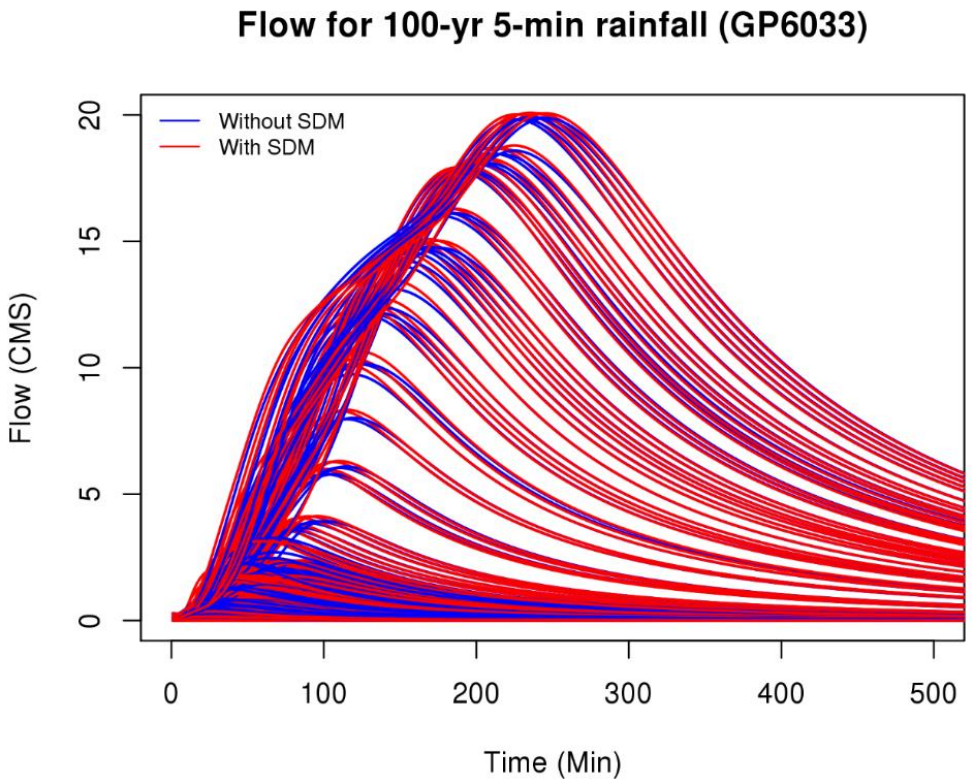

Figure 45 Simulated hydrographs of channel flow with and without storm drain modeling at all grid boxes in GP6033.

Though difficult to see in this figure, there are numerous hydrographs near the origin representing the response of very small contributing areas. To help discern the hydrographs associated with storm drains from those without, the box-and-whisker plots of the hydrographs in logarithmic scale with and without storm drain modeling is shown in Figure 46. In the figure, the upper and lower ends of the box represent the 75th and 25th percentiles. The line in the box represents the

median. The ends of the whiskers represent $median \pm 1.58 \times IQR/\sqrt{n}$ (where IQR is the inter-quartile range, or distance between the first and third quartiles). It is seen that the storm drains in this catchment reduce surface flow at most locations for about 30 min, and that at many locations the reduction persists well past 30 min.

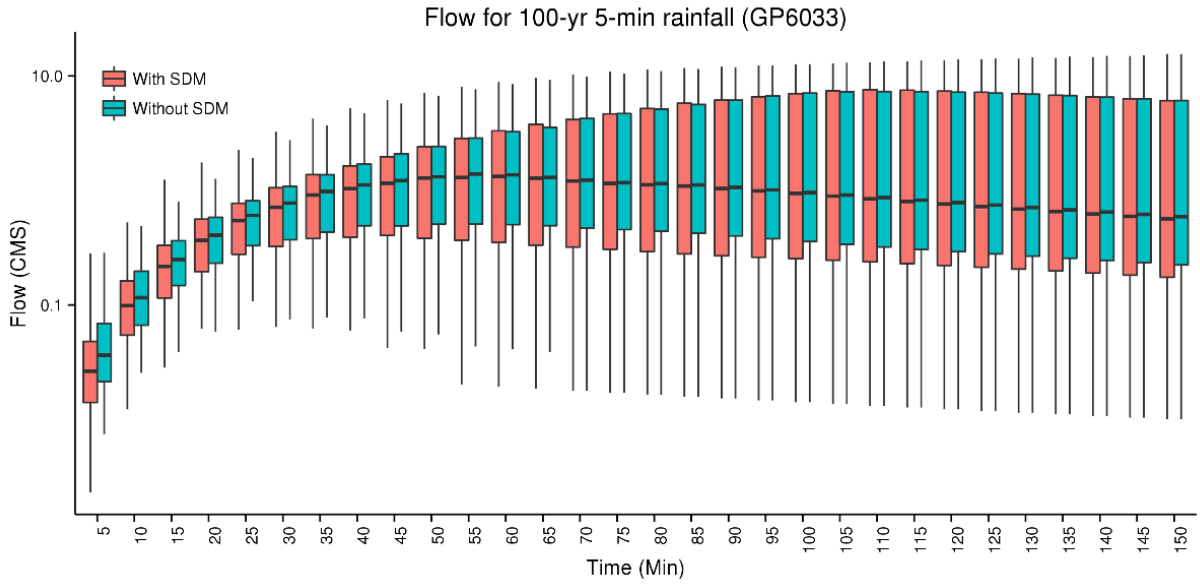

Figure 46 Box-and-whisker plots of the hydrographs of Fig 30 in logarithmic scale with and without storm drain modeling.

Figures 47 and 48 shows the results for the Fish Creek Catchment (Outlet 6133). For this cactcment, it was found that the storm drains reduce flow at most locations only for the first 10 min or less, and that, between 15 and 40 min or so, there is a noticeable increase in flow with storm drains modeled. The above

observations suggest that the Fish Creek Catchment may be susceptible to downstream flooding due to storm drains upstream.

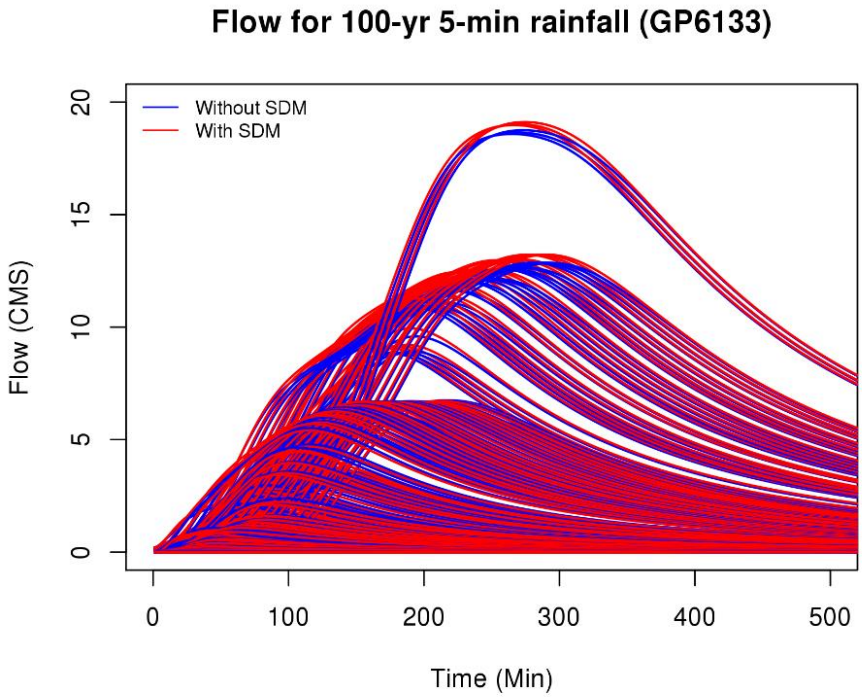

Figure 47 Simulated hydrographs of channel flow with and without storm drain modeling at all grid boxes in GP6133.

To track the impact of storm drains on surface flow at each grid box during the course of the catchment response following an impulse rainfall, the ratio of the flow with storm drains to that without at all grid boxes in the Johnson Creek Catchment and Fish Creek Catchment due to 100-yr 5-min rainfall are plotted in Figures 49 and 50. A ratio of less or greater than unity is an indication that the storm drains reduce or increase surface flow at that location, respectively. Note in the

figures that the storm drain reduces flow very significantly for a very short duration at almost all grid cells, that at many of the above locations the flow remains reduced for the entire duration, but that there are locations where the storm drains increase flow between 5 to 50 min. The results for other catchments are qualitatively similar and are shown in Appendix C. For stormwater planning and management, the locations where surface flow increases due to storm drains are of particular interest. Below is described how such areas may be identified by spatially mapping the changes in peak surface flow due to storm drains.

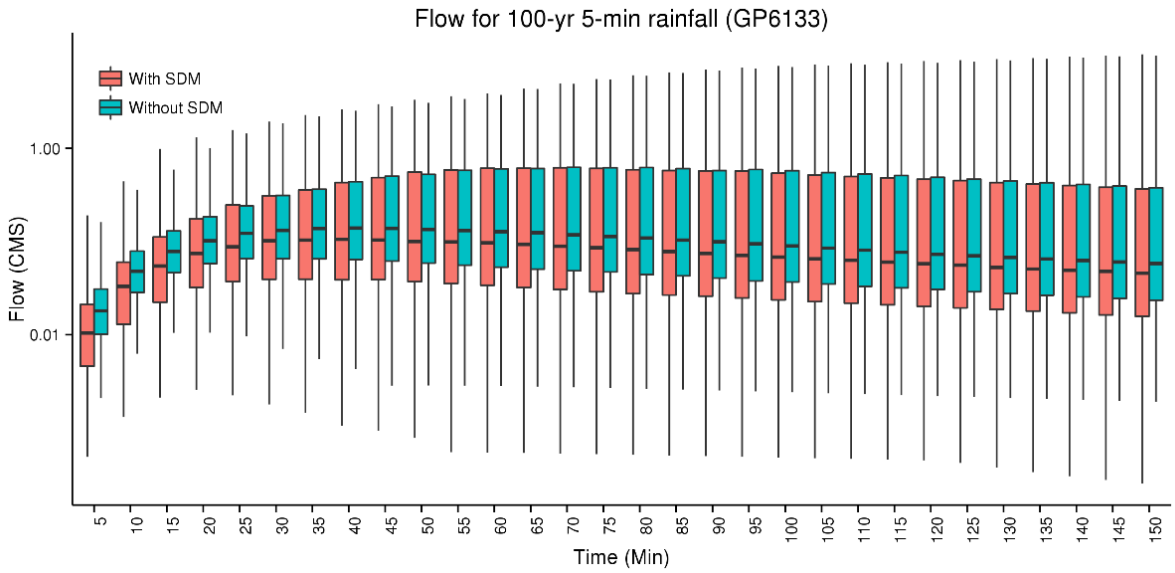

Figure 48 Box-and-whisker plots of the hydrographs of Fig 47 in logarithmic scale with and without storm drain modeling.

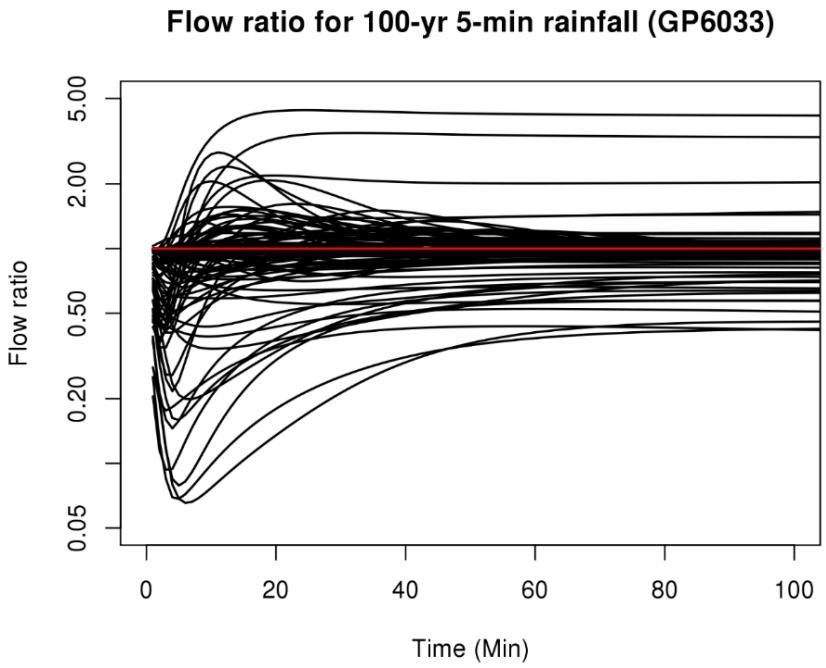

Figure 49 Ratio of the flow with storm drains to that without at all grid boxes in GP6033 due to 100-yr 5-min rainfall.

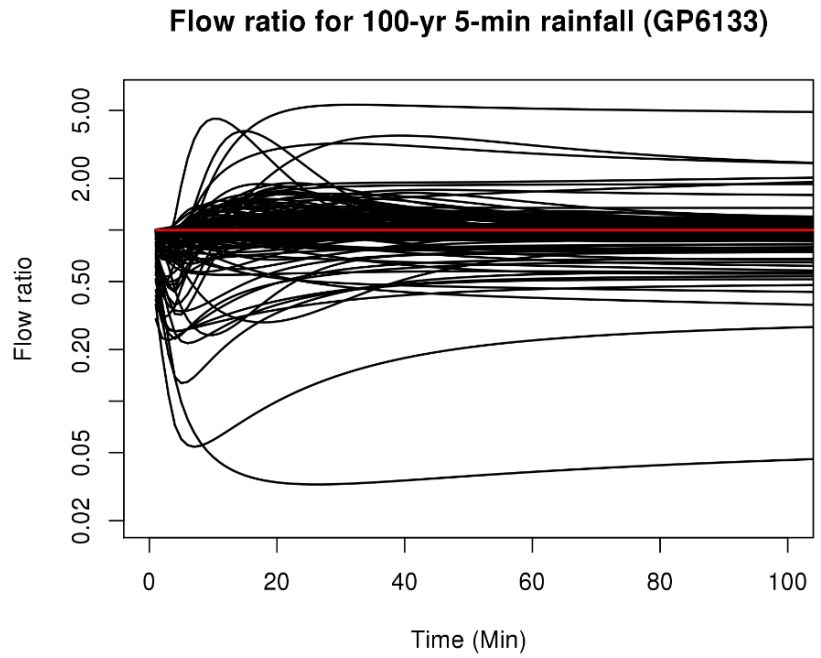

Figure 50 Ratio of the flow with storm drains to that without at all grid boxes in GP6133 due to 100-yr 5-min rainfall.

Also the performance of the coupled model is assessed using two extreme rainfal events over the five catchments. Rainfall events of May 29, 2015 and Januray 16, 2017 in Arlington and Grand Prairie are used for the twin simulations. Total rainfall of each event are shown in Figurs 51. Figures 52 and 53 show the simulated hydrographs with and without storm drain modeling and box-and-whisker plots of the hydrographs for the Johnson Creek Ctachment (GP6033).

For the storm drain simulations, we used completely empty boundying condition equivalent storm drain network. It is seen that the storm drains in this catchment (GP6033) reduce surface flow at most locations during both events, and that at many locations the reduction persists well past for the time of event. The simulation results for the other catchments are presented in the Appenix D.

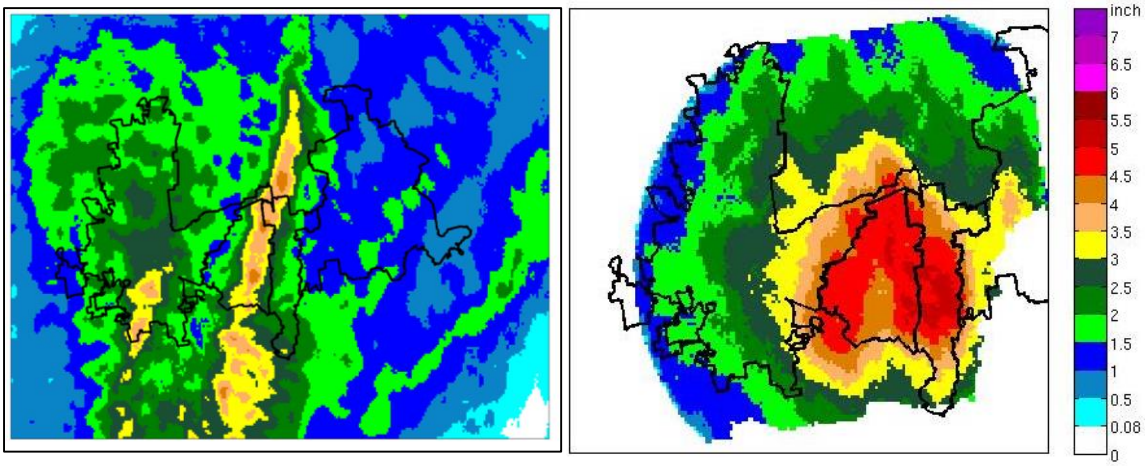

Figure 51 Total rainfal for January 16, 2017 (left) and for May 29, 2015 (right)

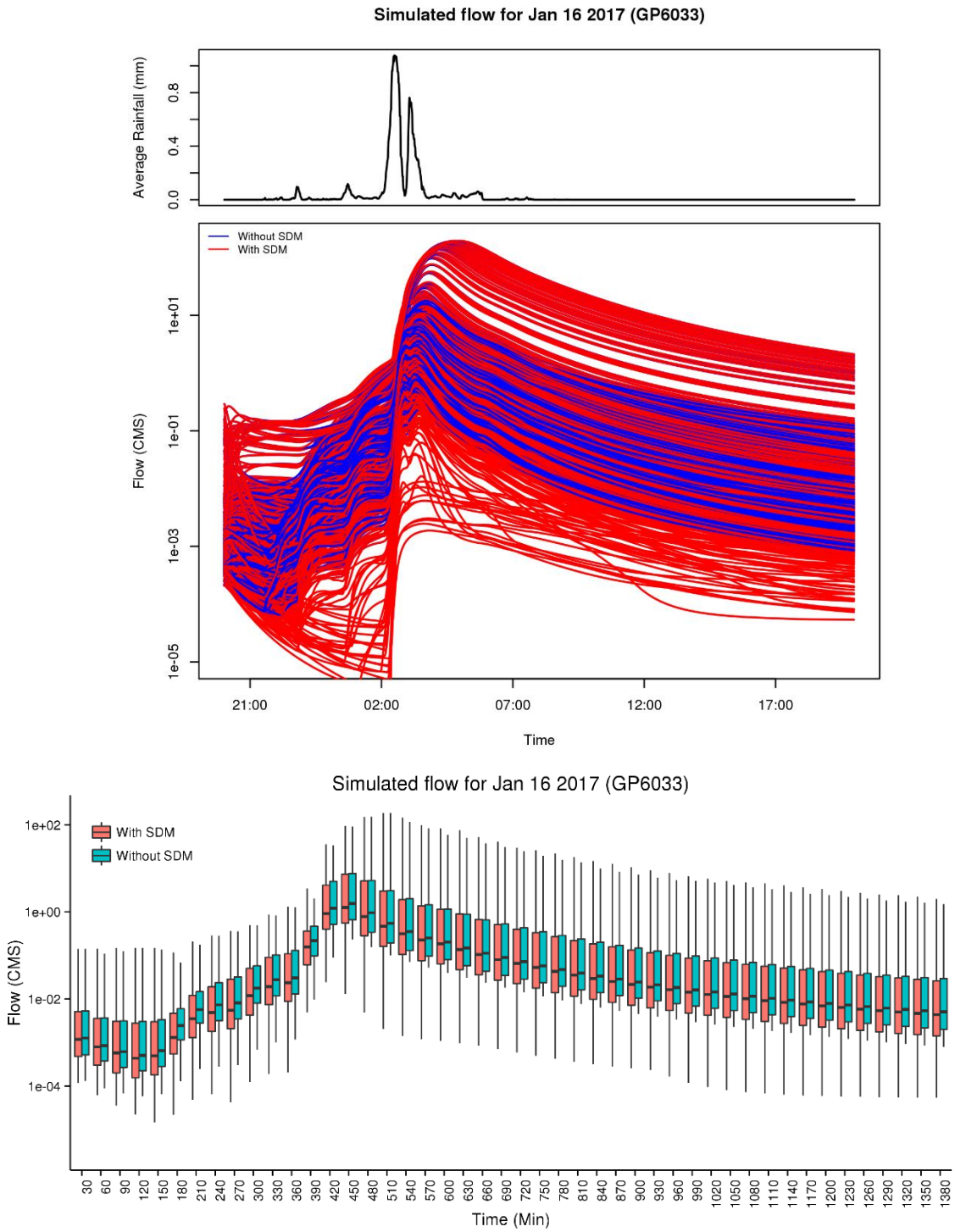

Figure 52 Simulated hydrographs of channel flow with and without storm drain modeling (upper panel) and box-and-whisker plots of the hydrographs in logarithmic scale (lower panel)

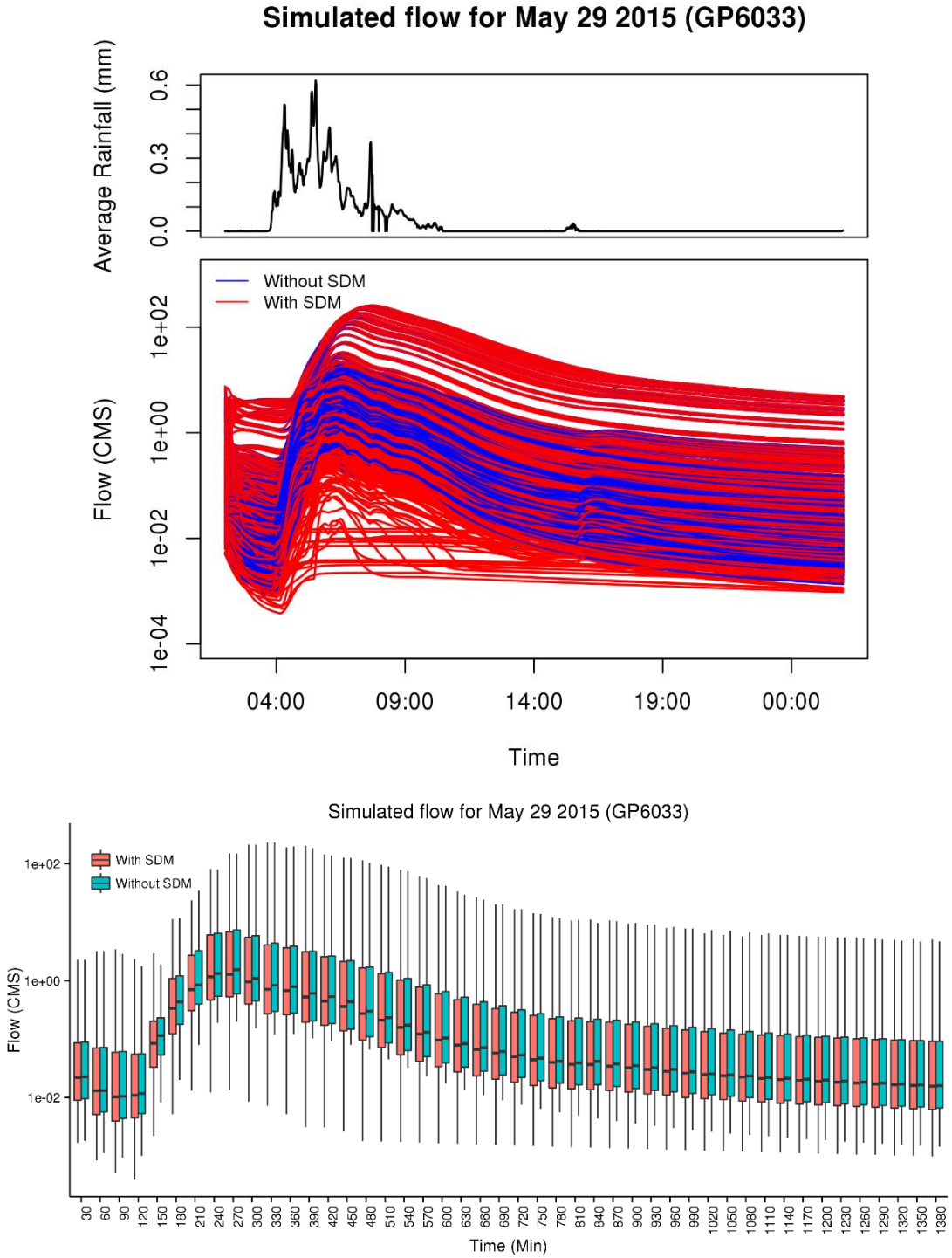

Figure 53 Simulated hydrographs of channel flow with and without storm drain modeling (upper panel) and box-and-whisker plots of the hydrographs in logarithmic scale (lower panel)

5.2.3 Impact of storm drains on peak flow

With the above analysis alone, it is not possible to associate the decrease or increase in surface flow due to storm drains with specific locations in the catchment. To that end, the ratio of the peak flow with storm drains to that without at each grid cell are calculated and the ratio over the entire catchment is mapped. This ratio is referred to herein as the peak flow ratio.

Figure 54 shows the map of the peak flow ratio for 100-yr 24-hr rainfall for the entire study area. Note in the figure that the peak flow ratio is less than unity for most cells (i.e. storm drains reduce peak flow), and that for many grid cells in which a large number of inlets are located the ratio is smaller. Figure 55 shows the map of the peak flow ratio exceeding unity but only for those cells that do not contain outfalls. In this way, those cells for which the increased peak flow may be due to direct discharges from storm drains are excluded from consideration. Because channel flows downstream may still be increased due to outfalls located upstream, some of the colored cells shown in Figure 55 are likely to be of higher-order natural streams for which storm drain systems are not of concern. All other colored cells in Figure 55 may be considered as not being served well by the existing stormwater infrastructure in that peak flow has increased due to storm drains compared to the storm drain-less conditions.

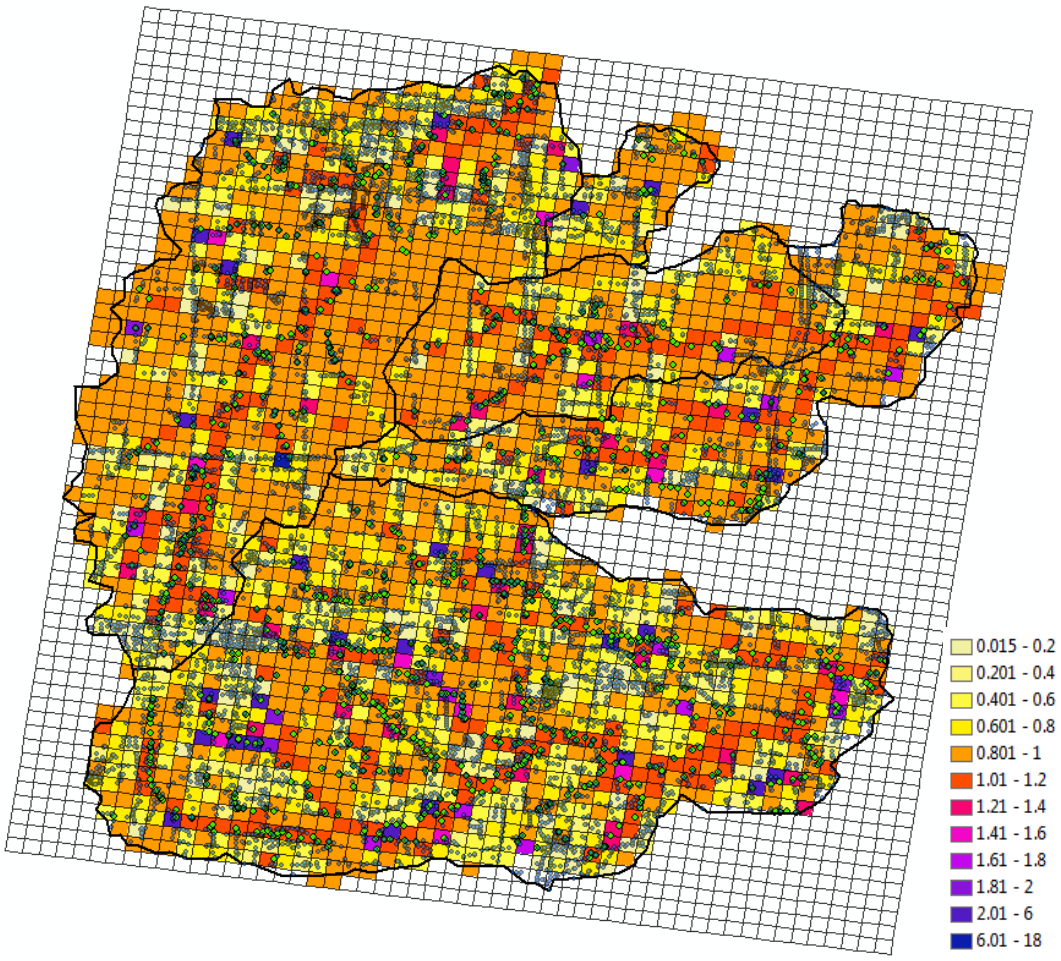

Figure 54 Map of the peak flow ratio for 100-yr 24-hr rainfall for the entire study area.

In the DFW area and elsewhere, continuing urbanization is expected to alter the hydrologic response of urban catchments. Analysis of the NLCD land cover of 2001, 2006 and 2011 for the DFW area indicates that imperviousness has increased by about 15 percent between 2001 and 2011. Figure 56 is the same as Figure 54 but the peak flow with storm drains under the existing condition (i.e., the denumerator in the peak flow ratio) has been replaced with that under a uniform 15% increase in

imperviousness in all catchments. Note that, with the increase in imperviousness, the area of the peak flow ratio exceeding unity has greatly increased, indicating that in many areas the existing storm drains would no longer be adequate 30%. The above maps demonstrate the value of integrated modeling of natural channels and storm drains for planning and management of stormwater infrastructure.

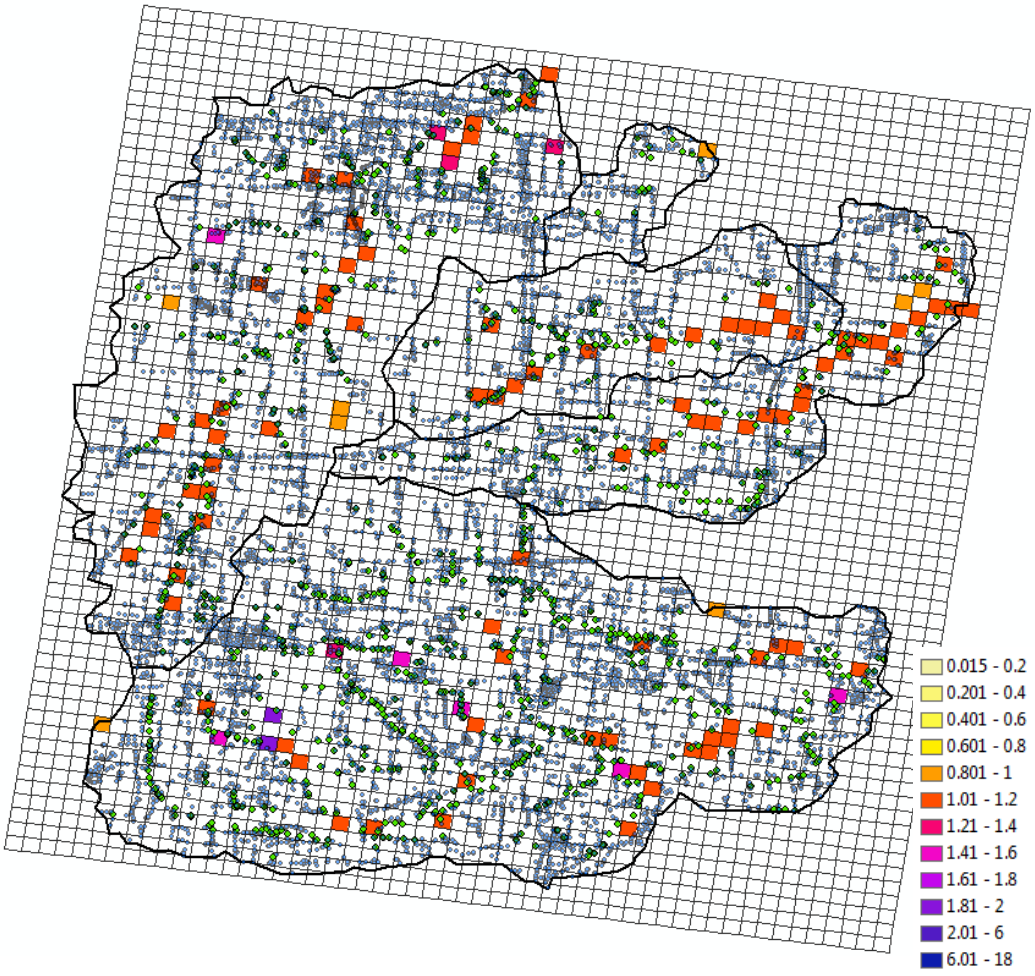

Figure 55 Map of the peak flow ratio exceeding unity but only for those cells that do not contain outfalls.

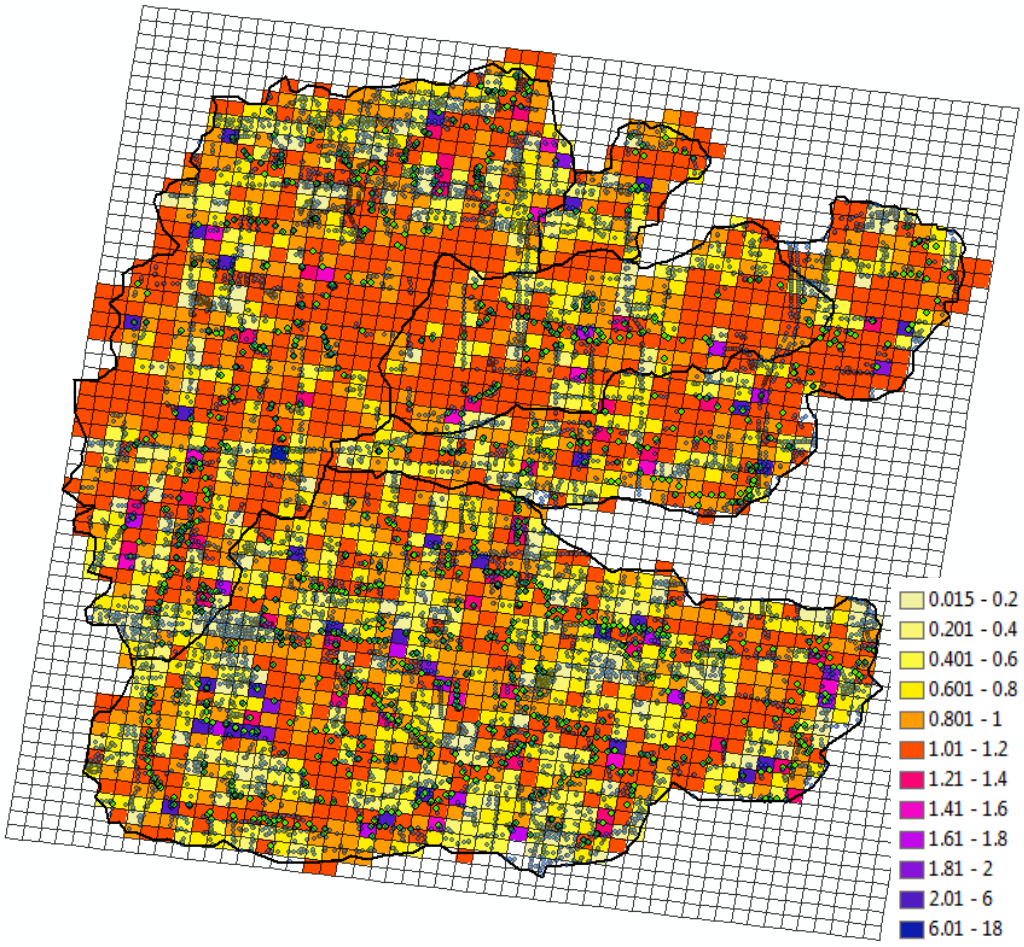

Figure 56 Same as Fig 54 but the peak flow with storm drains is under a uniform 15% increase in imperviousness in all catchments.

5.2.4 Sensitivity to Initial Condition (IC) of storm drain flow and inlet flow parameters

Because the residence time of stormwater in the storm drain network is only in the order of 10 hours or less for the study catchments, in most situations one may safely initialize the equivalent network with no flow conditions. During the course

of an event, however, the quality of the state of the storm drain model may deteriorate. It is hence instructive to assess the impact of the model state in the storm drain network on time-to-peak and peak flow. Figures 57 and 58 show the comparisons of time-to-peak and peak flow between the two bounding conditions of completely empty and full equivalent storm drain networks due to a 100-yr return period rainfall of 5-min duration.

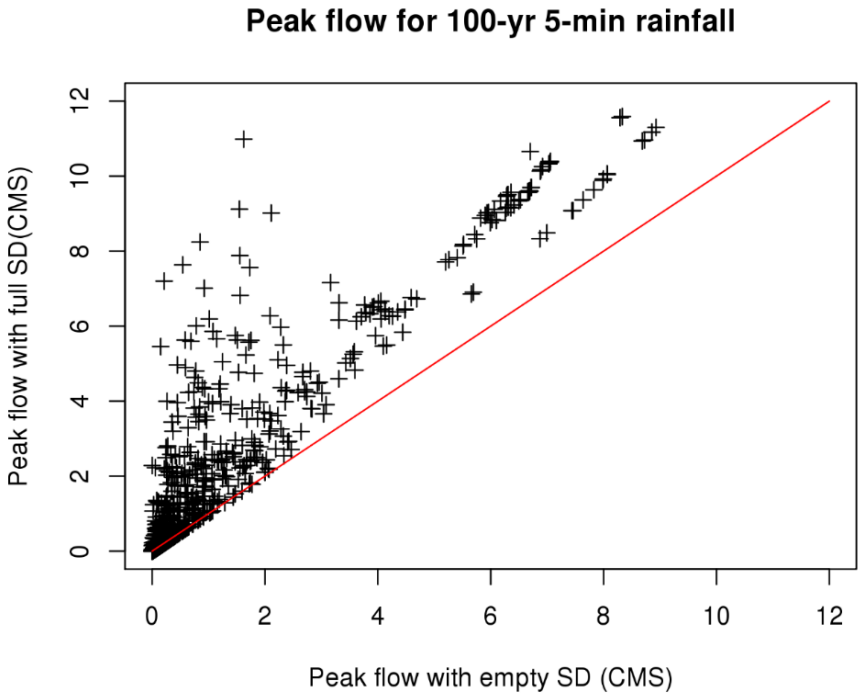

Figure 57 Comparisons of peak flow between the two bounding conditions of completely empty and full equivalent storm drain networks

The figures indicates that the accuracy of the state variable in the storm drain model, A_p in Eq.(15), may potentially impact the quality of simulation

significantly, particularly for those events in which the storm drains may undergo filling and draining successively, e.g., from successive short-duration pulses of rainfall.

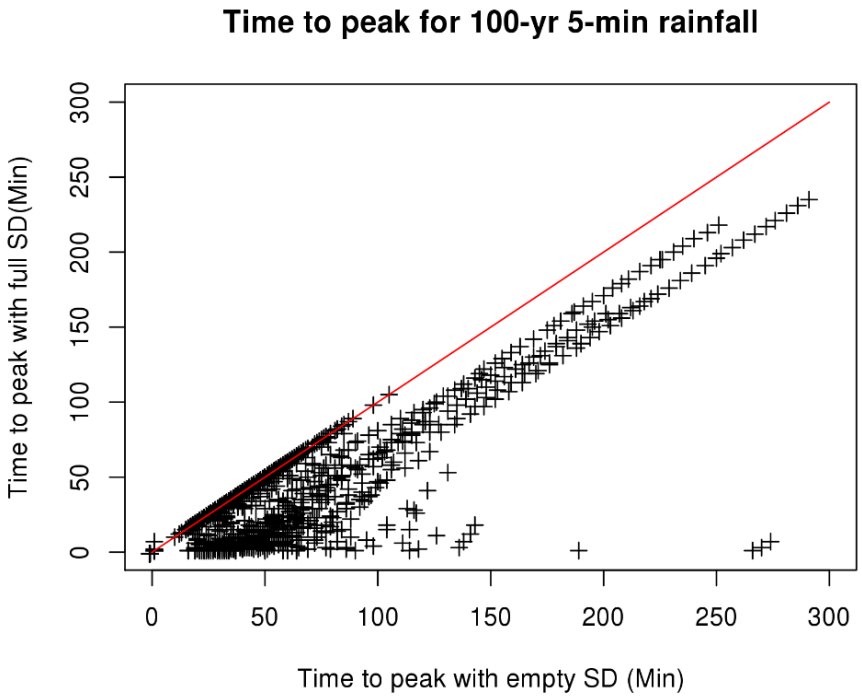

Figure 58 Comparisons of time to peak between the two bounding conditions of completely empty and full equivalent storm drain networks

Whereas flow through storm drain systems is well understood, modeling flow into storm drains is subject to significant sources of uncertainty. In this work, inlet flows are determined based on uniform kinematic-wave water depth over the paved areas in each grid cell assuming either weir or orifice flow. In reality, however, inlet flow is partitioned from gutter flow whose depth is typically larger

than the uniform water depth over the entire pavement. In inlet design, inlet flow is determined by the interception rate, or the efficiency of the inlet, which depends on the gutter flow (TxDOT 2016). In this work, the uncertainty associated with partitioning hillslope runoff into inlet and channel flows are assessed by evaluating the sensitivity of weir flow in Eq.(10) to the inlet length, L_w. Because changing N or C_w has the same effect as changing L_w, analysis of sensitivity on L_w amounts to that of all three parameters, N, C_w and L_w. For this reason, a wide range of values for L_w are choosen to encompass possible variations in N and C_w. Both curb-opening and depressed curb-opening inlets exist for which the weir discharge coefficient, C_w, is 0.374 and 0.286, respectively. In the study area, a curb-opening inlet has a length of 2.5 m. At many locations, however, the inlets are doubled to a length of 5.0 m. Inlets may be clogged which would effectively reduce N and/or L_w. In inlet design, clogging factors of 0.12 and 0.08 are suggested for one and two units of curb-opening inlets (Guo and MacKenzie 2012) which effectively reduces N in Eq.(10) to 0.88N and 0.92N, respectively. From the above, one may arrive at the smallest and largest values for NC_wL_w of 0.63N (=0.88Nx0.286x2.5) and 1.87N (=Nx0.374x5.0), respectively. To encompass approximately the above range of possible variations, L_w =1.7, 2.5 and 5.0 (m) are selected without reducing N and keeping C_w=0.374 which correspond to 0.63N, 0.94N and 1.87N, respectively. Then, L_w =10.0 and 50.0 (m) are added to assess the limiting conditions of effectively an unlimited inlet length. Figure 59 shows the volume of stormwater

conveyed by the natural channels vs. the storm drains from spatially uniform 100-yr return period 5-min rainfall over the five Catchments. The uppermost dotted brown line denotes the total storm water volume conveyed by both the natural and storm drain networks. Different colors represent different nominal inlet lengths. For each color, the solid and dashed lines denote the storm water conveyed via the natural channels and storm drains, respectively. The solid and dotted lines of the same color hence partition the total storm water volume into natural channel and storm water flow volume. The following observations may be made in Figures 59 and 60. The storm water volume conveyed by storm drains with a nominal inlet length of 2.5 and 5.0 m is approximately 22 and 38%, respectively, of the total runoff volume for both 5-min and 24-hr rainfall of 100-yr return period. The limiting conveyance volume by storm drains is reached at the nominal inlet length of 50 m where over 60% of the surface runoff is conveyed by storm drains. As expected, the rate of increase in the runoff volume conveyed by storm drains decreases as the nominal inlet length of the inlet increases, i.e., there is diminishing marginal value in increasing the inlet capacity. The above results suggest that significant uncertainties exist in partitioning surface runoff into natural channel and storm drain flows. Whereas uncertainty analysis for stormwater infrastructure for a large area using 1D-2D modeling would be an extremely expensive proposition for both modeling and computing, the integrated modeling approach described in this

work makes such analysis well within the realm of possibility even for very large areas.

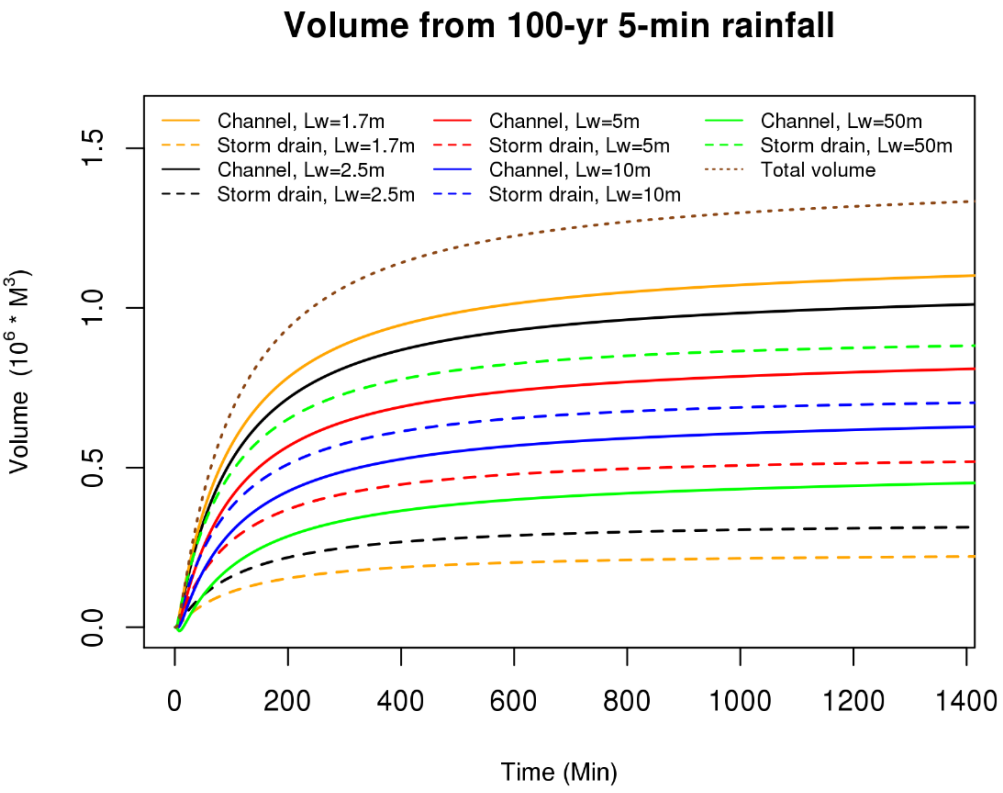

Figure 59 Volume of stormwater conveyed by the natural channels vs. the storm drains

Currently, simulation of the integrated model for a 24-hr event takes 3-4 hours and 25-30 min with 1-min time step at 250-m resolution for the study area (144.6 km^2) with and without the storm drain module, respectively. The current version of the integral model, however, has very large room for improvement in computational efficiency. It is expected that a two- to three-fold reduction in

computing time is easily achievable without parallelization, a task left for future endeavors.

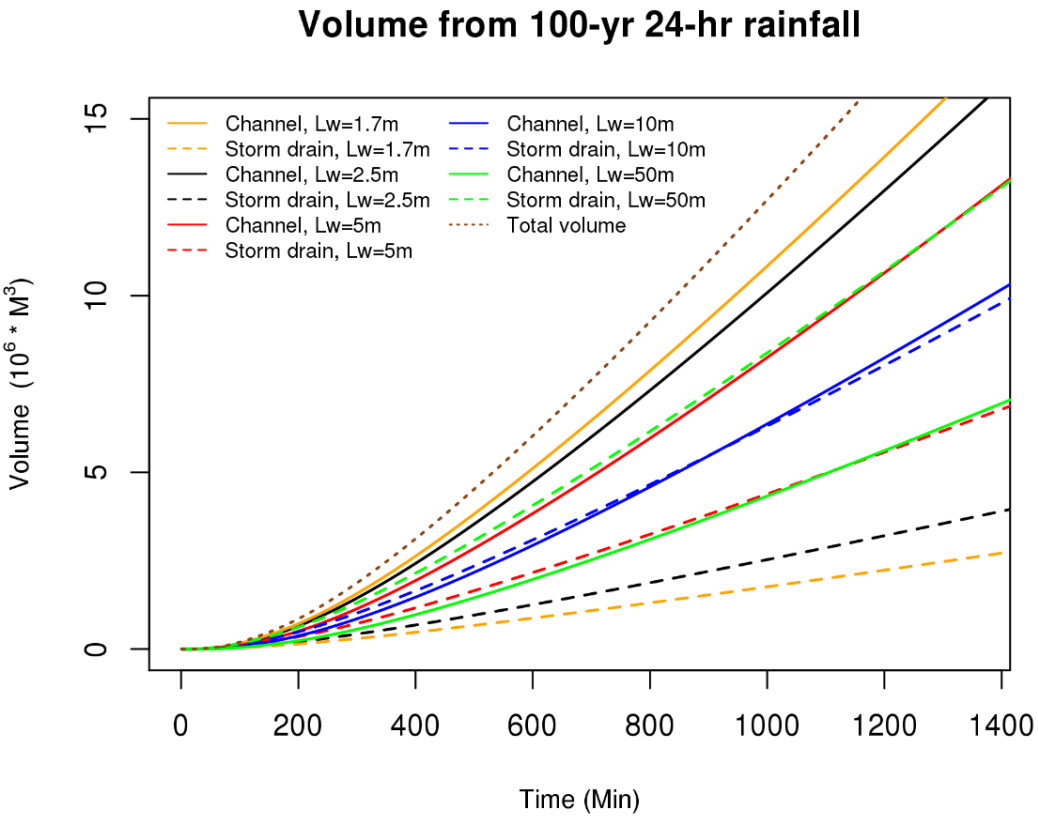

Figure 60 Volume of stormwater conveyed by the natural channels vs. the storm drains

Chapter 6

Conclusions and future research recommendations

Urban flooding is a serious problem in large and highly populated areas. If effective high-resolution prediction and warning capabilities exist for all urban areas, many lives would be saved and economic losses would be greatly reduced. The use of weather radar and distributed hydrologic modeling is a natural progression for high-resolution observation and modeling of large urban areas.

In the first part of this research, the potential value of a prototype high-resolution flash flood forecasting system for DFW is demonstrated through two case studies of the flash flooding events in Fort Worth. The hydrologic model used is HL-RDHM developed by the U.S. National Weather Service (NWS) operating at a 500-m resolution. The precipitation input used are the radar QPE at 500-m and 1-min resolution from the DFW Demonstration Network of CASA radars and the MPE product operationally produced by the West Gulf River Forecast Centre (WGRFC) with a spatiotemporal resolution of 4-km and 1-hr. The model simulation results are qualitatively assessed using the flooding reports received from the residents of the City of Fort Worth throughout the event. The results indicate that higher-resolution QPE and modeling improves location and temporal specificity of flooding threats, that high-quality QPE is necessary to benefit from

high-resolution modeling, and that translation of the base products into easy-to-understand and actionable information is necessary for decision support of the users. It is expected that the benefits from high-resolution distributed modelling are larger in large urban areas where population density is high and increasing urbanization changes watershed physiography. In such areas, the impact of climate change may be larger due to changing hydrologic and hydraulic conditions. The prototype flood prediction system have been implemented since spring 2015 and the hydrologic products (runoff rate, runoff 1 hr, runoff 3hr, streamflow and return period) are available in real time at http://droc1.srh.noaa.gov/dfw/.

For accurate flash flood forecasting and effective stormwater planning and management in urban areas, it is necessary to model not only the natural channel systems but also the large and complex networks of storm drains. In this work, a modular storm drain model is developed that may easily be coupled with existing gridded distributed hydrologic models for such applications and apply the integrated model to a 144.6 km^2 area consisting of five urban catchments in the Cities of Arlington and Grand Prairie in Texas, US. A salient feature of the proposed approach is the use of equivalent storm drain network. The equivalent network approximates the actual network on the same grid as the distributed hydrologic model and hence renders coupling of the storm drain module and the distributed model very simple. The gridded distributed hydrologic model used is the NWS's HLRDHM. The main findings are summarized below.

The equivalent storm drain network represents the real storm drain network very well in the study area. The proposed approach hence offers a practical pathway for integrated modeling of storm drains with gridded distributed hydrologic models for large urban areas. Comparison of simulated flow with the observed was possible only at catchment outlets due to lack of observations for smaller contributing areas. Because outlet flows integrate both the natural channel and storm drain flows in the study area, the impact of storm drains is not readily discernable. It is seen that storm drain modeling increases peak outlet flow for significant events very slightly only for smaller catchments. To assess the impact of the storm drain network, twin simulation experiments were carried out in which the integrated model was run with and without the storm drain module using impulse- and step-function representation of design rainfall. It was found that, for the highly impervious and highly urbanized Johnson Creek Catchment, the storm drain network reduces surface flow at most locations for about 30 min, and that at many locations the reduction persists well past 30 min. For the least impervious Fish Creek Catchment (Outlet 6133), on the other hand, the storm drain network reduces surface flow at most locations only for the first 10 min or less, and noticeably increase between 15 and 40 min. The above suggests that the Fish Creek Catchment may be susceptible to downstream flooding due to storm drain flow from upstream.

The twin simulation experiments also show that the storm drains reduce surface flow very significantly for a short duration at almost all grid cells in the

study area, and that at many locations the flow remains reduced for the entire duration. The results also reveal that there are locations in the Johnson Creek Catchment where the existing storm drain network increases peak flow compared to the storm drain-less conditions. The study area has experienced approximately 15% increase in imperviousness from 2001 to 2011. The integrated model simulation results indicate that, with a 15% increase in imperviousness relative to the current conditions, the existing stormwater infrastructure would lose effectiveness for approximately 30% of the study area. The above results demonstrate the potential power of the proposed integrated model not only for real-time flash flood forecasting but also for planning and management of stormwater infrastructure.

The integrated model simulations show that, for the study area, the storm water volume conveyed by storm drains with a nominal inlet length of 2.5 and 5.0 m is approximately 22 and 38%, respectively, of the total runoff volume for both 5-min and 24-hr rainfall of 100-yr return period. The above range reflects possible variations in inlet length, type and clogging. Additional uncertainties exist due to sheet flow approximation of gutter flow. As expected, the rate of increase in the runoff volume conveyed by storm drains decreases as the nominal inlet length of the inlet increases, indicating diminishing marginal value in increasing the inlet capacity. The above results suggest that significant uncertainties exist in partitioning surface runoff into natural channel and storm drain flows. Whereas

uncertainty analysis for stormwater infrastructure for a large area using 1D-2D modeling would be an extremely expensive proposition for both modeling and computing, the integrated modeling approach proposed in this work makes such analysis feasible even for very large areas. Validation of simulation results is a large challenge due to lack of streamflow sensing at sufficiently small spatial scales. It is noted here that water level sensors are in the process of deploying in the study area and elsewhere in DFW and have also launched the crowdsourcing app, iSeeFlood (Choe et al. 2017, http://ispuw.uta.edu/nsf/8-1-1description.html), to aid validation as well as real-time warning. Finally, though there are significant differences in routing operations between the HLRDHM and WRF-Hydro, the primary model in the recently launched NWM, it is expected that the storm drain module developed in this work can also be integrated with the latter for nested domains of large urban area. For such implementation, additional research is needed.

The following areas of improvement have been identified for high resolution flash flood forecasting for DFW area thus far:

- Verification
- Observation of water level, flow, soil moisture and rainfall
- Reservoir and lake modeling
- Flood frequency analysis for improved estimation of return period
- Real-time prescription of upstream boundary conditions for large rivers

- High-performance computing for hyper-resolution modeling
- Optimization of model parameters
- Real-time assimilation of water and soil moisture data to improve initialization

The following areas are future recommendations for integrated modeling of storm drain and natural channel systems thus far:

- Rigorous uncertainty analysis is necessary for the coupled model with respect to partitioning of runoff and infiltration and of storm drain flow and natural channel flow
- Assess impact of changes in precipitation frequency due to climate change
- Assess sensitivity to grid resolution
- Implement the coupled model for real time flash flood forecasting
- Integrate the storm drain module with WRF-Hydro for nested domains of large urban area
- Improve computational efficiency, robustness and operational worthiness of the modeling software

Appendix A

Time series of simulation and observation results for GP6363 using CASA QPE and MPE

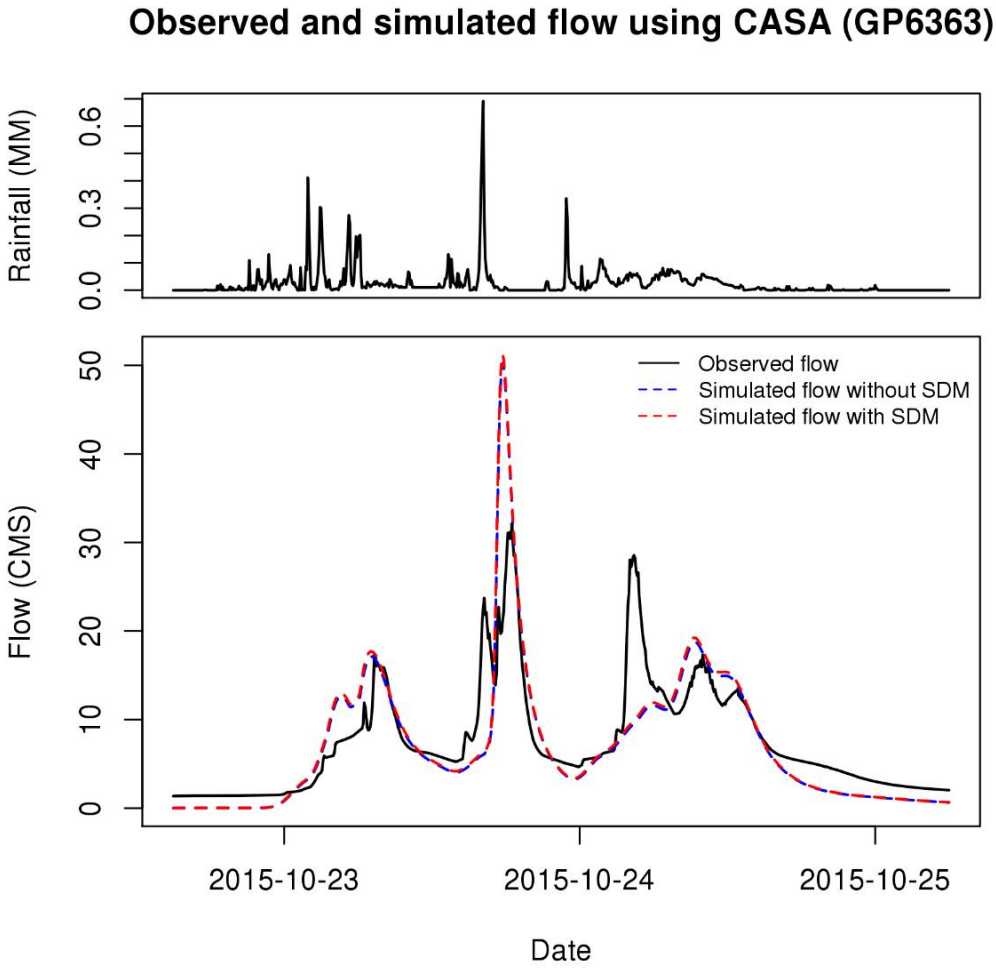

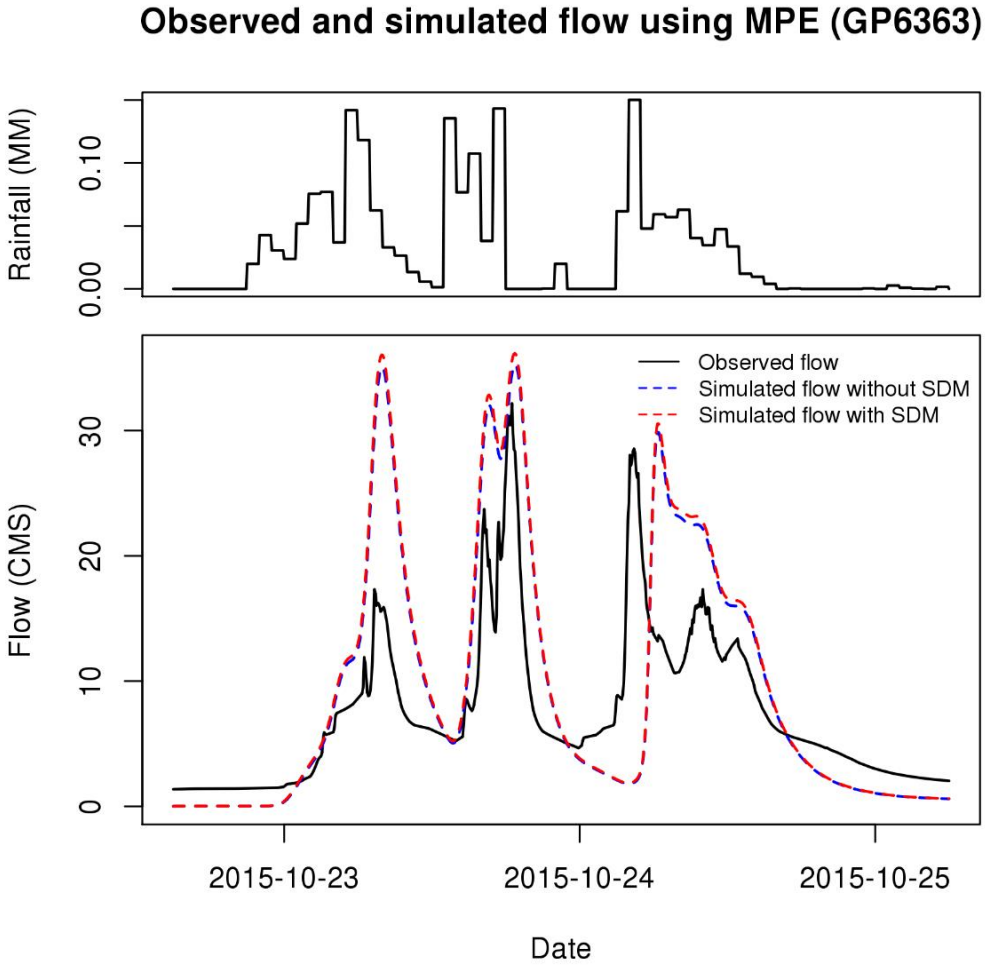
Observed and simulated flow using MPE (GP6363)
Rainfall (MM)
0.00
0.10
Flow (CMS)
0
10
20
30
Observed flow
Simulated flow without SDM
Simulated flow with SDM
2015-10-23
2015-10-24
2015-10-25
Date

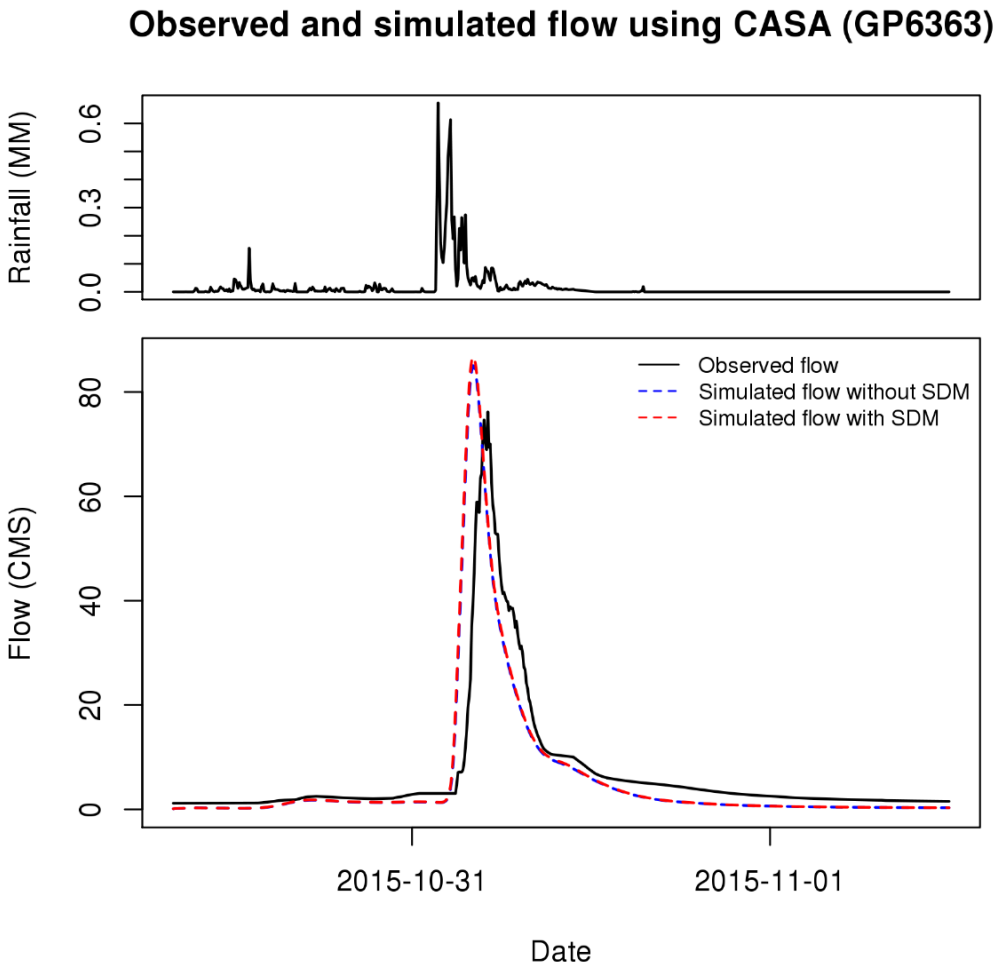
Observed and simulated flow using CASA (GP6363)
Rainfall (MM)
0.0
0.3
0.6
Flow (CMS)
0
20
40
60
80
Observed flow
Simulated flow without SDM
Simulated flow with SDM
2015-10-31
2015-11-01
Date

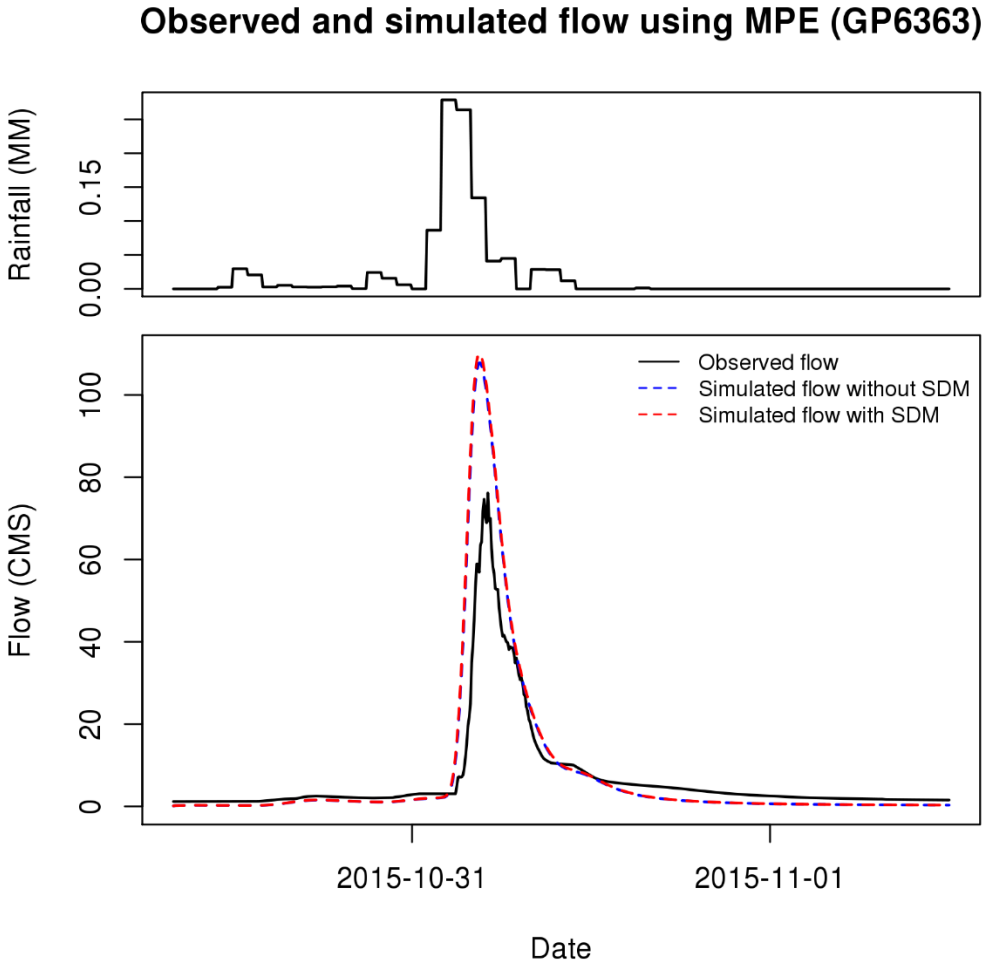
Observed and simulated flow using MPE (GP6363)
Rainfall (MM)
0.00
0.15
Flow (CMS)
0
20
40
60
80
100
Observed flow
Simulated flow without SDM
Simulated flow with SDM
2015-10-31
2015-11-01
Date

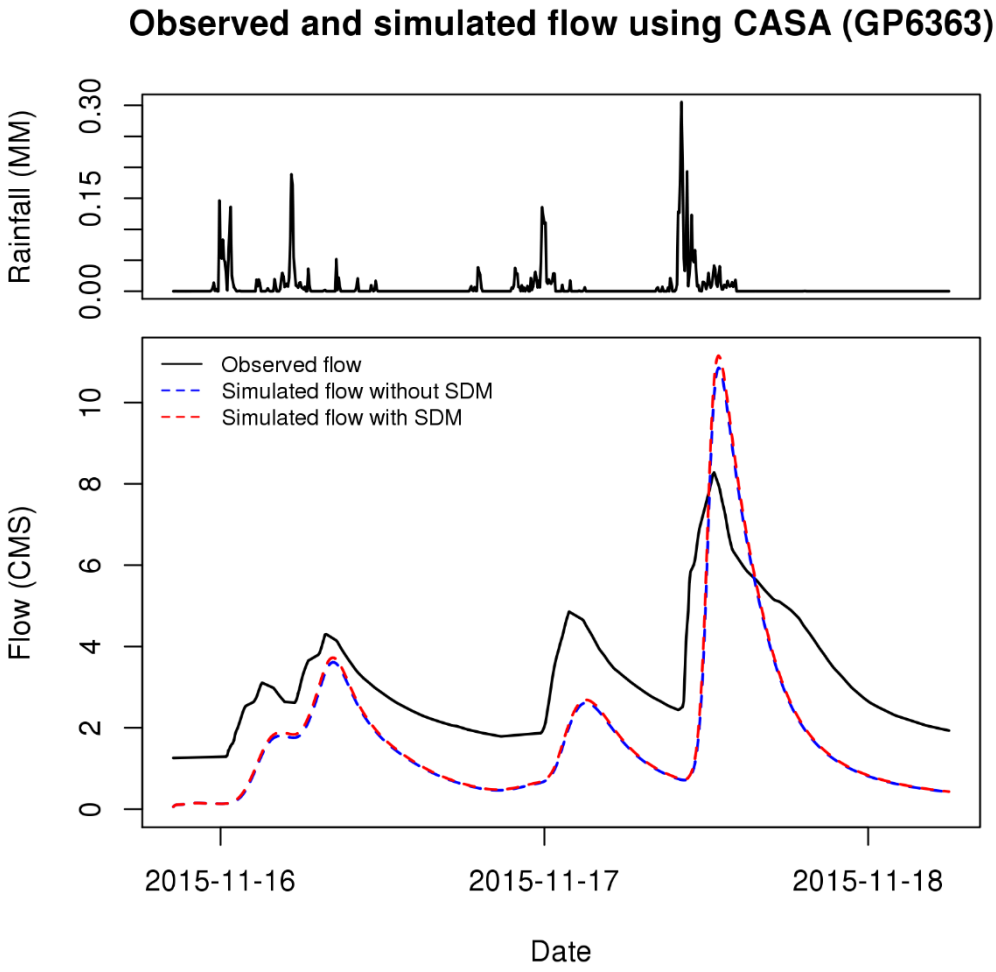
Observed and simulated flow using CASA (GP6363)
Rainfall (MM)
0.00
0.15
0.30
Flow (CMS)
0
2
4
6
8
10
Observed flow
Simulated flow without SDM
Simulated flow with SDM
2015-11-16
2015-11-17
2015-11-18
Date

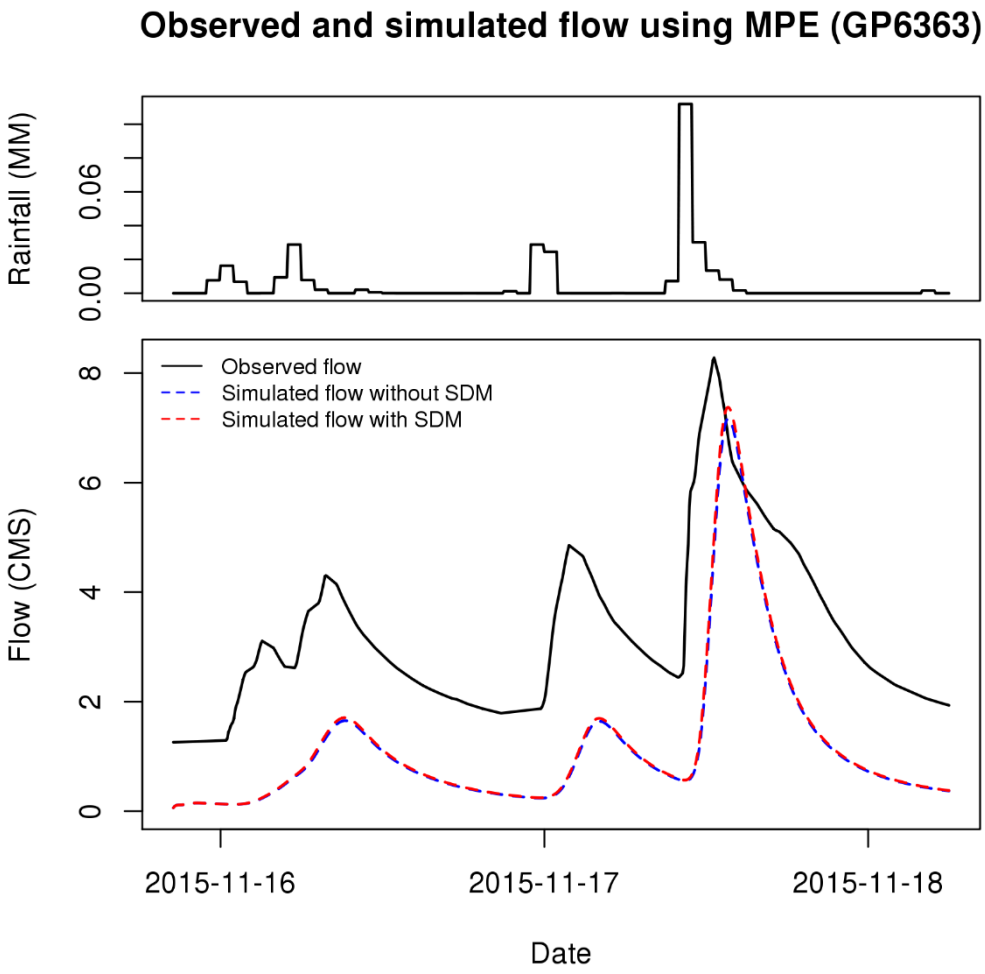
Observed and simulated flow using MPE (GP6363)
Rainfall (MM)
0.00
0.06
Flow (CMS)
0
2
4
6
8
Observed flow
Simulated flow without SDM
Simulated flow with SDM
2015-11-16
2015-11-17
2015-11-18
Date

Appendix B

Time series of simulation and observation results for GP6043 using CASA QPE and MPE

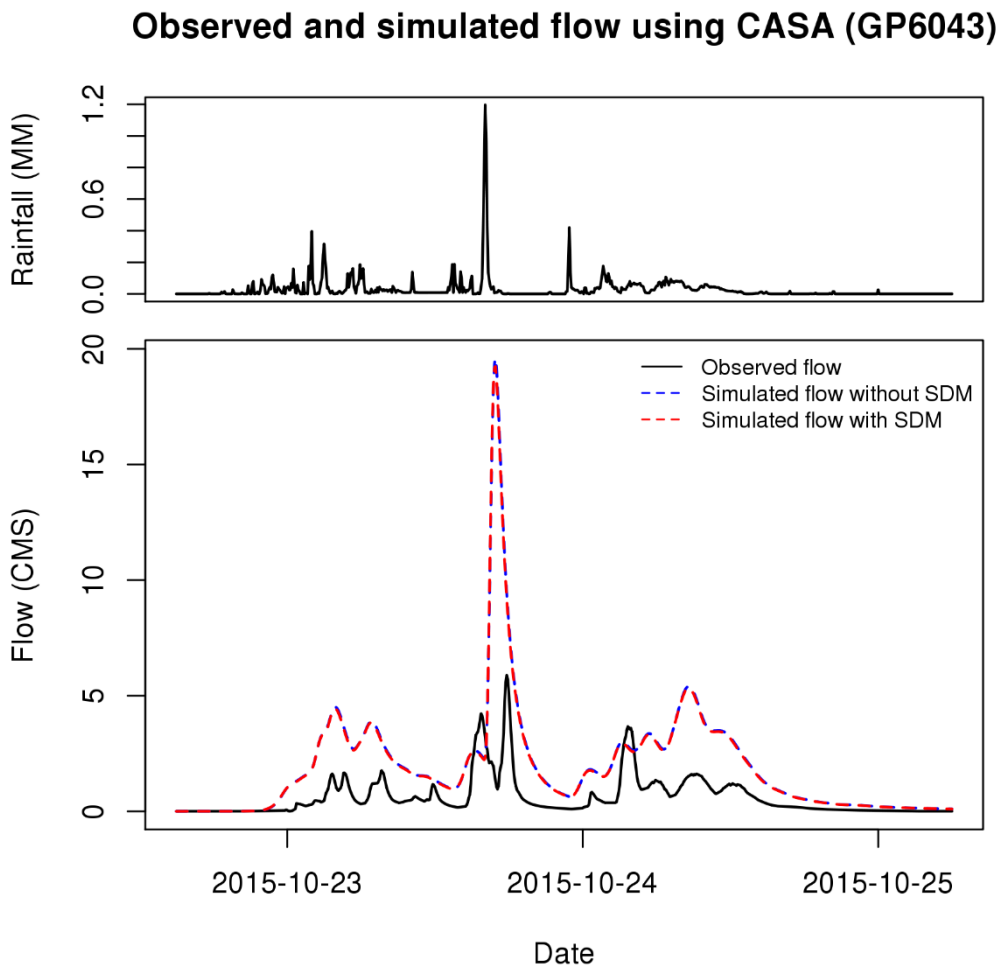

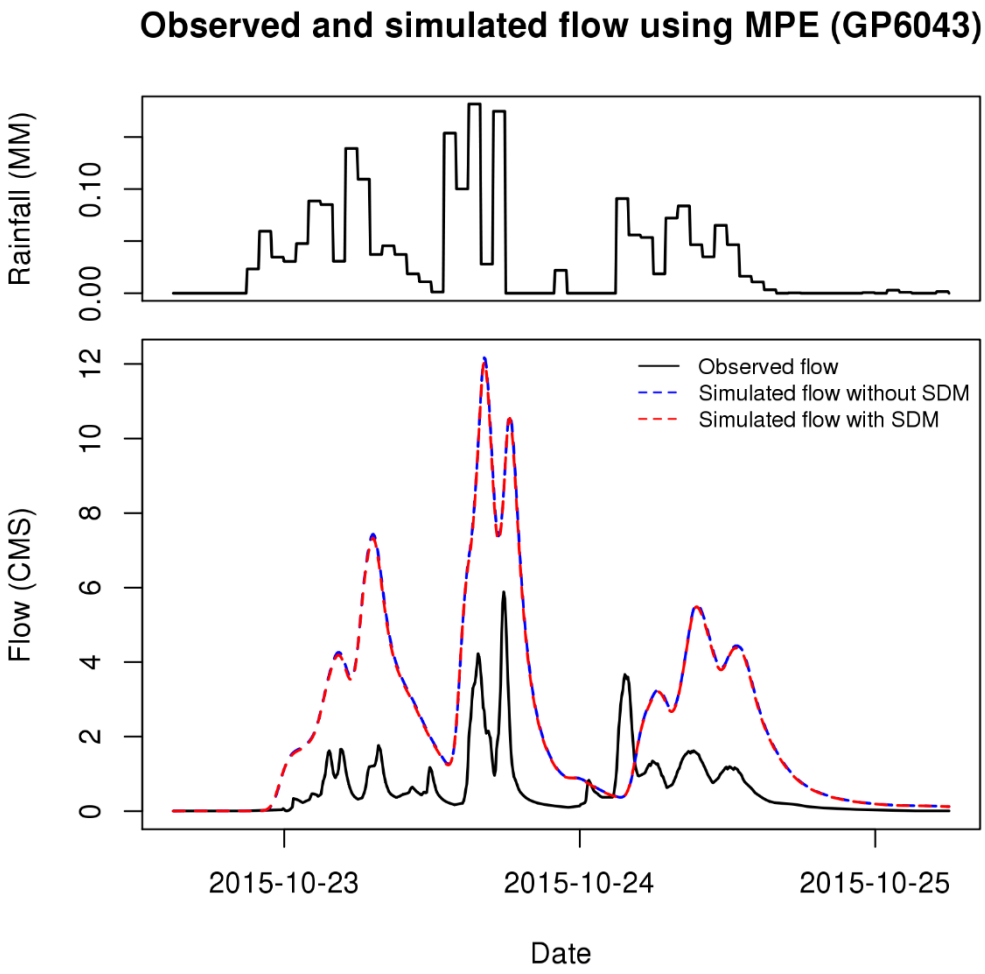
Observed and simulated flow using MPE (GP6043)
Rainfall (MM)
0.00
0.10
Flow (CMS)
0
2
4
6
8
10
12
Observed flow
Simulated flow without SDM
Simulated flow with SDM
2015-10-23
2015-10-24
2015-10-25
Date

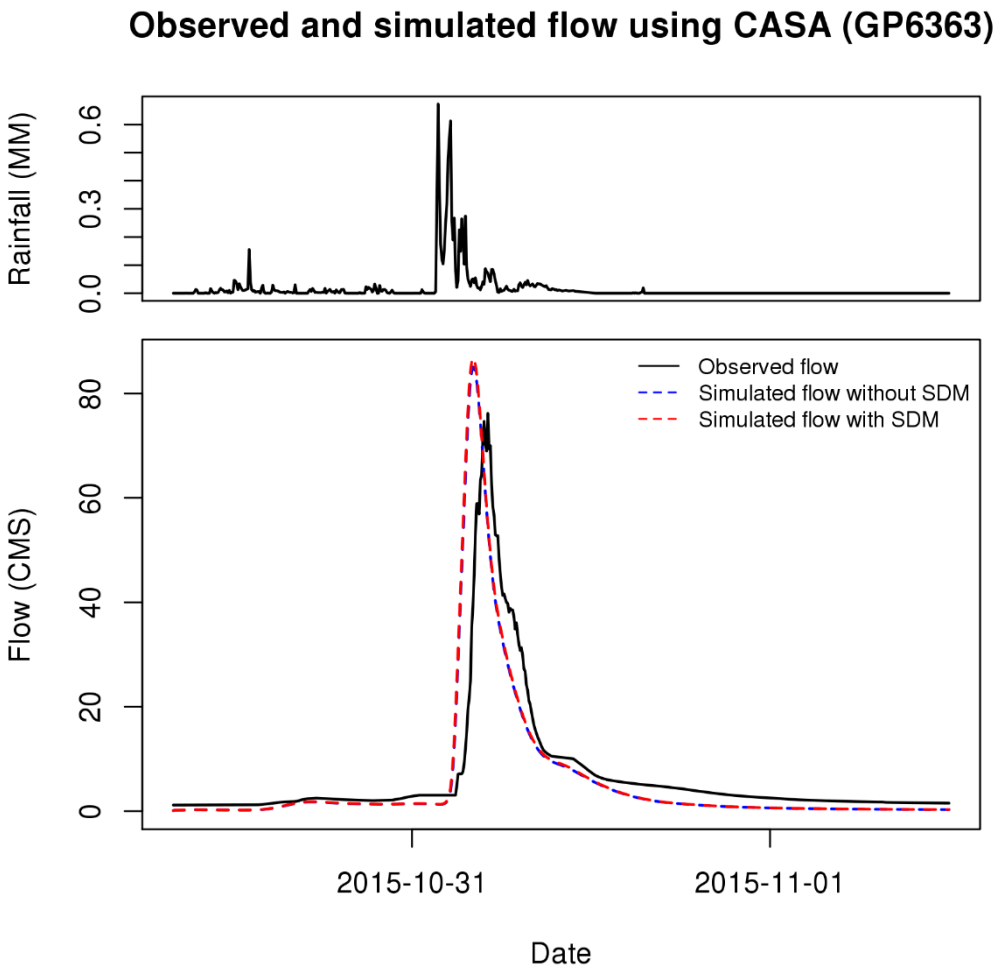
Observed and simulated flow using CASA (GP6363)
Rainfall (MM)
0.0
0.3
0.6
Flow (CMS)
0
20
40
60
80
Observed flow
Simulated flow without SDM
Simulated flow with SDM
2015-10-31
2015-11-01
Date

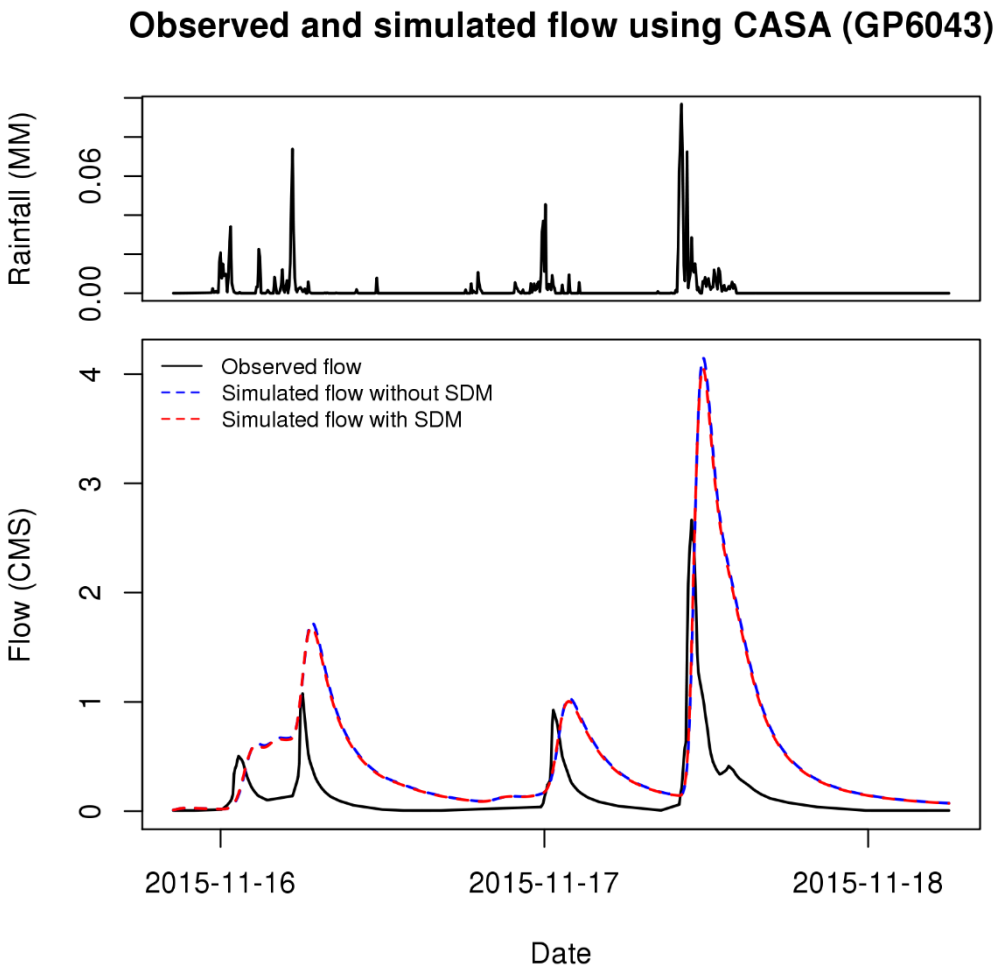
Observed and simulated flow using CASA (GP6043)
Rainfall (MM)
0.00
0.06
Flow (CMS)
0
1
2
3
4
Observed flow
Simulated flow without SDM
Simulated flow with SDM
2015-11-16
2015-11-17
2015-11-18
Date

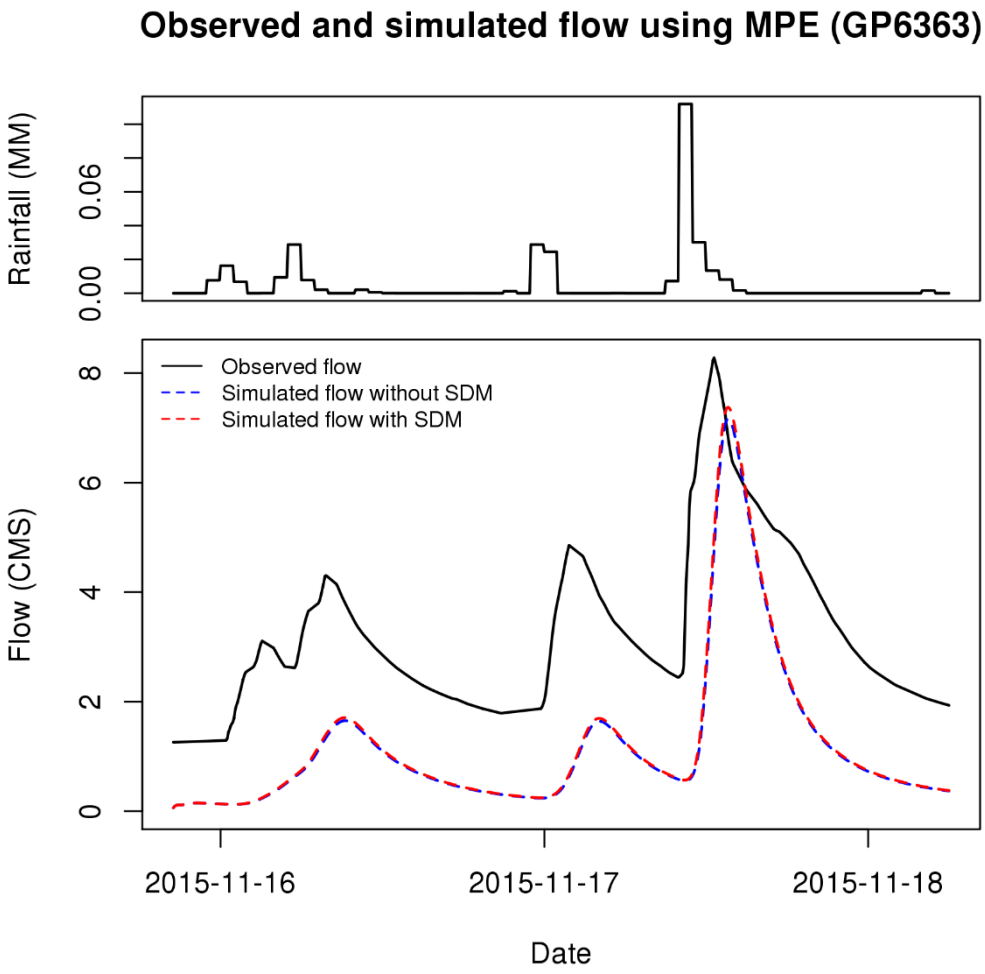
Observed and simulated flow using MPE (GP6363)
Rainfall (MM)
0.00
0.06
Flow (CMS)
0
2
4
6
8
Observed flow
Simulated flow without SDM
Simulated flow with SDM
2015-11-16
2015-11-17
2015-11-18
Date

Appendix C

Simulated hydrographs and box-and whisker plots of channel flow with and without storm drain modeling (design rainfall)

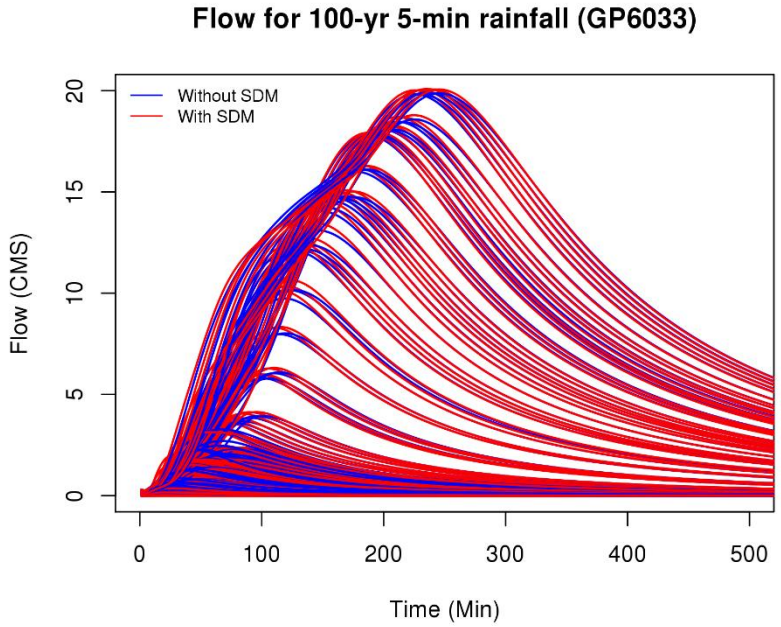

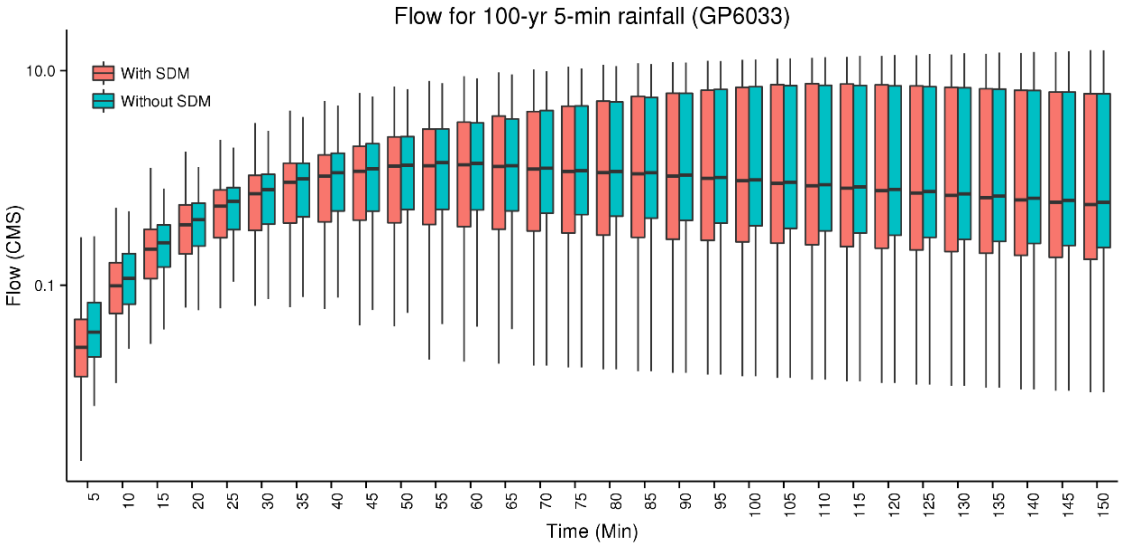

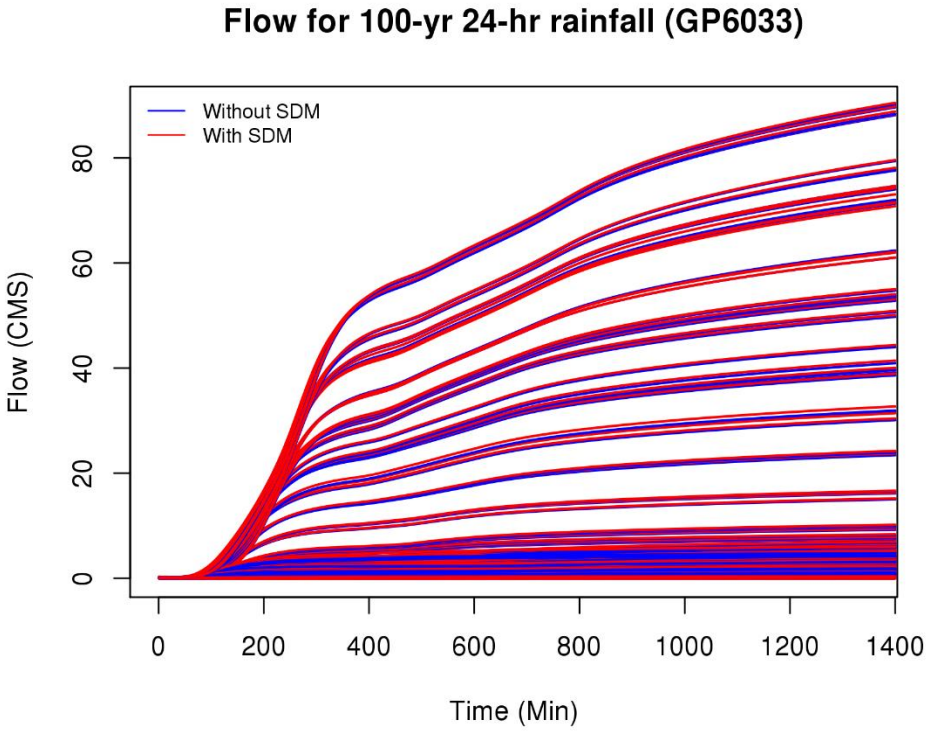
Flow for 100-yr 24-hr rainfall (GP6033)
Without SDM
With SDM
Flow (CMS)
0
20
40
60
80
0
200
400
600
800
1000
1200
1400
Time (Min)

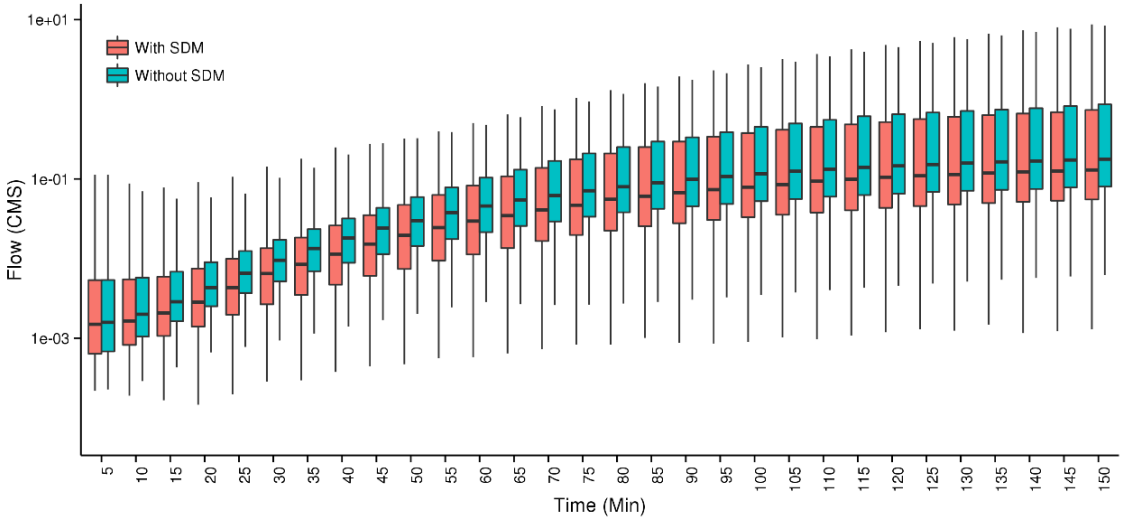
With SDM
Without SDM
Flow (CMS)
1e+01
1e-01
1e-03
5
10
15
20
25
30
35
40
45
50
55
60
65
70
75
80
85
90
95
100
105
110
115
120
125
130
135
140
145
150
Time (Min)

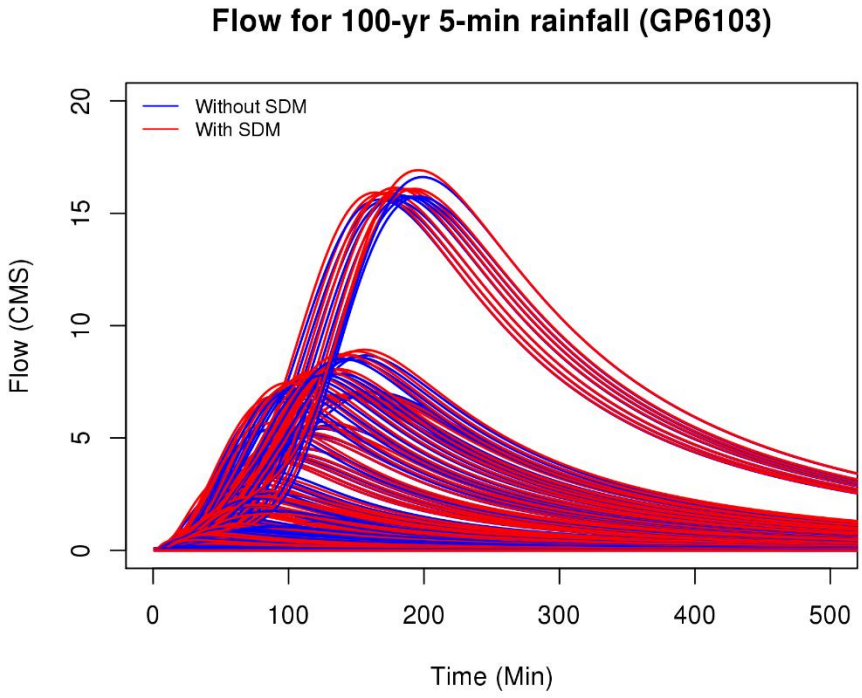
Flow for 100-yr 5-min rainfall (GP6103)
Without SDM
With SDM
Flow (CMS)
0
5
10
15
20
0
100
200
300
400
500
Time (Min)

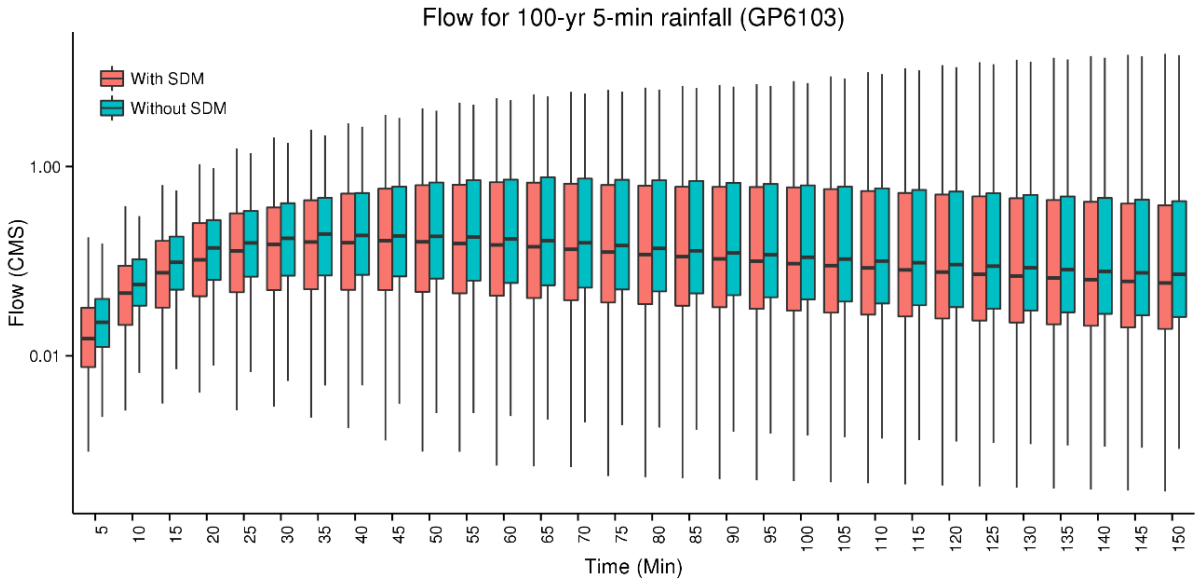
Flow for 100-yr 5-min rainfall (GP6103)
With SDM
Without SDM
Flow (CMS)
1.00
0.01
5
10
15
20
25
30
35
40
45
50
55
60
65
70
75
80
85
90
95
100
105
110
115
120
125
130
135
140
145
150
Time (Min)

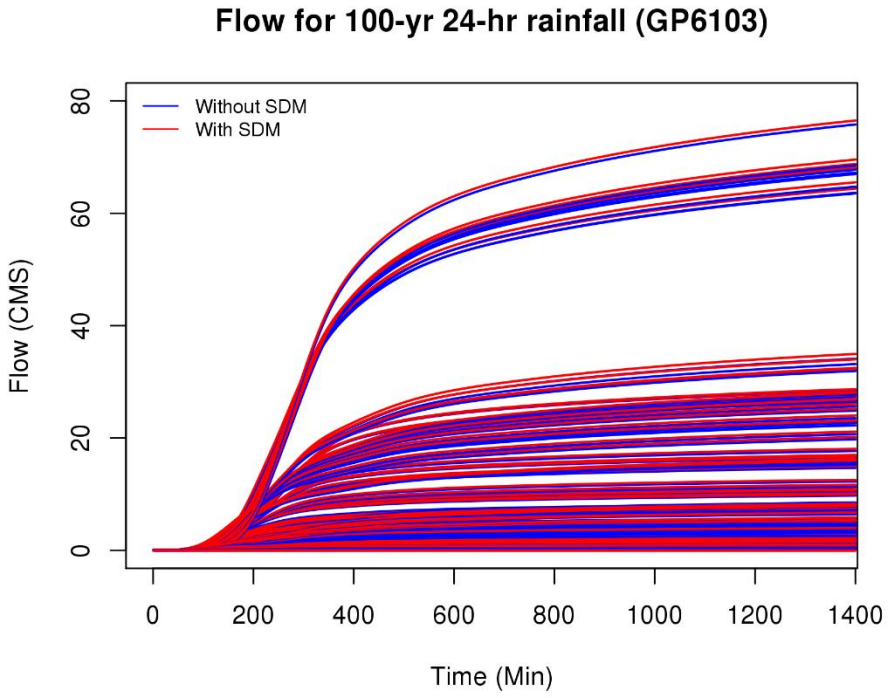
Flow for 100-yr 24-hr rainfall (GP6103)
Without SDM
With SDM
Flow (CMS)
0
20
40
60
80
0
200
400
600
800
1000
1200
1400
Time (Min)

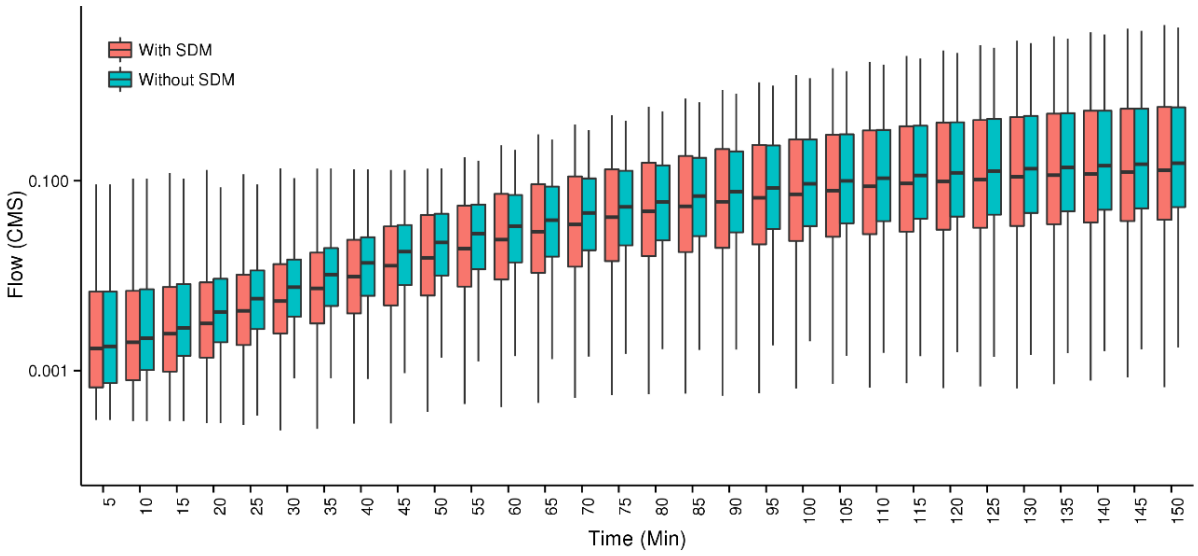
With SDM
Without SDM
Flow (CMS)
0.100
0.001
5
10
15
20
25
30
35
40
45
50
55
60
65
70
75
80
85
90
95
100
105
110
115
120
125
130
135
140
145
150
Time (Min)

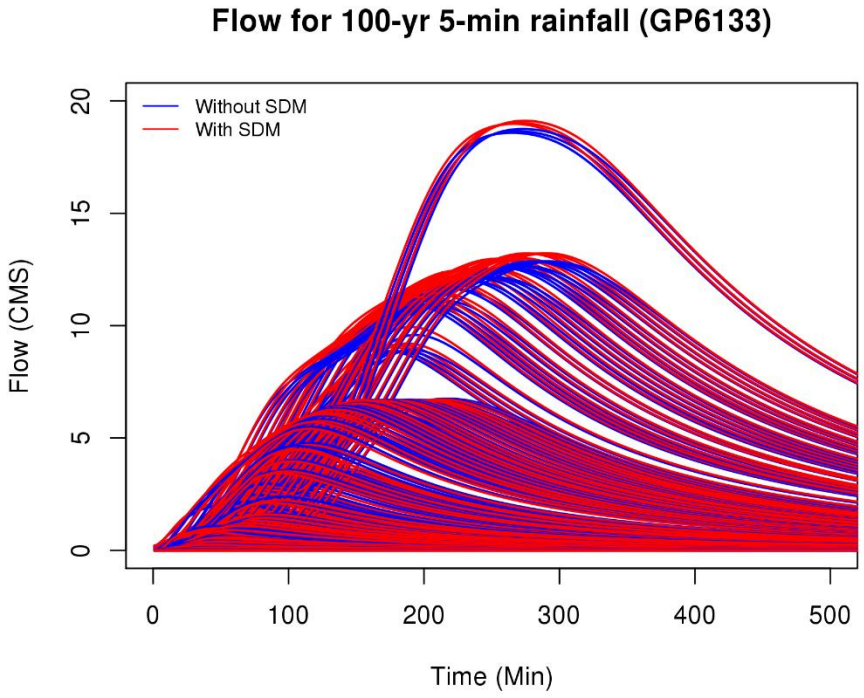
Flow for 100-yr 5-min rainfall (GP6133)
Without SDM
With SDM
Flow (CMS)
0
5
10
15
20
0
100
200
300
400
500
Time (Min)

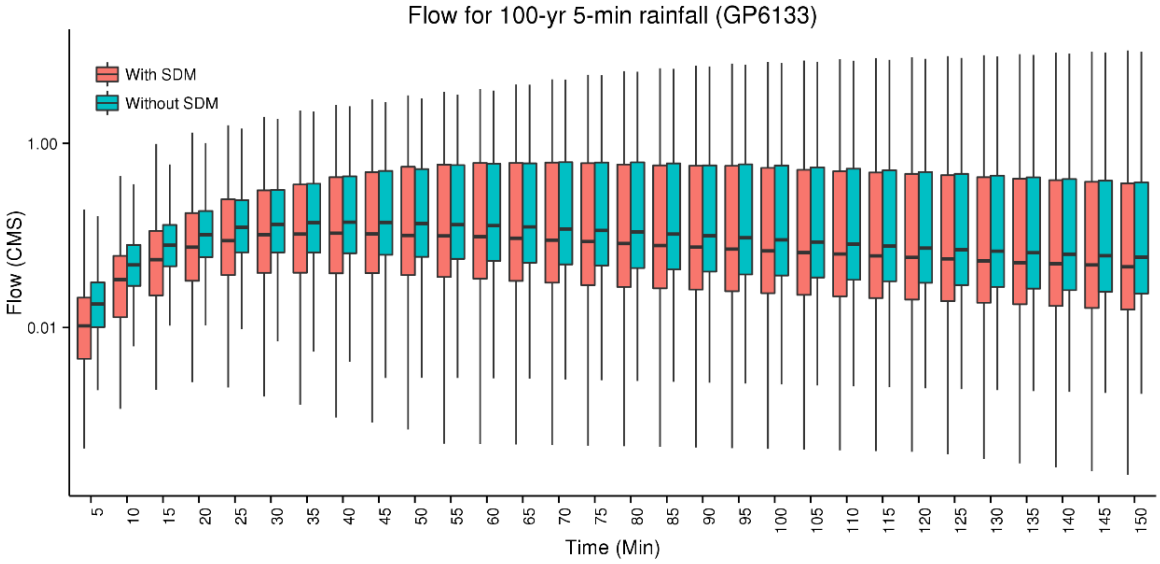
Flow for 100-yr 5-min rainfall (GP6133)
With SDM
Without SDM
Flow (CMS)
1.00
0.01
5
10
15
20
25
30
35
40
45
50
55
60
65
70
75
80
85
90
95
100
105
110
115
120
125
130
135
140
145
150
Time (Min)

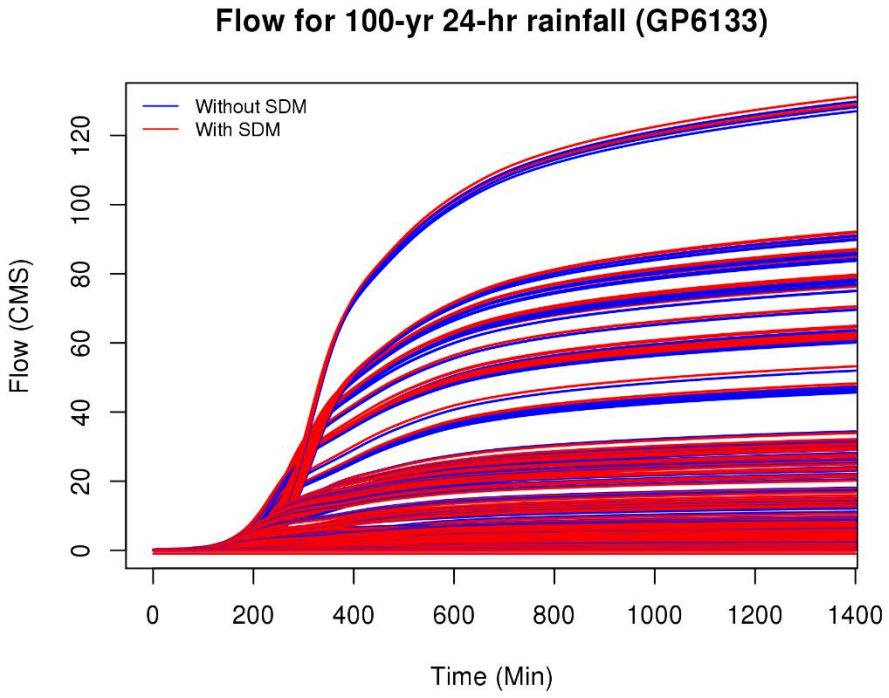
Flow for 100-yr 24-hr rainfall (GP6133)
Without SDM
With SDM
Flow (CMS)
0
20
40
60
80
100
120
0
200
400
600
800
1000
1200
1400
Time (Min)

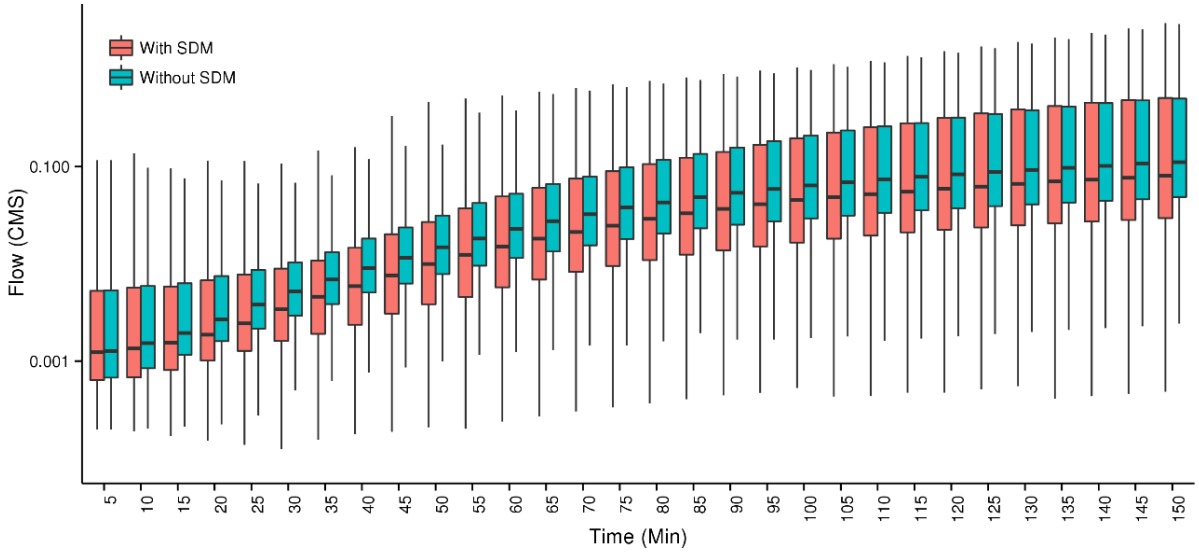
With SDM
Without SDM
Flow (CMS)
0.100
0.001
5
10
15
20
25
30
35
40
45
50
55
60
65
70
75
80
85
90
95
100
105
110
115
120
125
130
135
140
145
150
Time (Min)

Appendix D
Simulated hydrographs and box-and whisker plots of channel flow woth and without storm drain modeling (real cases)

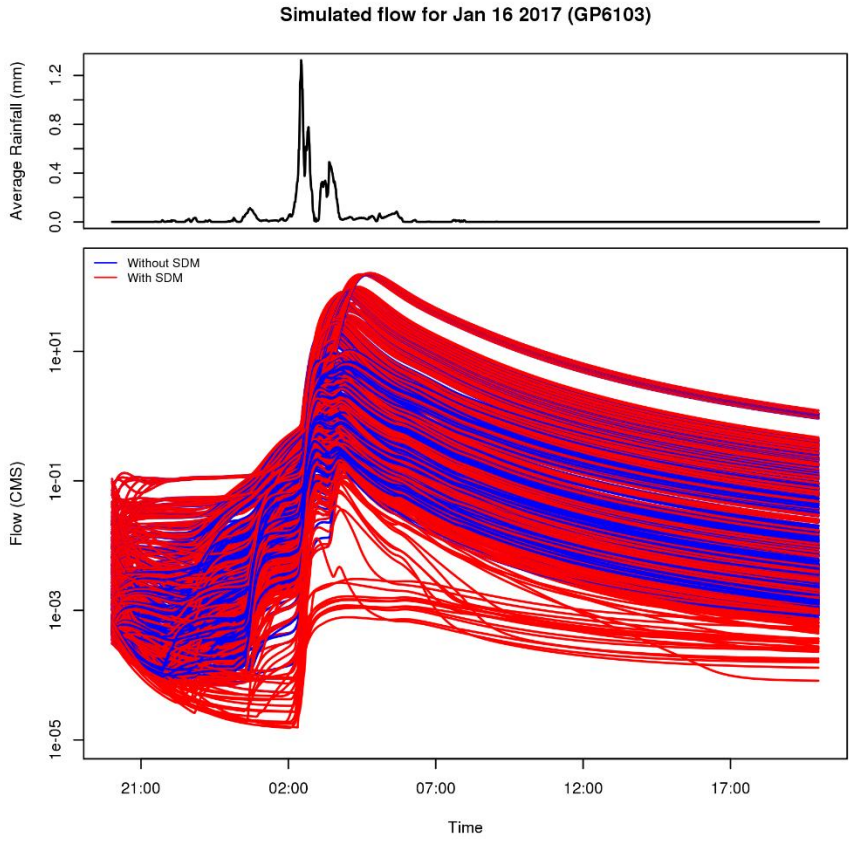

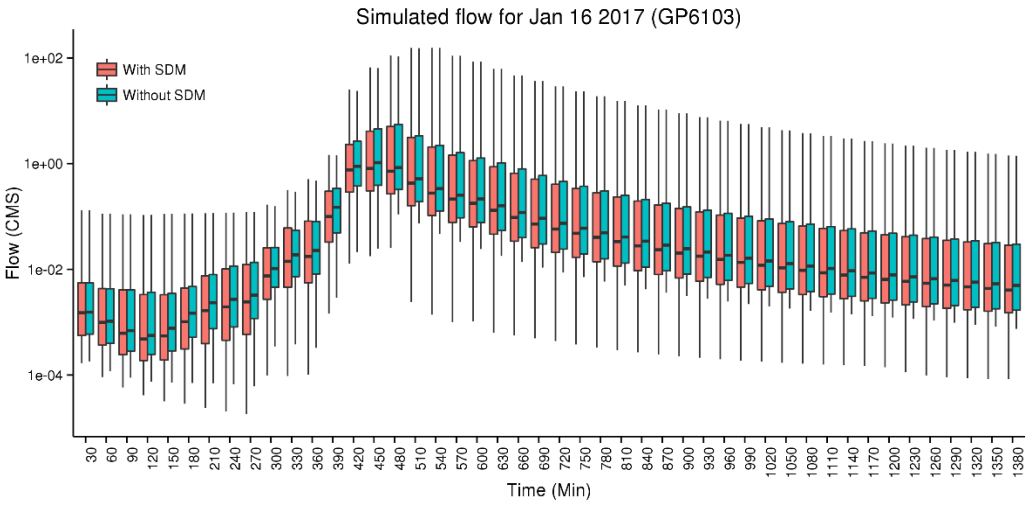

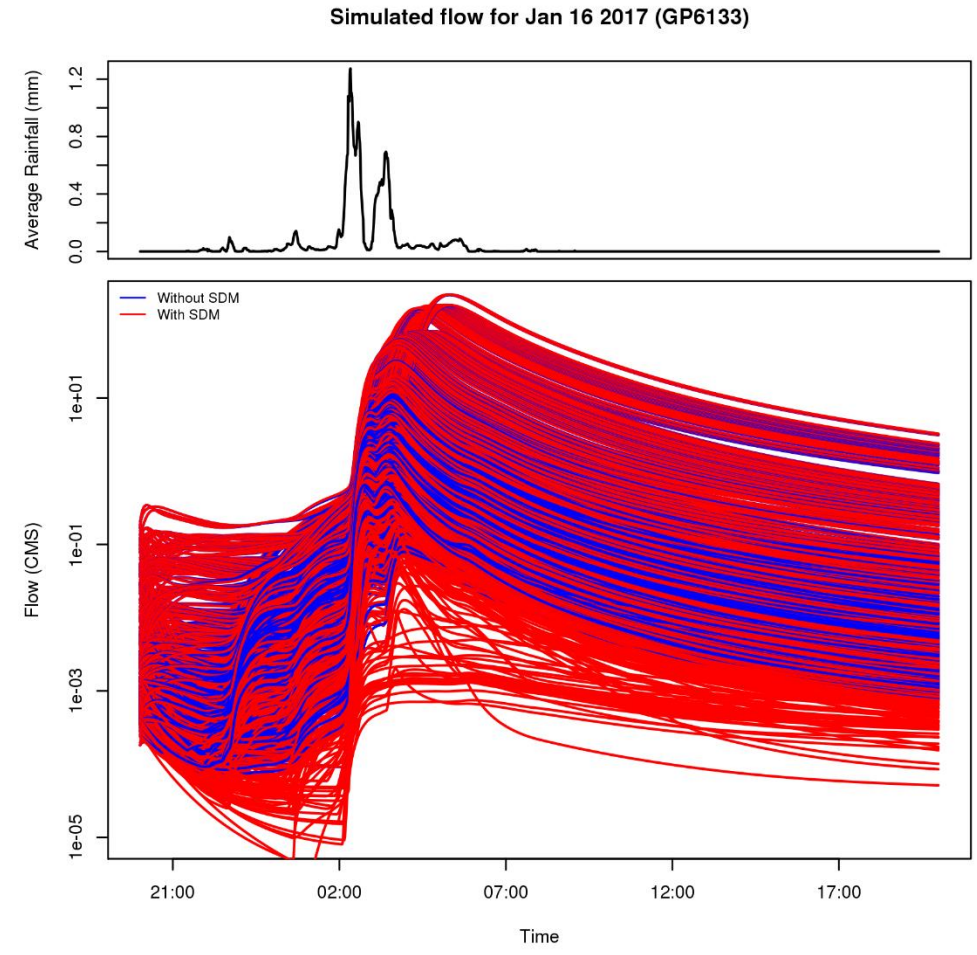
Simulated flow for Jan 16 2017 (GP6133)
Average Rainfall (mm)
0.0
0.4
0.8
1.2
Without SDM
With SDM
Flow (CMS)
1e+01
1e-01
1e-03
1e-05
21:00
02:00
07:00
12:00
17:00
Time

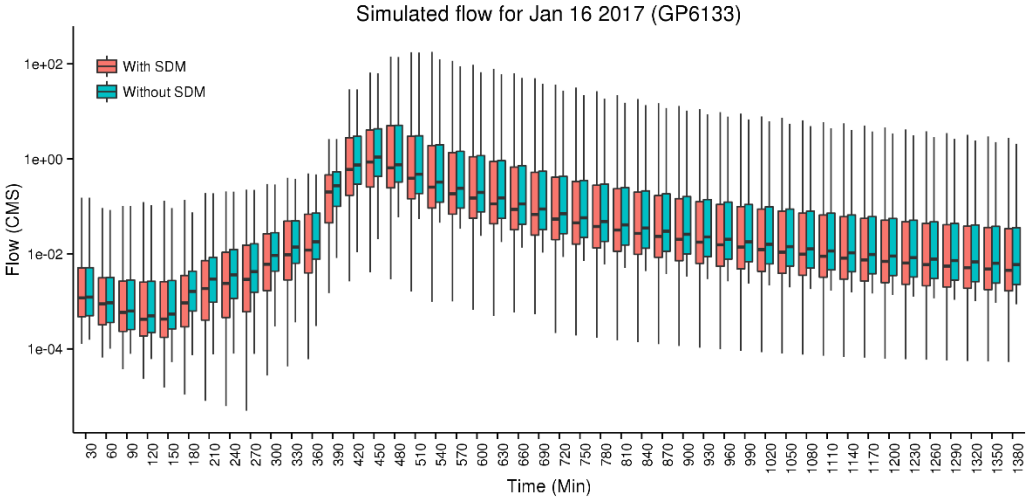
Simulated flow for Jan 16 2017 (GP6133)
With SDM
Without SDM
Flow (CMS)
1e+02
1e+00
1e-02
1e-04
30
60
90
120
150
180
210
240
270
300
330
360
390
420
450
480
510
540
570
600
630
660
690
720
750
780
810
840
870
900
930
960
990
1020
1050
1080
1110
1140
1170
1200
1230
1260
1290
1320
1350
1380
Time (Min)

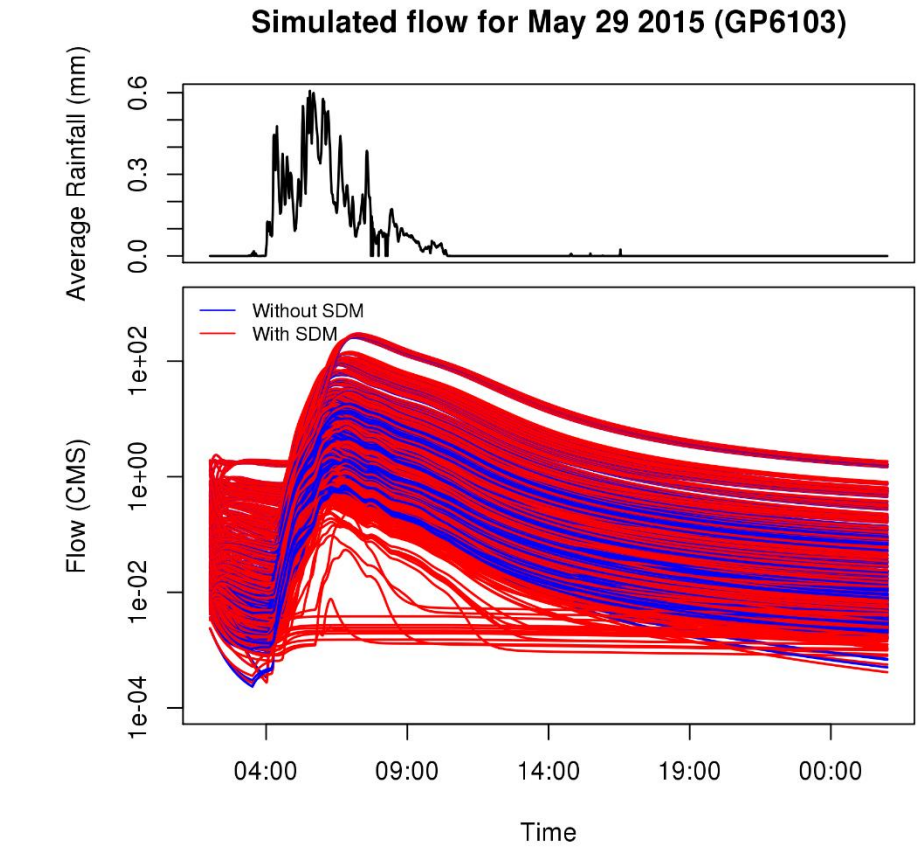
Simulated flow for May 29 2015 (GP6103)
Average Rainfall (mm)
0.0
0.3
0.6
Without SDM
With SDM
Flow (CMS)
1e-04
1e-02
1e+00
1e+02
04:00
09:00
14:00
19:00
00:00
Time

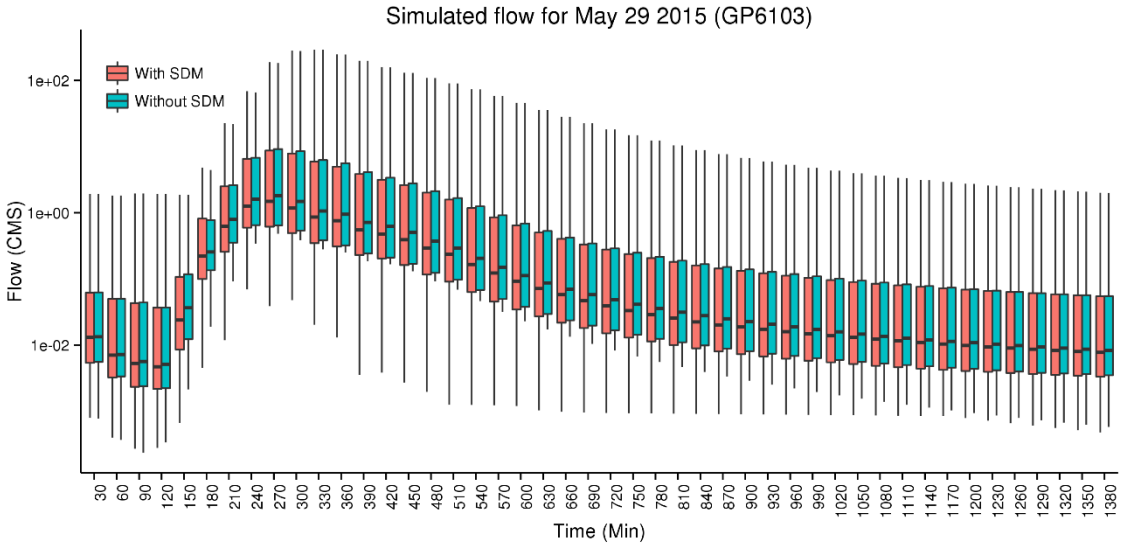
Simulated flow for May 29 2015 (GP6103)
With SDM
Without SDM
Flow (CMS)
1e-02
1e+00
1e+02
30
60
90
120
150
180
210
240
270
300
330
360
390
420
450
480
510
540
570
600
630
660
690
720
750
780
810
840
870
900
930
960
990
1020
1050
1080
1110
1140
1170
1200
1230
1260
1290
1320
1350
1380
Time (Min)

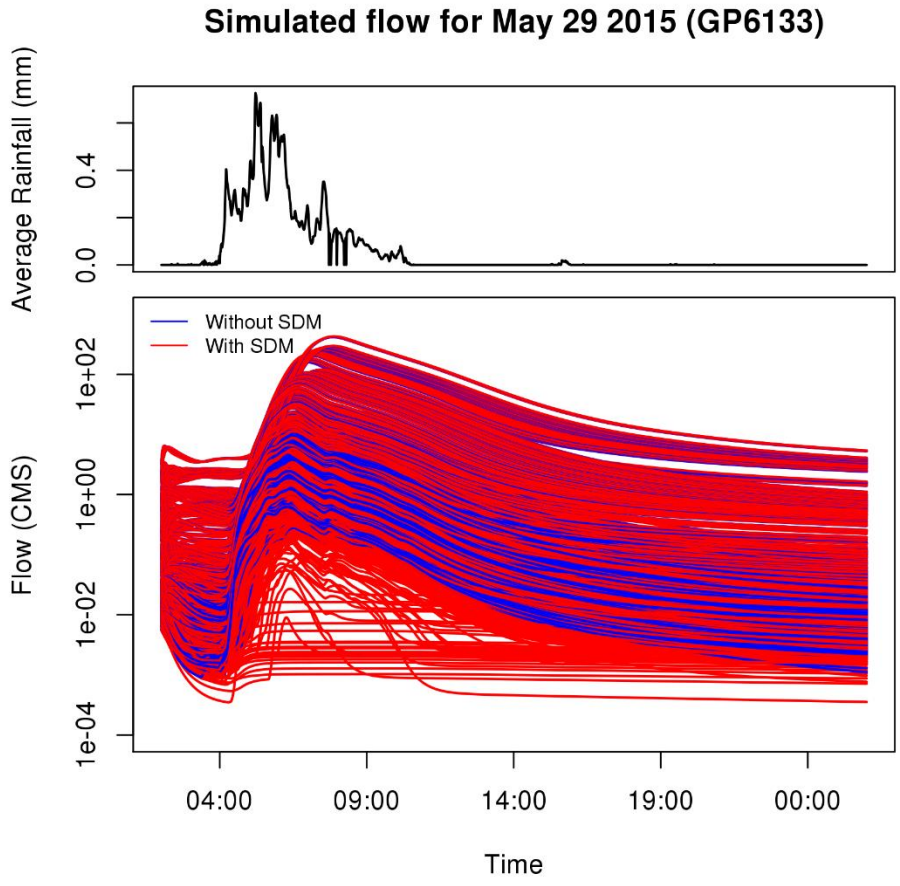
Simulated flow for May 29 2015 (GP6133)
Average Rainfall (mm)
0.0
0.4
Flow (CMS)
1e-04
1e-02
1e+00
1e+02
Without SDM
With SDM
04:00
09:00
14:00
19:00
00:00
Time

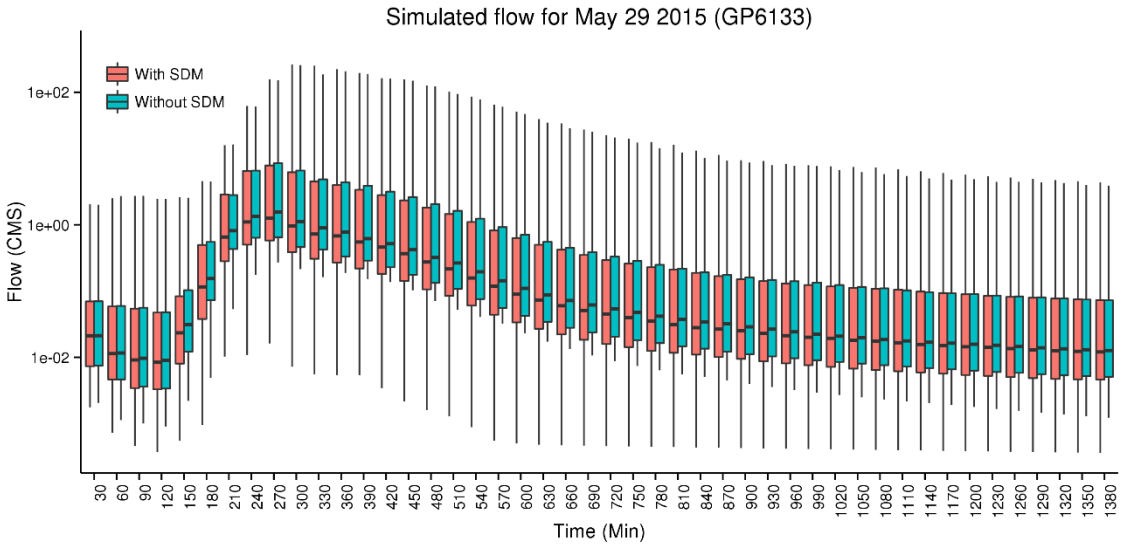
Simulated flow for May 29 2015 (GP6133)
With SDM
Without SDM
Flow (CMS)
1e-02
1e+00
1e+02
30
60
90
120
150
180
210
240
270
300
330
360
390
420
450
480
510
540
570
600
630
660
690
720
750
780
810
840
870
900
930
960
990
1020
1050
1080
1110
1140
1170
1200
1230
1260
1290
1320
1350
1380
Time (Min)

Appendix E

Script of derivation of flow direction of storm drain network

```
# This code is written by Hamideh Habibi for pipe order analysis
# 11/10/2016
##########################################        Reading input files
#####################################################################
# Pipe file
library(foreign)
library(miscTools)
pipe<-read.dbf("F:/UTA/Pojects/Natural cannel and pipe system
modeling/5catchments/Inputs/pipe_5catchmets.dbf")
A<-dim(pipe)
# GP types file
GP_types<-read.dbf("F:/UTA/Pojects/Natural cannel and pipe system
modeling/5catchments/Inputs/GP_TypesP.dbf")
C<-dim(GP_types)
# Arlington file
Arlington_types<-read.dbf("F:/UTA/Pojects/Natural cannel and pipe system
modeling/5catchments/Inputs/Arlington_TypesP.dbf")
D<-dim(Arlington_types)
# outfall  file
outfall<-read.dbf("F:/UTA/Pojects/Natural cannel and pipe system
modeling/5catchments/Inputs/outfall_5catchmets.dbf")
E<-dim(outfall)
# SLOP
groundSlop<-read.table("F:/UTA/Pojects/Natural cannel and pipe system
modeling/5catchments/Inputs/rutpix_SLOPH.asc", header=FALSE,skip =6, sep =")

##############################################      Generate empty Matrix      ##############
# for attrebiute table of pipe
Pipe_line<-matrix(-1,1,31)
colnames(Pipe_line)<-
c("Outfall_ID","Pipe_ID","Upstream","Up_type","DownStream","Down_type","Point1_x","Point1_y","Point2_x",
"Point2_y","Upstream_x","Upstream_y",

"pipe_row","culvert_row",'L_ft','D_in','W_ft','H_ft','S','A_ft2','P_ft','R_ft','Qmax_cfs','Hf_ft','HRAP_cell','HRAP_pi
pe','ID',
                'order', 'FID','order2','Manning_num')
Pipe_line<-Pipe_line[-1,]
write.csv(Pipe_line, file = "F:/UTA/Pojects/Natural cannel and pipe system
modeling/5catchments/Merging_process/Main system/Output_main/Pipe_line.csv",row.names = FALSE)

##############################################      Main Code boundary        #############
options(digits=12)
p=1
outfall_X=(outfall$START_X*(-1)*10^(10));    outfall_X=floor(outfall_X/(10^p))/((-1)*10^(10-p));
outfall_Y=(outfall$START_Y*(10^(10)));       outfall_Y=floor(outfall_Y/(10^p))/(10^(10-p));
pipe_X1=(pipe$START_X*(-1)*10^(10));      pipe_X1=floor(pipe_X1/(10^p))/((-1)*10^(10-p));
pipe_Y1=(pipe$START_Y*(10^(10)));         pipe_Y1=floor(pipe_Y1/(10^p))/(10^(10-p));
pipe_X2=(pipe$END_X*(-1)*10^(10));        pipe_X2=floor(pipe_X2/(10^p))/((-1)*10^(10-p));
pipe_Y2=(pipe$END_Y*(10^(10)));           pipe_Y2=floor(pipe_Y2/(10^p))/(10^(10-p));
GP_types_X=(GP_types$X*(-1)*10^(10));             GP_types_X=floor(GP_types_X/(10^p))/((-1)*10^(10-p));
GP_types_Y=(GP_types$Y*(10^(10)));                GP_types_Y=floor(GP_types_Y/(10^p))/(10^(10-p));
AR_types_X=(Arlington_types$X*(-1)*10^(10));          AR_types_X=floor(AR_types_X/(10^p))/((-1)*10^(10-p));
AR_types_Y=(Arlington_types$Y*(10^(10)));             AR_types_Y=floor(AR_types_Y/(10^p))/(10^(10-p));
```

```
################### To find the points in pipe and culvert files ###################
func1<-function(px,py,listx1,listy1,listx2,listy2)
{
 points_1=which((listx1==px)&(listy1==py));
 points_2=which((listx2==px)&(listy2==py));
 rows<-c(points_1,points_2);
 num<-length(rows);
 result <- list("rows" =rows, "num" =num)
 return(result)
}

#################  To find matches #########

func2<-function(p1,p2)
{
 match<-intersect(p1,p2)
 return(match)
}

#################### To find non matched between vectors and put as upstream.

func3<-function(po1,po2,po3)
{
 var1<-c(po1,po2);
 var2<-c(po3);
 matched<-intersect(var1,var2);
 all<-union(var1, var2);
 non.matched<-all[!all %in% matched];
 return(non.matched)
}

###################### to find the name and type #############
func4<-function(x,y,list1x,list1y,list2x,list2y,list3x,list3y)
{
 GP=which((list1x==x)&(list1y==y))
 AR=which((list2x==x)&(list2y==y))
 OF=which((list3x==x)&(list3y==y))
 result<-list("AR"=AR,"GP"=GP,"OF"=OF);
 return(result)
}

############

func5<-function(var1,var2)
{
 matched_points<-intersect(var1,var2);
 non.matched_points<-var1[!var1 %in% matched_points];
 number_rows<-length(non.matched_points)
 mylist<-list("n_row"=number_rows,"rows"=non.matched_points)
 return(mylist)
}

N=1                                          # for unknowns
#################################################################################################
#################################
for(i in 1:1184){  #for each row outfall location
 Pipe_line<-read.csv(file="F:/UTA/Pojects/Natural cannel and pipe system
modeling/5catchments/Merging_process/Main system/Output_main/Pipe_line.csv",head=TRUE)
```

```
 if (dim(Pipe_line)[1]==0){          # this is for numbering system of pipes
   ID=1
 }else if (dim(Pipe_line)[1]!=0){
   ID=as.numeric(max(Pipe_line$ID))+1
 }

 Order=1
 print (i)
 # First reading the outfall X,Y coordinate and ID

 outfall_ID=outfall$DES_GISID[i];
 if (paste(outfall_ID)=="NA"){
   outfall_ID=paste("outfall_",i,sep='')
 }
 x=outfall_X[i];
 y=outfall_Y[i];

 # I will search for strat and end points in pipe and culvert files to find the outfall location.
 pipe_points<-func1(x,y,pipe_X1,pipe_Y1,pipe_X2,pipe_Y2)
   if (pipe_points$num==0){
   next
 }

 matches<-func2(c(pipe_points$rows),c(Pipe_line[1:dim(Pipe_line)[1],13]))
 if (length(matches)>0) {
   next
 }

 Dstream_x=x; Dstream_y=y; Dstream_ID=outfall_ID;Dstream_type="outfall"
 output<-matrix(-1,1, 31)
 colnames(output)<-
c("Outfall_ID","Pipe_ID","Upstream","Up_type","DownStream","Down_type","Point1_x","Point1_y","Point2_x",
"Point2_y","Upstream_x","Upstream_y",

"pipe_row","culvert_row",'L_ft','D_in','W_ft','H_ft','S','A_ft2','P_ft','R_ft','Qmax_cfs','Hf_ft','HRAP_cell','HRAP_pi
pe','ID',
                'order', 'FID','order2',"Manning_num")
 output<-output[-1,]
  # I will start to find upstream locations.
   if (pipe_points$num>0){
   m=1
   output_pipe<-matrix(-1,pipe_points$num, 31)
   colnames(output_pipe)<-
c("Outfall_ID","Pipe_ID","Upstream","Up_type","DownStream","Down_type","Point1_x","Point1_y","Point2_x",
"Point2_y","Upstream_x","Upstream_y",

"pipe_row","culvert_row",'L_ft','D_in','W_ft','H_ft','S','A_ft2','P_ft','R_ft','Qmax_cfs','Hf_ft','HRAP_cell','HRAP_pi
pe','ID',
                    'order', 'FID','order2',"Manning_num")
   for (j in 1:pipe_points$num){
     k=pipe_points$rows[j]
     output_pipe<-
func6(m,k,output_pipe,outfall_ID,pipe,Dstream_ID,Dstream_type,pipe_X1,pipe_Y1,pipe_X2,pipe_Y2,13,pipe$PIP
EDIAMET,pipe$PIPEWIDTH,pipe$PIPEHEIGHT,pipe$FID_pipes,groundSlop,pipe$PIPEMATERI)
     non.matched_XX<-func3(pipe_X1[k],pipe_X2[k],Dstream_x)
     if (length(non.matched_XX)==0){
       non.matched_XX=Dstream_x
     }
```

```
    output_pipe[m,11]=non.matched_XX;
    non.matched_YY<-func3(pipe_Y1[k],pipe_Y2[k],Dstream_y)
    if (length(non.matched_YY)==0){
      non.matched_YY=Dstream_y
    }
    output_pipe[m,12]=non.matched_YY;
    Names<-
func4(non.matched_XX,non.matched_YY,GP_types_X,GP_types_Y,AR_types_X,AR_types_Y,outfall_X,outfall_
Y)
    output_pipe<-func7(m,output_pipe,Names)
    if (output_pipe[m,3]==-100){
      output_pipe[m,3]=paste("UnkT_",N,sep='')
      N=N+1
    }
    output_pipe[m,27]=ID
    output_pipe[m,28]=Order
    output_pipe[m,29]=k-1
    m=m+1
   }
   }
 output<-output_pipe

 ## keep track of cells and ID
 cells<-matrix(-1,4000,4)                    # I need to increase the number of rows if I have more outfalls.
 colnames(cells)<- c('ID_up','ID_DS','Upcell','Dscell')
 cells[ID,1]=ID
 cells[ID,2]='outfall to channel'
 ## Now I have the first row of output file, I need to complete it based on upstraem and downstraem location.
 ################################
 n=1
 repeat{
   # find the non matched points for pipe
   n_rows1<-func5(c(rows1$rows),c(output[1:dim(output)[1],13]))

   if (n_rows1$n_row>0){
     work<-matrix(-1,n_rows1$n_row,31)
     colnames(work)<-
c("Outfall_ID","Pipe_ID","Upstream","Up_type","DownStream","Down_type","Point1_x","Point1_y","Point2_x",
"Point2_y","Upstream_x","Upstream_y",

"pipe_row","culvert_row",'L_ft','D_in','W_ft','H_ft','S','A_ft2','P_ft','R_ft','Qmax_cfs','Hf_ft','HRAP_cell','HRAP_pi
pe','ID',
                  'order', 'FID','order2',"Manning_num")
       for (e in 1:n_rows1$n_row){ ## For
        g=n_rows1$rows[e]
        work<-
func6(e,g,work,outfall_ID,pipe,output[n,3],output[n,4],pipe_X1,pipe_Y1,pipe_X2,pipe_Y2,13,pipe$PIPEDIAMET
,pipe$PIPEWIDTH,pipe$PIPEHEIGHT,pipe$FID_pipes,groundSlop,pipe$PIPEMATERI)
        non.matched_x<-func3(pipe_X1[g],pipe_X2[g],output[n,11])
        if (length(non.matched_x)==0){
          non.matched_x=pipe_X1[g]
        }
        work[e,11]=non.matched_x;
        non.matched_y<-func3(pipe_Y1[g],pipe_Y2[g],output[n,12])
        if (length(non.matched_y)==0){
          non.matched_y=pipe_Y1[g]
        }
        work[e,12]=non.matched_y;
```

```
        # find the name of secend point in the pipe line between points files (outfall, inlet, junction, stormfitting)
        Names3<-
func4(non.matched_x,non.matched_y,GP_types_X,GP_types_Y,AR_types_X,AR_types_Y,outfall_X,outfall_Y)
        work<-func7(e,work,Names3)
        if (work[e,3]==-100){
          work[e,3]=paste("UnkT_",N,sep='')
          N=N+1
        }
        #### find the ID ####
        ID_pipe<-which((pipe$FID_pipes==pipe$FID_pipes[g]));
        if (length(ID_pipe)==1){
          work[e,27]=output[n,27]
        }else if ((length(ID_pipe)>1)&(work[e,25]==output[n,25])){
          work[e,27]=output[n,27]
        }else if ((length(ID_pipe)>1)&(work[e,25]!=output[n,25])){
          upcell=work[e,25]
          Dscell=output[n,25]
          ID_DS=output[n,27]
          cell_check<-
which((c(cells[1:dim(cells)[1],2])==ID_DS)&(c(cells[1:dim(cells)[1],3])==upcell)&(c(cells[1:dim(cells)[1],4])==D
scell));
          if (length(cell_check)==1){
            work[e,27]=cells[cell_check,1]
          }else if (length(cell_check)==0){
            ID=ID+1
            cells[ID,1]=ID
            cells[ID,2]=ID_DS
            cells[ID,3]=upcell
            cells[ID,4]=Dscell
            work[e,27]=ID
          }
        }
        ####find Order ###
        DownpipeOrder=output[n,28]
        Areadownp=output[n,20]
        Areacurrentp=work[e,20]
        if (n_rows1$n_row==1){
          work[e,28]=as.numeric(DownpipeOrder)
        }else {
          if (as.numeric(Areadownp)<=as.numeric(Areacurrentp)){
            work[e,28]=as.numeric(DownpipeOrder)

          }else{
            work[e,28]=as.numeric(DownpipeOrder)+1
          }
        }
        #####
        work[e,29]=g-1
      }## For
      output<-rbind2(output,work)
    }
    size<-dim(output);
    if(n==size[1]){
      break
    }
    n=n+1;
  }  ### REPEAT
```

```
 # I need to do a modification for the times that I have 2 outfalls in the output file ########################

 HRAP_1=as.numeric(output[1,25])                  # HRAP# of main outfall
 ID_1=as.numeric(output[1,27])                   # ID# of main outfall
 outfalls_US=which(c(output[1:dim(output)[1],4])=="outfall");
 z=1
 if (length(outfalls_US)>=1){
  HRAP_2<-as.numeric(output[outfalls_US[z],25])
  ID_2<-as.numeric(output[outfalls_US[z],27])
  repeat{
   if ((HRAP_2==HRAP_1)&(ID_2!=ID_1)){
    output[outfalls_US[z],27]=ID_1
    non.matched_data2<-
func3(output[outfalls_US[z],7],output[outfalls_US[z],8],output[outfalls_US[z],9],output[outfalls_US[z],10],output[
outfalls_US[z],11],output[outfalls_US[z],12])

match.data2=which((c(output[1:dim(output)[1],27])==ID_2)&(c(output[1:dim(output)[1],11])==non.matched_data
2[1])&(c(output[1:dim(output)[1],12]))==non.matched_data2[2]);
     outfalls_US=c(outfalls_US,match.data2)
   }
    L<-length(outfalls_US);
   if(z==L){
    break
   }
   z=z+1;
  }
  New_ID_DS=which(c(cells[1:dim(cells)[1],2]==ID_2))
  if (length(New_ID_DS)>=1){
   for (W in 1:length(New_ID_DS)){
    cells[New_ID_DS,2]=ID_1
  }
  }
 }
 ## generate order:
 # find head pipes and get them order 1
 matched_order<-intersect(output[,3],output[,5]);
 all=output[,3]
 orders1<-all[!all %in% matched_order];
 for (l in 1:length(orders1)){
  roworders1<-which(output[,3]==orders1[l])
  output[roworders1,30]=1
 }
 #####

 for (v in dim(output)[1]:1){
  if (output[v,30]>0){
   next
  }
  uppipe=which(output[v,3]==output[,5])
  upOrder=as.numeric(output[uppipe,30])       # read orders of upstream
  maxorder=as.numeric(max(upOrder))
  minorder=as.numeric(min(upOrder))
  if (length(upOrder)==1){
   output[v,30]=maxorder
  }else if (length(upOrder)>1){
   if (maxorder==minorder){
    output[v,30]=maxorder+1
   }else if (maxorder!=minorder){
```

```
      output[v,30]=maxorder
     }
    }
  }
  #####
  #write.csv(cells, file = paste('F:/UTA/Pojects/Natural cannel and pipe system modeling/pipe order
analysis/Outputs/cell',i,'.csv'))
  write.csv(output, file = paste('F:/UTA/Pojects/Natural cannel and pipe system
modeling/5catchments/Merging_process/Main system/Output_main/output',i,'.csv',sep=''),row.names = FALSE)
  Pipe_line<-rbind(Pipe_line,output)
  write.csv(Pipe_line, file = "F:/UTA/Pojects/Natural cannel and pipe system
modeling/5catchments/Merging_process/Main system/Output_main/Pipe_line.csv",row.names = FALSE)
  ID=ID+1
}#for each row outfall location

#################################################################################################
########## Merge order ones
Indir=paste("F:/UTA/Pojects/Natural cannel and pipe system modeling/5catchments/Merging_process/Main
system")
Main<-matrix(-9999,1,25)
colnames(Main)<-
c("Outfall_ID","Pipe_ID","Upstream","Up_type","DownStream","inlets_num","Point1_x","Point1_y","Point2_x","
Point2_y",

"L_ft","D_in","W_in","H_in","S","Qmax_cfs","Hf_ft","HRAP_cell","Order","Upstream_x","Upstream_y",
                  "A_ft2","R_ft","Manning_num",'ID')
for (j in 1:1184){  #293
  print(j)

#################################################################################################
  infile=paste(file=Indir,"/Output_main/output",j,".csv",sep="")
  if (!file.exists(infile)){
    next
  }
  connectivity=read.csv(file=infile,head=TRUE)
  newconn<-matrix(-9999,1,25) # empty matrix for output
  colnames(newconn)<-
c("Outfall_ID","Pipe_ID","Upstream","Up_type","DownStream","inlets_num","Point1_x","Point1_y","Point2_x","
Point2_y",

"L_ft","D_in","W_in","H_in","S","Qmax_cfs","Hf_ft","HRAP_cell","Order","Upstream_x","Upstream_y",
                "A_ft2","R_ft","Manning_num",'ID')
  IDpipes=0
  ###
  for (i in dim(connectivity)[1]:1){ # ## FOR PIPE i
     work<-matrix(-1,1,25)
     colnames(work)<-
c("Outfall_ID","Pipe_ID","Upstream","Up_type","DownStream","inlets_num","Point1_x","Point1_y","Point2_x","
Point2_y",

"L_ft","D_in","W_in","H_in","S","Qmax_cfs","Hf_ft","HRAP_cell","Order","Upstream_x","Upstream_y",
                  "A_ft2","R_ft","Manning_num","ID")
     pipe_series=i
     N=0
     #USpipe=which(connectivity$DownStream==paste(connectivity$Upstream[i]))
     if ((connectivity$Up_type[i]=="Inlet")||(connectivity$Up_type[i]=="GRATE
INLET")||(connectivity$Up_type[i]=="CURB INLET")||(connectivity$Up_type[i]=="Y-INLET")){
       N=1
```

```
  }
   work[1,1]=paste(connectivity$Outfall_ID[i])
   work[1,2]=paste(connectivity$Pipe_ID[i])
   work[1,3]=paste(connectivity$Upstream[i])
   work[1,4]=paste(connectivity$Up_type[i])
   work[1,5]=paste(connectivity$DownStream[i])
   work[1,6]=N
   work[1,7]=connectivity$Point1_x[i]
   work[1,8]=connectivity$Point1_y[i]
   work[1,9]=connectivity$Point2_x[i]
   work[1,10]=connectivity$Point2_y[i]
   work[1,11]=round(connectivity$L_ft[i], digits=6)
   work[1,12]=connectivity$D_in[i]
   work[1,13]=connectivity$W_ft[i]
   work[1,14]=connectivity$H_ft[i]
   if (connectivity$S[i]<0){
    connectivity$S[i]=0.1
   }
   work[1,15]=connectivity$S[i]
   if(connectivity$D_in[i]>0){
    A=pi*(connectivity$D_in[i]/12)^2/4    #ft^2
    P=pi*(connectivity$D_in[i]/12)        #ft
    R=A/P
   }else if (connectivity$D_in[i]<0){
    ## the data in the shape file is strange, we have calverts as small as 5
    ## and as large as 120 so it doesnt make sese if we consider foot or inch for all
    ## so I consider a threshold 20
    if (connectivity$W_ft[i]<20){  # the colverts unit are feet
     A=connectivity$W_ft[i]*connectivity$H_ft[i]   #ft^2
     P=connectivity$W_ft[i]+2*connectivity$H_ft[i] #ft
     R=A/P
    }else if ((connectivity$W_ft[i]>20))  # the calvrets unit are inch
     A=(connectivity$W_ft[i]*connectivity$H_ft[i])/(12*12)   #ft^2
     P=connectivity$W_ft[i]/12+2*connectivity$H_ft[i]/12 #ft
     R=A/P
   }
   Q=(1.49/connectivity$Manning_num[i])*A*R^(2/3)*(connectivity$S[i]/100)^0.5  #ft3/s
   #Q=1.318**A*R^0.63*(connectivity$S[i]/100)^0.54
   hf=connectivity$L_ft[i]*(connectivity$S[i]/100)
   work[1,16]=round(Q, digits=6)
   work[1,17]=round(hf, digits=6)
   work[1,18]=connectivity$HRAP_cell[i]
   work[1,19]=connectivity$order2[i]
   work[1,20]=connectivity$Upstream_x[i]
   work[1,21]=connectivity$Upstream_y[i]
   work[1,22]=round(A, digits=6)
   work[1,23]=round(R, digits=6)
   work[1,24]=connectivity$Manning_num[i]
   work[1,25]=paste(connectivity$ID[i])
   newconn<-rbind(newconn,work)
}## FOR PIPE SERIES i
write.csv(newconn, file =paste(Indir,'/Real/Real_',j,'.csv', sep=''), row.names=FALSE)

################################
infile2=paste(file=Indir,"/Real/Real_",j,".csv",sep="")
connectivity=read.csv(file=infile2,head=TRUE)
Row=0
for (d in dim(connectivity)[1]:2){## check the X Y coordinates
```

```
  Row=c(Row,d)
  up=connectivity$Upstream[d]
  up_x=connectivity$Upstream_x[d]
  up_y=connectivity$Upstream_y[d]
  up_pipe=which(connectivity$DownStream==paste(up))
  if (length(up_pipe)==0){
    next
  }
  for (l in 1:length(up_pipe)){
    if ((connectivity$Point2_x[up_pipe[l]]!=up_x)&(connectivity$Point2_y[up_pipe[l]]!=up_y)){
      Point1_x=connectivity$Point2_x[up_pipe[l]]
      Point1_y=connectivity$Point2_y[up_pipe[l]]
      connectivity$Point2_x[up_pipe[l]]=up_x
      connectivity$Point2_y[up_pipe[l]]=up_y
      connectivity$Point1_x[up_pipe[l]]=Point1_x
      connectivity$Point1_y[up_pipe[l]]=Point1_y
    }
  }
 }## check the X Y coordinates
 write.csv(connectivity, file =paste(Indir,'/Real/Real_',j,'.csv', sep=''), row.names=FALSE)
 Main<-rbind(Main,connectivity)
}### for every system
Main<-Main[-which(Main[,1]==-9999),]
write.csv(Main, file =paste(Indir,'/Real/Real.csv', sep=''), row.names=FALSE)
```

Appendix F

Script of storm drain flow modeling

```
#### START TIME ###
iyr_s=2017
imon_s=1
iday_s=16
ihr_s=12
imin_s=0
isec_s=0
#### END TIME
iyr_e=2017
imon_e=1
iday_e=16
ihr_e=12
imin_e=1
isec_e=0
#### TIME step in RDHM (seconds)
dt=60
#### Input and Output directory
InOudir="/home/hhabibi/Stormdrain_model/Preparation_RDHM/5catchments/xmrg_2/output_TS_10s"
#### Area of a cell in sqr KM
resolution=0.0625
#### create the input file (for now surface flow) and make it asc and return to xmrg format
func_time<-function(y,d,mo,h,mi,se,dtx){
  if (dtx<=60){
    time1=mo*10000000000+d*100000000+y*10000+h*100+mi
    if (dtx==60){
      time1=paste(time1,'00',sep='')
    }else{
      if (se<10){
        se=paste ("0",se,sep='')
      }
      time1=paste(time1,se,sep='')
    }

  }else if (dtx==3600){
    time1=mo*100000000+d*1000000+y*100+h
  }
  if (mo<10){
    time1=paste ("0",time1,sep='')
  }
  return(time1)
}
#### Libraries
library(rootSolve)
library(foreign)
#### Area of each cell
A1celldir=paste(InOudir,'/Area_cell_Mi2.asc', sep = '') # ,Connectivity_ Connectivity_Merged
A1cell<-read.table(file=A1celldir,skip=6,head=FALSE,sep="")
A1cell=A1cell*2.58985  #MI2 to KM2
#A1cell=0.0603435                # KM2 for 1/16 HRAP, getting fro, connectivity file
#A2cell=4.7625*4.7625*resolution^2  # Km2  (using cell size and HRAP)
#################################
#### read pipe connectivity file
connectivitydir=paste(InOudir,'/connectivity/pipeconn_250m.csv', sep = '') # ,Connectivity_ Connectivity_Merged
```

```
connectivity<-read.csv(file=connectivitydir,head=TRUE)
############################################################ main code
dt_sd=dt  # change the time sterp of Storm drain
yr=iyr_s;mon=imon_s;day=iday_s;hr=ihr_s;min=imin_s;sec=isec_s
g=9.81
CW=(2/3)^(1.5)*g^(0.5)                  # discharge coefficent (m^0.5/s)^M
Pw=5      # m
Iheight=250    # mm
Maxiter=25
herror=0.000005
alpha=1
repeat{ # for the start and end time of simualtion
  # for RDHM state variables
  date_forward=strptime(paste(yr,mon,day,hr,min,sec), "%Y %m %d %H %M %S")+dt
  stime <- data.frame(year = as.numeric(format(date_forward, format = "%Y")),
                      month = as.numeric(format(date_forward, format = "%m")),
                      day = as.numeric(format(date_forward, format = "%d")),
                      hour = as.numeric(format(date_forward, format = "%H")),
                      minute = as.numeric(format(date_forward, format = "%M")),
                      second = as.numeric(format(date_forward, format = "%S")))
  syr=stime$year;smon=stime$month;sday=stime$day;shr=stime$hour;smin=stime$minute;ssec=stime$second #
use this
  time_new=func_time(syr,sday,smon,shr,smin,0,dt)
  #print(time_new)
  ######################################## Creat the file path and read the input file (hillslopedepth)
  #Un ZIP
  Input_name=paste(InOudir,'/hslopedepth/','depth',time_new,'z.gz',sep='')
  system(paste('gunzip ',Input_name))
  # ASC
  Input_name2=paste(InOudir,'/hslopedepth/','depth',time_new,'z',sep='')
  system(paste('/home/hhabibi/Stormdrain_model/HL-RDHM/hl-rdhm-release-3.5.4/bin/xmrgtoasc ',Input_name2,
sep=''))
  # Read ASC
  Input_name3=paste(InOudir,'/hslopedepth/','depth',time_new,'z.asc',sep='')
  hdepth<-read.table(file=Input_name3,skip=6,head=FALSE,sep="") #mm
  size=dim(hdepth)
  cells=which(hdepth==-1)
  system(paste('rm -rf ',Input_name3))
  system(paste('gzip ',Input_name2))
  ######################################## Creat the file path and read the input file (hillslopeflow)
  #UnZIP
  Input_name=paste(InOudir,'/hslopeflow/','hillslopinflow',time_new,'z.gz',sep='')
  system(paste('gunzip ',Input_name))
  # ASC
  Input_name2=paste(InOudir,'/hslopeflow/','hillslopinflow',time_new,'z',sep='')
  system(paste('/home/hhabibi/Stormdrain_model/HL-RDHM/hl-rdhm-release-3.5.4/bin/xmrgtoasc ',Input_name2,
sep=''))
  # Read ASC
  Input_name3=paste(InOudir,'/hslopeflow/','hillslopinflow',time_new,'z.asc',sep='')
  hflow<-read.table(file=Input_name3,skip=6,head=FALSE,sep="")  ##mm/s
  system(paste('rm -rf ',Input_name3))
  system(paste('gzip ',Input_name2))
  tt=0
  repeat{ # for dt_SD<dt time storm drain model
    time_current<-strptime(paste(yr,mon,day,hr,min,sec), "%Y %m %d %H %M %S")
    time<-func_time(yr,day,mon,hr,min,sec,dt_sd)
    date_forward_SD=strptime(paste(yr,mon,day,hr,min,sec), "%Y %m %d %H %M %S")+dt_sd
    stime_SD <- data.frame(year = as.numeric(format(date_forward_SD, format = "%Y")),
```

```
                month = as.numeric(format(date_forward_SD, format = "%m")),
                day = as.numeric(format(date_forward_SD, format = "%d")),
                hour = as.numeric(format(date_forward_SD, format = "%H")),
                minute = as.numeric(format(date_forward_SD, format = "%M")),
                second = as.numeric(format(date_forward_SD, format = "%S")))

syr_SD=stime_SD$year;smon_SD=stime_SD$month;sday_SD=stime_SD$day;shr_SD=stime_SD$hour;smin_SD=
stime_SD$minute;ssec_SD=stime_SD$second
  time_SD=func_time(syr_SD,sday_SD,smon_SD,shr_SD,smin_SD,ssec_SD,dt_sd)
  print(time_SD)
  ##################################### Creat the file path and read the pipe state variable
  SV_dir=paste(InOudir,'/State_variable/','PipeSV',time,'z.csv',sep="")
  SV=read.csv(file=SV_dir,head=TRUE)

  ##################################### create a new files
  SV_new<-matrix(0,dim(connectivity)[1],6)
  colnames(SV_new)<- c("Name","Qin","Qo","depth","Area","P")
  outfall=matrix(0,size[1],size[2])
  pinflow=matrix(0,size[1],size[2])
  flowresidual=matrix(0,size[1],size[2])
  flowinpipes=matrix(0,size[1],size[2])
  tt=tt+dt_sd
  for (i in 1:dim(connectivity)[1]){ ### for all pipes of current time  #dim(connectivity)[1]
   #   print(i)
   # reading information
   n=connectivity$Manning_num[i]
   S=connectivity$S[i]/100                  # pipe slope
   D=connectivity$D_in[i]*0.0254            # pipe diameter (m)
   A=connectivity$A_ft2[i]*(0.3048)^2       # M2
   R=connectivity$R_ft[i]*(0.3048)          # M
   L=connectivity$L_ft[i]*0.3048            # Convert ft to m
   P=A/R                                    # M
   Q_max=(1/n)*A*R^(2/3)*S^(1/2)            # CMS
   # Read state variables
   Q_out_dt=as.numeric(SV[i,3])
   h_dt=as.numeric(SV[i,4])
   A_dt=as.numeric(SV[i,5])
   P_dt=as.numeric(SV[i,6])

   ### calculate inflow to pipe if there are inlets (if there is no inlet, Q would be 0)
   # 1) first find the value of surfaceflow /hillslope of corresponding to the location of each pipe.
   cell=connectivity$HRAP_cell[i]
   ROW=ceiling(cell/size[2])
   Coll=cell-floor(cell/size[2])*size[2]
   if (connectivity$inlets_num[i]>0){
    Hw=hdepth[ROW,Coll]                     #mm
    qs=hflow[ROW,Coll]                      #mm/s
    Acell=A1cell[ROW,Coll]                  #km2
    #     subf=subsurfaceFlow[ROW,Coll]/dt          #mm/s
    if (Hw==-1){  # HW if -1
     #find the closest possitive value in a Row
     data_in_row=hdepth[ROW,]-Hw
     data_in_row_pos=which(data_in_row>0)
     dist_row=abs(data_in_row_pos-Coll)
     closest_dist_row=which(dist_row==min(dist_row))
     if (length(closest_dist_row)>1){
      closest_dist_row=closest_dist_row[1]
     }
```

```
  dist_ro=dist_row[closest_dist_row]
  #find the closest possitive value in a Collumn
  data_in_col=hdepth[,Coll]-Hw
  data_in_col_pos=which(data_in_col>0)
  dist_col=abs(data_in_col_pos-ROW)
  closest_dist_col=which(dist_col==min(dist_col))
  if (length(closest_dist_col)>1){
   closest_dist_col=closest_dist_col[1]
  }
  dist_co=dist_col[closest_dist_col]
  ## select one of them which is closest
  if (dist_co>dist_ro){
   Hw=hdepth[ROW,data_in_row_pos[closest_dist_row]]
   qs=hflow[ROW,data_in_row_pos[closest_dist_row]]                    #mm/s
   Acell=A1cell[ROW,data_in_row_pos[closest_dist_row]]                #km2
   #       subf=subsurfaceFlow[ROW,data_in_row_pos[closest_dist_row]]/dt          #mm/s
  }else if (dist_co<=dist_ro){
   Hw=hdepth[data_in_col_pos[closest_dist_col],Coll]
   qs=hflow[data_in_col_pos[closest_dist_col],Coll]
   Acell=A1cell[data_in_col_pos[closest_dist_col],Coll]        #km2
   #       subf=subsurfaceFlow[data_in_col_pos[closest_dist_col],Coll]/dt          #mm/s
  }
 } # HW if -1
                  # Total number of inlets in the cell
       HR_cells=which(connectivity$HRAP_cell==connectivity$HRAP_cell[i])
 total_inlet=sum(connectivity$inlets_num[HR_cells])
       Qweir=CW*Pw*(Hw/1000)^(1.5)*total_inlet
       Qorifice=0.67*(Iheight/1000)*Pw*(2*9.81*Hw/1000)^(0.5)*total_inlet
 if (Hw<=(1.4*Iheight)){ # The inlets operates as weir
   #thr=qs*(Acell*1000)/(CW*Pw*(Hw/1000)^(1.5)*total_inlet)
         #Qinlets=CW*Pw*(Hw/1000)^(1.5)*total_inlet*(thr*0.96)
    Qinlets=Qweir
 }else if (Hw>Iheight){ #The inlets operates as Orifice
    Qinlets=Qorifice
 }else if ((Hw>Iheight)&(Hw<=(1.4*Iheight))){
          Qinlets=max(c(Qorifice,Qweir))
       }
       qin=Qinlets/(Acell*1000)  #mm/s
       if (qin>qs){
          Qinlets=qs*(Acell*1000)
       }
       Qinlet=Qinlets*connectivity$inlets_num[i]/total_inlet
}else{
 Qinlet=0
}
j=1
if (Qinlet>connectivity$Qin_max_CMS[i]){
 Qinlet=connectivity$Qin_max_CMS[i]
}
# Need to find if there is an upream pipes or not
if (j==1){
 Up_pipe=which(connectivity$DownStream==paste(connectivity$Upstream[i]))
 Nup_pipes=length(Up_pipe)
 if (Nup_pipes>=1){
  Qup_pipes=0
  Qup=0
  for (z in 1:Nup_pipes){
   # create file name to read the coresponding pipe file
```

```
    f=Up_pipe[z]
    #ID_uppipe=connectivity$Upstream[f]
    Qup=as.numeric(SV_new[f,3])
    Qup_pipes=Qup+Qup_pipes
   }
  }else{
   Qup_pipes=0
  }
}
Qinflow=Qup_pipes+Qinlet              # CMS
if (Qinflow>Q_max){
  Qresi=Qinflow-Q_max             # CMS
  Qinflow=Q_max                   # CMS
}else if (Qinflow<=Q_max){
  Qresi=0                       #mm
}
#### lphato prevent non-convergence
rr=1
dtx=dt_sd
repeat{# For convergence
  A_wetted=A_dt
  P_wetted=P_dt
  Q_out=Q_out_dt
  for (k in 1:rr){ # for repeat 1:r time
    Constant=dtx*Qinflow/(L)+A_wetted
    nn=1
    repeat{
      a=(n*P_wetted^(2/3)/S^0.5)^(3/5)
      fQ=dtx*Q_out/L+a*Q_out^(3/5)-Constant
      if (Q_out==0){
        dfQ=dtx/L
      }else{
        dfQ=dtx/L+3/5*a*Q_out^(-2/5)
      }
      Q_out_k=Q_out-alpha*(fQ/dfQ)
      error=abs(Q_out_k-Q_out)
      #      print(Q_out_k)
      if (Q_out_k<0){
        Q_out_k=0.000000000000000001
      }
      ### For pipes
      if (D>0){
        if (Q_out_k>Q_max/2){
          fun1<- function (y) {((S^0.5/n)*(pi*D^2/4-(D^2*(y-sin(y)/8)))^(5/3)/(pi*D-D*y/2)^(2/3))-Q_out_k}
          tet<-uniroot.all(fun1, interval=c(0.00000000000000000000001,3.1415933333333333))
          if (length(tet)==0){
            tet=0.0000000000000000000001
          }
          A_wetted=pi*D^2/4-(D^2*(tet-sin(tet)/8))
          P_wetted=pi*D-tet*(D)/2
          fun3<- function (y) {2*acos(1-2*y/D)-tet}
          h<-uniroot.all(fun3, interval=c(0.000000000000000000000001,D))
          if (length(h)==0){
            h=0.0000000000000000000001
          }
          depth=D-h
        }else if (Q_out_k<=Q_max/2){
          fun<- function (x) {(0.04960628*S^0.5*(D)^(8/3)*(x-sin(x))^(5/3)/(n*(x)^(2/3)))-Q_out_k}
```

```
          tet<-uniroot.all(fun, interval=c(0.00000000000000000000001,3.1415933333333333))
          A_wetted=(tet-sin(tet))*(D)^2/8  # m^2
          P_wetted=tet*(D)/2               #m
          fun2<- function (y) {2*acos(1-2*y/D)-tet}
          depth<-uniroot.all(fun2, interval=c(0.00000000000000000000001,D))
         }
        }
        ### For Culverts^M
        if (D<0){
         fun4<- function (x) {((S^0.5/n)*(W*x)^(5/3)/(W+2*x)^(2/3))-Q_out_k}
         depth<-uniroot.all(fun4, interval=c(0.00000000000000000000001,H))
         if (length(depth)==0){
          depth=0.000000000000000000000001
         }
         A_wetted=W*depth      #m^2^M
         P_wetted=(W+2*depth)  #m^M
        }
        R_wetted=A_wetted/P_wetted  #m^M
        Q_out=Q_out_k
        if ((error<=herror) || (nn==Maxiter)){
         break
        }
        nn=nn+1
       } ## for repeat until get the least error
      } # for repeat 1:r time
      if (error<=herror){
       break
      }else if((error>herror)&(nn==Maxiter)){
       dtx=dtx/2
       rr=rr*2
      }
     }# For convergence

     # write the data in State variable file
     SV_new[i,1]=paste(connectivity$Upstream[i])
     SV_new[i,2]=Qinflow
     SV_new[i,3]=Q_out
     SV_new[i,4]=depth
     SV_new[i,5]=A_wetted
     SV_new[i,6]=P_wetted
     outfile_ID=connectivity$Outfall_ID[i]
     if (connectivity$DownStream[i]==paste(outfile_ID)){
      outfall[ROW,Coll]=outfall[ROW,Coll]+Q_out              #CMS
     }
     pinflow[ROW,Coll]=pinflow[ROW,Coll]+Qinlet                    #CMS
     flowresidual[ROW,Coll]=flowresidual[ROW,Coll]+Qresi       #CMS
     flowinpipes[ROW,Coll]=flowinpipes[ROW,Coll]+Q_out         #CMS
    } ### for all pipes of current time
    ####################
    # 1) pipe state variables
    #time_new=func_time(syr,sday,smon,shr,smin,dt_sd)
    SV_new_dir=paste(InOudir,'/State_variable/','PipeSV',time_SD,'z.csv',sep="")
    write.csv(SV_new, file =SV_new_dir, row.names=FALSE)

    # # 2) flow at outfall locations (CMS)
     outfall[cells]=-1
     pipeoutflow=paste(InOudir,'/pipeoutflow/','pipeoutflow',time_SD,'z.asc',sep='')
     write(c("ncols 53","nrows 60","xllcorner 587.625000","yllcorner 248.437500",
```

```
          "cellsize 0.062500","NODATA_value -1.000000"), file=pipeoutflow,append = FALSE)
    write.table(outfall,file=pipeoutflow, sep="\t", append = TRUE,  row.names = FALSE, col.names = FALSE)
    system(paste('/home/hhabibi/Stormdrain_model/HL-RDHM/hl-rdhm-release-3.5.4/bin/asctoxmrg -f par
',pipeoutflow, sep=''))
    system(paste('rm -rf ',pipeoutflow))
   #
   # # 3) Inflow to pipe at each cell (CMS)
    pinflow[cells]=-1
    pipeinflow=paste(InOudir,'/pipeinflow/','pipeinflow',time_SD,'z.asc',sep='')
    write(c("ncols 53","nrows 60","xllcorner 587.625000","yllcorner 248.437500",
          "cellsize 0.062500","NODATA_value -1.000000"), file=pipeinflow,append = FALSE)
    write.table(pinflow,file=pipeinflow, sep="\t", append = TRUE,  row.names = FALSE, col.names = FALSE)
    system(paste('/home/hhabibi/Stormdrain_model/HL-RDHM/hl-rdhm-release-3.5.4/bin/asctoxmrg -f par
',pipeinflow, sep=''))
    system(paste('rm -rf ',pipeinflow))
   #
   # # 4) back to surface runoff   (CMS)
    flowresidual[cells]=-1
    pipeflow2surface=paste(InOudir,'/pipeflow2surface/','pipeflow2surface',time_SD,'z.asc',sep='')
    write(c("ncols 53","nrows 60","xllcorner 587.625000","yllcorner 248.437500",
          "cellsize 0.062500","NODATA_value -1.000000"), file=pipeflow2surface,append = FALSE)
    write.table(flowresidual,file=pipeflow2surface, sep="\t", append = TRUE,  row.names = FALSE, col.names =
FALSE)
    system(paste('/home/hhabibi/Stormdrain_model/HL-RDHM/hl-rdhm-release-3.5.4/bin/asctoxmrg -f par
',pipeflow2surface, sep=''))
    system(paste('rm -rf ',pipeflow2surface))

   # # 5) Flow in pipes          (CMS)
    flowinpipes[cells]=-1
    flowinpipesdir=paste(InOudir,'/flowinpipes/','flowinpipes',time_SD,'z.asc',sep='')
    write(c("ncols 53","nrows 60","xllcorner 587.625000","yllcorner 248.437500",
          "cellsize 0.062500","NODATA_value -1.000000"), file=flowinpipesdir,append = FALSE)
    write.table(flowinpipes,file=flowinpipesdir, sep="\t", append = TRUE,  row.names = FALSE, col.names =
FALSE)
    system(paste('/home/hhabibi/Stormdrain_model/HL-RDHM/hl-rdhm-release-3.5.4/bin/asctoxmrg -f par
',flowinpipesdir, sep=''))
    system(paste('rm -rf ',flowinpipesdir))
   ####################
   difftime_last_SD<-as.numeric(difftime(strptime(paste(syr_SD,smon_SD,sday_SD,shr_SD,smin_SD,ssec_SD),
"%Y %m %d %H %M %S"),
                          strptime(paste(syr,smon,sday,shr,smin,ssec), "%Y %m %d %H %M %S")))
   if (difftime_last_SD>=0){
     break
   }
   yr=syr_SD;mon=smon_SD;day=sday_SD;hr=shr_SD;min=smin_SD;sec=ssec_SD
  } # for dt_SD<dt time storm drain model

  difftime_last<-as.numeric(difftime(strptime(paste(syr_SD,smon_SD,sday_SD,shr_SD,smin_SD,ssec_SD), "%Y
%m %d %H %M %S"),
                          strptime(paste(iyr_e,imon_e,iday_e,ihr_e,imin_e,isec_e), "%Y %m %d %H %M %S")))
  if (difftime_last>=0){
    break
  }
  yr=syr_SD;mon=smon_SD;day=sday_SD;hr=shr_SD;min=smin_SD;sec=ssec_SD
  #SV=SV_new
} # # for the start and end time of simualtion
```

References

Akan, A.O. and Houghtalen, R.J., 2003. Urban hydrology, hydraulics, and stormwater quality: engineering applications and computer modeling. John Wiley & Sons.

Anderson, R.M., Koren, V., Reed, S.M., 2006. Using SSURGO Data to Improve Sacramento Model a-priori Parameter Estimates. J. of Hydrol, 320(1): 103-116.

Anderson, Edward J., and Khairy H. Al-Jamal. 1995. Hydraulic-network simplification. Journal of Water Resources Planning and Management 121 (3): 235-40.

Ashley, R. M., Balmforth, D. J., Saul, A. J., and Blanskby, D. J., 2005. Flooding in the future-Predicting climate change, risks, and responses in urban areas.Water Sci. Technol., 52(5), 265–273.

Arnell, N. W.: Relative effects of multi-decadal climatic variability and changes in the mean and variability of climate due to global warming: future streamflows in Britain, J. Hydrol., 270(3–4), 195–213, 2003.

Butler, D., & Davies, J. (2004). Urban drainage. CRC Press.

Berne, A., and W. F. Krajewski, 2013. Radar for hydrology: Unfulfilled promise or unrecognized potential? Advances in Water Resources, 51, 357–366.

Bringi, V. N. Chandrasekar, V., 2001. Polarimetric Doppler Weather Radar: Principles and applications, Cambridge University Press, 648 pp., 2001.

Brown, J. D. and D.-J. Seo, 2012. Evaluation of a nonparametric post-processor for bias correction and uncertainty estimation of hydrologic predictions, Hydrol. Process. Published online in Wiley Online Library (wileyonlinelibrary.com) DOI: 10.1002/hyp.9263.

Burnash, R.J.C., Ferral, R.L., McGuire, R.A., McGuire, R.A., 1973. A generalized streamflow simulation system: conceptual modeling for digital computers. US Department of Commerce National Weather Service and State of California Department of Water Resources.

Bhaduri, B., Minner, M., Tatalovich, S., and Harbor, J., 2001. Longterm hydrologic impact of urbanization: A tale of two models." J. Water Resour. Plann. Manage. 127-1, 13-19.

Biancamaria, Sylvain, Paul D. Bates, Aaron Boone, and Nelly M. Mognard. "Large-scale coupled hydrologic and hydraulic modelling of the Ob River in Siberia." Journal of Hydrology 379, no. 1 (2009): 136-150.

Biancamaria, S., Bates, P.D., Boone, A., Mognard, N.M., 2009. Large-scale coupled hydrologic and hydraulic modelling of the Ob river in Siberia. J. Hydrol. 379, 136–150.

Brun, S. E. and Band, L. E.: Simulating runoff behavior in an urbanizing watershed, Computers, Environ. Urban Syst., 24(1), 5–22, 2000.

Bonnifait, L., Delrieua, G., Laya, M.L., Boudevillaina, B., Massonb, A., Belleudya, P.,Gaumec, E., Saulnier, G.M., 2009. Distributed hydrologic and hydraulic modelling with radar rainfall input: Reconstruction of the 8–9 September 2002 catastrophic flood event in the Gard region, France. Adv. Water Resour. 32, 1077–1089.

Chang, H. and Franczyk, J.: Climate change, land use change, and floods: Toward an integrated assessment, Geography Compass, 2(5), 1549–1579, 2008.

Changnon, S. A. and Demissie, M.: Detection of changes in streamflow and floods resulting from climate fluctuations and land usedrainage changes, Climatic Change, 32(4), 411 421, 1996.

Chandrasekar, V., Cifelli, R., 2012. Concept and principles of rainfall estimation from radar: Multi sensor environment and data fusion. Indian Journal of Radio & Space Physics, Vol 41, August, 389-402.

Chandasekar, V., Lim, S., 2008. Retrieval of reflectivity in a networked radar environment. Journal of Atmospheric and Oceanic Technology, 25, 1755-1767.

Campbell, C. W., and Sullivan, S. M., 2002. Simulating time-varying cave flow and water levels using the storm water management model. Eng. Geol., 65(2), 133-139.

Chen, H, and Chandrasekar, V., 2015. The quantitative precipitation estimation system for Dallas-Fort Worth (DFW) urban remote sensing network. J. Hydrol. 531,259–271

Choe, C., Seo, S., Sreetharan, S., 2017. Real-time, Crowd-Sourced Flood Mapping & Analytics via iSeeFlood. Paper presented at the meeting of New York State Floodplain and Stormwater Managers Association Conference, Binghamton, New York.

Chow, V. T., Maidment, D. R. and Mays, L. W., 1988. Applied Hydrology. New York: McGraw-Hill.

Dallas news, (http://thescoopblog.dallasnews.com/2014/06/page/4/).

Fox4 news, (http://www.fox4news.com/story/25860827/flash-flooding-across-tarrant-county-on-tuesday)

Danish Hydraulic Institute, 1995. Mouse: User's manual and tutorial, Horsholm, Denmark.

David, C. H., Maidment, D. R., Niu, G.Y., Yang, Z.L., Habets, F. and Eijkhout, V., 2011. River Network Routing on the NHDPlus Dataset. Journal of Hydrometeorology 12:913–34.

Denault, C., Millar, R. G., and Lence, B. J. 2006. Assessment of possible impacts of climate change in an urban catchment. J. Am. Water Resour. Assoc., 42(3), 685–697.

Dittman, R. H., 1994: Annual flood death statistics per state per capita for the United States and Puerto Rico during the period 1959–1991. NOAA Tech. Memo. NWS SR-153, 11 pp.

Emerson, C. H., Welty, C., and Traver, R. G., 2005. Watershed-scale evaluation of a system of storm water detention basins, J. Hydrol. Eng., 10, 237–242.

Fares, A., Awal, R., Michaud, J., Chu, P.S., Fares, S., Kodama, K. and Rosener, M., (2014). Rainfall-runoff modeling in a flashy tropical watershed using the distributed HL-RDHM model. Journal of Hydrology, 519, 3436-3447.

French, R. Ing, S. Von Allmen, and R. Wood, 1983: Mortality from flash floods: A review of the National Weather Service reports, 1969–1981. Public Health Rep., 98, 584–588.

Gaume, E., Bain, V., Bernardara, P., Newinger, O., Barbuc, M., Bateman, Dumitrescu A, and Daliakopoulos I. (2009). A compilation of data on European flash floods. Journal of Hydrology, 367(1), 70-78

Gires, A. I., & ten Veldhuis, M. C. (2013). URBAN PLUVIAL FLOOD MODELLING: CURRENT THEORY AND PRACTICE.

Graziano, T., Clark, E., Cosgrove, B., and Gochis, D., 2017. Transforming National Oceanic and Atmospheric Administration (NOAA) Water Resources Prediction, AMS Meeting, Seattle, WA.

Greene, D.R., and Hudlow, M.D., 1982: Hydrometeorological grid mapping procedures. AWRA Int. Symp. Hydrometeorology, AWRA, Bethesda, MD

Gochis, D.J., Yu, W., Yates, D.N., 2014. The WRF-Hydro model technical description and user's guide, version 2.0. NCAR Technical Document Available at: https://www.ral.ucar.edu/projects/wrf_hydro (last access Feb 2017).

Guo, J. C. Y., MacKenzie K., 2012. Hydraulic efficiency of grate and curb-opening inlets under clogging effect. Colorado department of transportation DTD applied research and innovation branch. CDOT-2012-3. Denver, CO, 84pp.

Guo, Y. P., 2006. Updating rainfall IDF relationships to maintain urban drainage design standards. J. Hydrol. Eng., 11(5), 506–509.

Hamlet, A. F. and Lettenmaier, D. P.: Effects of 20th century warming and climate variability on flood risk in the Western US, Water Resour. Res., 43(6), W06427, doi:10.1029/2006wr005099, 2007.

Habibi, H., Nasab, A. R., Norouzi, A., Nazari, B., Seo, D. J., Muttiah, R., & Davis, C., 2016. High Resolution Flash Flood Forecasting for the Dallas-Fort Worth Metroplex. Journal of Water Management Modeling.

HL-RDHM. 2009. Hydrology Laboratory-Research Distributed Hydrologic Model (HL-RDHM) User Manual v. 3.0.0.

HL-RDHM. 2009. Hydrology Laboratory-Research Distributed Hydrologic Model (HL-RDHM) Developer Manual v. 3.0.0.

Hsu, M. H., Chen, S. H., and Chang, T. J., (2000). "Inundation simulation for urban drainage basin with storm sewer system." J. Hydrol., 234(1), 21–37.

Huber, W. C., and Dickinson, R. E., 1988. Storm water management model user's manual, version 4, EPA/600/3-88/001a (NTIS PB88- 236641/AS), Environmental Protection Agency, Athens, Ga.

Huntington, T. G.: Evidence for intensification of the global water cycle: Review and synthesis, J. Hydrol., 319(1–4), 83–95, 2006.

Jeppson RW., 1974. Steady flow analysis of pipe networks: an instructional manual. Department of Civil Engineering and Utah Water Research Laboratory, College of Engineering, Utah State University, Logan, Utah.

Jonkman, S. N., and I. Kelman, 2005: An analysis of the causes and circumstancesof flood disaster deaths. Disasters, 29, 75–97.

Junyent, F., Chandrasekar, v., McLaughlin, D., Insanic, D., Bharadwaj, N., 2010: The CASA Integrated Project 1 Networked Radar System. J. Atmos. Oceanic Technol., 27, 61–78. doi: http://dx.doi.org/10.1175/2009JTECHA1296.1

Kim, J., Warnock, A., Ivanov, V.Y., Katopodes, N.D., 2012. Coupled modeling of hydrologic and hydrodynamic processes including overland and channel flow. Adv. Water Resour. 37, 104–126.

Kean, J.W., Smith, J.D., 2005. Generation and verification of theoretical rating curves in the Whitewater River Basin, Kansas. J. Geophys. Res., 110

Koren, V.I., Smith, M., Wang, D., and Zhang, Z., 2000. Use of soil property data in the derivation of conceptual rainfall-runoff model parameters, American Meteorological Society 15th Conference on Hydrology, Long Beach, CA, pp. 103-106.

Koren, V.I., Smith, M.B., and Duan, Q., 2003. Use of a priori parameter estimates in the derivation of spatially consistent parameter sets of rainfall-runoff

models. In: Q. Duan, S. Sorooshian, H. Gupta, H. Rosseau and R. Turcotte (Editors), Calibration of Watershed Models. Water Science and Applications. AGU, 239-254.

Koren, V., Reed, S., Smith, M., Zhang, Z., Seo, D.J., 2004. Hydrologic Laboratory Modeling System (HL-RMS) of the US National Weather Service. J. of Hydrol, 291, 297-318.

Lim, S., Chandrasekar, V., Lee, P., Jayasumana, A.P., 2011: Real-Time Implementation of a Network-Based Attenuation Correction in the CASA IP1 Testbed. J. Atmos. Oceanic Technol., 28, 197–209. doi: http://dx.doi.org/10.1175/2010JTECHA1441.1

Leandro, J., Chen, A., Djordjevic, S. and Savic, D., 2009. A comparison of 1D/1D and 1D/2D coupled hydraulic models (sewer/surface) for urban flood simulation. Journal of Hydraulic Engineering, 135(6), 495-504.

Liang, X., Lettenmaier, D.P., Wood, E.F., Burges, S.J., 1994. A simple hydrologically based model of land surface water and energy fluxes for GSMs. J. Geophys. Res. 99, 415–428.

Mailhot, A., Duchesne, S., Rivard, G., Nantel, E., Caya, D., and Villeneuve, J. P., 2006a. “Climate change impacts on the performance of urban drainage

systems for southern Québec." Proc., EIC Climate Change Technology Conference, Engineering Institute of Canada, Ottawa.

Mailhot A, Duchesne S. Design Criteria of Urban Drainage Infrastructures under Climate Change.Journal of Water Resources Planning & Management [serial online]. March 2010; 136 (2):201-208.

Milly, P. C. D., Betancourt, J., Falkenmark, M., Hirsch, R. M., Kundzewicz, Z. W., Lettenmaier, D. P., and Stouffer, R. J.: Climate change – Stationarity is dead: whither water management?, Science, 319(5863), 573–574, 2008.

McCuen, R. H., 1979. Statistical terminology: definitions and interpretation for flood peak estimation. Journal of the American Water Resources Association, 15: 1106–1116. doi:10.1111/j.1752-1688.1979.tb01089.x

Motiee, H., 1996. Un-modèle numérique pour la simulation des réseaux d'assainissement pluvial fondésur le concept de stockage. Ph.D. Thesis. Lyon, France: Institut National des Sciences Appliquées de Lyon.

Moreda, F., Koren, V., Zhang, Z., Reed, S., and Smith, M., 2006: Parameterization of distributed hydrological models: Learning from the experiences of lumped modeling. J. Hydrol., 320, 218–237.

Nazari, B., Seo, D.J., Muttiah, R., 2014. Hydraulic modeling for inundation mapping using radar rainfall data-a case study for the city of Fort Worth. In:

International Symposium, Weather Radar and Hydrology, Washington, DC. April 7‐10.

Niemczynowicz, J., 1989. Impact of the greenhouse effect on sewerage systems-Lund case study. Hydrol. Sci. J., 34(6), 651–666.

Norouzi, A., 2016. Evaluation and improvement of fine-scale and hydrologic modeling of large urban areas using hydrometeorological and hydrologic observations. PhD dissertation, Dept of Civil Eng, The University of Texas at Arlington, Arlington, TX.

Norouzi, A., A. Rafieeinasab, D.J. Seo, J. Lee, 2015. Estimation of Stage-Discharge Relationships in Urban Streams Using a Fluid-Mechanically-Based Model. EWRI Congress, May, Austin, TX.

Neal, J.C., Schumann, G., Bates, P.D., 2012. A subgrid channel model for simulating river hydraulics and floodplain inundation over large and data sparse areas. Water Resour. Res. 48 (11), 16W11506.

Nguyen, P., Thorstensen, A., Sorooshian, S., Hsu, K., AghaKouchak, A., Sanders, B., Koren, V., Cui, Z. and Smith, M. (2015). A high resolution coupled hydrologic–hydraulic model (HiResFlood-UCI) for flash flood modeling. Journal of Hydrology.

Oki, T. and Kanae, S.: Global hydrological cycles and world water resources, Science, 313(5790), 1068–1072, 2006.

Ott, B. and Uhlenbrook, S.: Quantifying the impact of land-use changes at the event and seasonal time scale using a processoriented catchment model, Hydrol. Earth Syst. Sci., 8, 62–78, doi:10.5194/hess-8-62-2004, 2004.

Rappaport, E. N., 2000: Loss of life in the United States associated with recent Atlantic tropical cyclones. Bull. Amer. Meteor. Soc., 81, 2065–2073.

Raczynski A., Kirkpatrick W., Rehnstrom, D., Boulos, P., and Lansey, K, 2008. Developing hydraulic and water quality equivalent systems, Water Distribution Systems Analysis, doi:10.1061/41024(340)73.

Rafieeinasab, A., A. Norouzi, and D.-J. Seo, B. Nelson, 2015. Improving High-Resolution Quantitative Precipitation Estimation via Fusion of Multiple Radar-Based Precipitation Products, submitted to Radar Hydrology Special Issue of Journal of Hydrology.

Rafieeinasab, A., A. Norouzi, T. Mathew, D.-J. Seo, H. Chen, V. Chandrasekar, P. Rees, and B. Nelson, 2014. Comparative evaluation of multiple radar-based QPEs for North Texas, International Symposium Weather Radar and Hydrology, Apr 7-10, Reston, VA.

Rafieeinasab, A., Norouzi, A., Kim, S., Habibi, H., Nazari, B., Seo, D. J., Lee, H., Cosgrove, B., & Cui, Z. (2015). Toward high-resolution flash flood prediction in large urban areas–Analysis of sensitivity to spatiotemporal resolution of rainfall input and hydrologic modeling. Journal of Hydrology, 531, 370-388.

Reed, S., Koren, V., Smith, M., Zhang, Z., Moreda, F., Seo, D. J., and Participants, D. M. I. P., 2004. Overall distributed model intercomparison project results. Journal of Hydrology, 298(1), 27-60.

Reed, S., Schaake, J., Zhang, Z.Y., 2007. A distributed hydrologic model and threshold frequency-based method for flash flood forecasting at ungauged locations. J. Hydrol. 337 (3–4), 402–420.

Reed, S.M., 2003. Deriving flow directions for coarse-resolution (1-4 km) gridded hydrologic modeling. Water Resources Research, 39(9).

Rosso, R. and Rulli, M. C.: An integrated simulation method for flash-flood risk assessment: 2. Effects of changes in land-use under a historical perspective, Hydrol. Earth Syst. Sci., 6, 285–294, doi:10.5194/hess-6-285-2002, 2002.

Selvalingam, S., Liong, S. Y., and Manoharan, P. C., 1987. Use of RORB and SWMM models to an urban catchment in Singapore. Adv. Water Resour. 10-2, 79–86.

Seo, D.-J., Nonlinear Estimation of Spatial Distribution of Rainfall - An Indicator Cokriging, Stoch. Hydrol. Hydraul., 10(2), 1996.

Seo, D.J., Seed, A., Delrieu, G., 2010. Radar-based rainfall estimation, chapter in AGU Book Volume on Rainfall: State of the Science, F. Testik and M. Gebremichael, Editors. Geophys. Monogr. Ser. 191. doi:10.1029/GM191.

Smith, M., Koren, V., Zhang, Z., Reed, S., Seo, D.J., Moreda, F., Kuzmin, V., Cui, Z., Anderson, R., 2004b. NOAA NWS distributed hydrologic and modeling research and development. NOAA Technical Report NWS 51, US.

Smith, J. A., Baeck, M. L., Morrison, J. E., Sturdevant-Rees, P., Turner-Gillespie, D. F., & Bates, P. D. (2002). The regional hydrology of extreme floods in an urbanizing drainage basin. Journal of Hydrometeorology, 3(3), 267-282.

Smith, M. B., D. P. Laurine, V. I. Koren, S. Reed, and Z. Zhang, 2003: Hydrologic model calibration in the National Weather Service. Calibration of Watershed Models, Q. Duan et al., Eds., Water Science and Application Series, Vol. 6, Amer. Geophys. Union, 133–152.

Smith, M. B., Koren, V., Zhang, Z., Zhang, Y., Reed, S. M., Cui, Z., Moreda, F., Cosgrove, B.A., Mizukami, N. and Anderson, E.A. (2012). Results of the DMIP 2 Oklahoma experiments. Journal of Hydrology, 418, 17-48.

Soil Conservation Service, 1983. TR-20: Computer programs for projects formulations-hydrology. Tech. Release 20, U.S. Department of Agriculture, Washington, D.C.

Soil Conservation Service, 1986. TR-55: Urban hydrology for small watersheds. Tech. Release 55, U.S. Department of Agriculture, Washington, D.C.

Texas Department of Transportation (TxDOT), 2016. Hydraulic Design Manual, http://onlinemanuals.txdot.gov/txdotmanuals/hyd/hyd.pdf

Thomas, D. S. K., and J. T. Mitchell, 2001: Which are the most hazardous states? American Hazardscapes: The Regionalization of Hazards and Disasters, S. L. Cutter, Ed., Joseph Henry Press, 115–155.

U.S. Army Corp. of Engineers, 1985. HEC-1: Flood hydrograph package. Hydrologic Engineering Center, Davis, Calif.

Watt, W. E., Waters, D., and McLean, R., 2003. Climate change and urban stormwater infrastructure in Canada: Context and case studies. Toronto-Niagara Region Study Report and Working Paper Series Rep. No. 2003-1, Meteorological Service of Canada, Waterloo, Ontario.

Wallingford Ltd, 1997. HydroWorks on-line manual, Wallingford, U.K.

Warwick, J. J., and Tadepalli, P., 1991. Efficacy of SWMM application. J. Water Resour. Plann. Manage, 117(3), 352-366.

Willems, P., Arnbjerg-Nielsen, K., Olsson, J., Nguyen, V.T.V., 2012. Climate change impact assessment on urban rainfall extremes and urban drainage: Methods and shortcomings, Atmospheric Research, Volume 103, Pages 106-118, ISSN 0169-8095

Wheater, H. and Evans, E.: Land use, water management and future flood risk, Land Use Policy, 26, S251–S264, 2009

Zaghloul, N. A., 1998. Flow simulation in circular pipes with variable roughness using SWMM-EXTRAN Model. J. Hydraul. Eng., 124(1), 73–76.

Zhang, Z., Koren, V., Reed, S., Smith, M.B. and Moreda, F., 2006. Comparison of simulation results using SSURGO-based and STATSGO-based parameters in a distributed hydrologic model. 3rd Federal Interagency Hydrologic Modeling Conference, Reno, NV.

Zhu, T. J., Lund, J. R., Jenkins, M. W., Marques, G. F., and Ritzema, R. S.: Climate change, urbanization, and optimal longterm floodplain protection, Water Resour. Res., 43(6), W06421, doi: 10.1029/2004wr003516, 2007.